Longitudinal analysis of Brain Metabolite levels for HIV infected Children from ages five to eleven.

Noëlle van Biljon

MSc specialising in Biostatistics Dissertation

Supervisor: Assoc. Prof Francesca Little.

Co-supervisors: Prof Ernesta Meintjes,
Dr Martha Holmes,
Dr Frances Robertson.

January 2020

Declaration

I know that plagiarism is wrong. Plagiarism is to use another's work and pretend that it is one's own. I have used the Harvard convention for citation and referencing. Each contribution to, and quotation in, this dissertation from the work(s) of other people has been attributed, and has been cited and referenced. This dissertation is my own work.

Signature: Signed by candidate

Date: 31/01/2020

Acknowledgements

I would like to thank my supervisor Associate Professor Francesca Little who has taught me and guided me throughout this entire process and without whom I would not confidently call myself a Biostatistician.

I would also like to thank my co-supervisors Professor Ernesta Meintjes, Dr Frances Robertson and Dr Martha Holmes for their guidance and for exposing me to the world of MR spectroscopy and neuro-metabolism.

Thank you to the numerous research staff that worked to acquire this data and thank you to the children and parents who participated in this study, without whom this dissertation would not be possible.

This work was supported in part by the National Institutes of Health under grants R01DC015984, R01HD071664, R21MH096559, R21MH108346, U19AI53217; the NRF/DST through the South African Research Chairs Initiative; GlaxoSmithKline/ Viivhealthcare and Medical Research Council of South Africa; NRF grants CPR20110614000019421 and CPRR1-50723129691; UCT VC INTERIM FUNDING, and a UCT Postgraduate Conference Travel Award.

Abstract

HIV infected (HIV+) children initiate antiretroviral therapy (ART) early in life and remain on it lifelong. However, the long-term impact of ART and HIV on the maturing brain is not well documented and longitudinal neuroimaging studies are rare, especially in developing countries most heavily impacted by HIV/AIDS where access to imaging resources are limited. We have examined HIV related changes in metabolite level trajectories from 5-11 years in three brain regions using Magnetic Resonance Spectroscopy (MRS). We used univariate linear mixed effect models to identify independent profiles of the metabolites measured in each region of the brain. To explore the metabolite trends in a multivariate setting we generated multilevel mixed effects models, and correlated response models. There was an element of confounding introduced through the change of MRI scanner during the follow-up period and we compare different methods to resolve this issue. Consequently, we did observe differences in metabolite profiles from HIV+ children compared to HIV uninfected (HIV-) controls. This suggests that while these children are on ART treatment, there is still some underlying effect on their neurochemistry which sets their development apart from the normal healthy profiles we expect.

Table of Contents:

List of Figures:

List of Tables:

Abbreviations

Abbreviation	Definition
HIV	Human Immunodeficiency Virus
AIDS	Acquired Immunodeficiency Syndrome
MRI	Magnetic Resonance Imaging
MRS	Magnetic Resonance Spectroscopy
GM	Gray Matter
WM	White Matter
CSF	Cerebrospinal Fluid
BG	Basal Ganglia
PWM	Peritrigonal White Matter
MFGM	Midfrontal Gray Matter
Cr+PCr	Creatine-Phosphocreatine
Glu	Glutamate
Glu+Gln	Glutamate + glutamine
Ins	Myo-Inositol
NAA	N-acetyl aspartate
NAA+NAAG	N-acetyl aspartate +N-acetyl-aspartyl-glutamate
GPC+PCh	Choline
HUU	HIV Unexposed Uninfected
HEU	HIV Exposed Uninfected
HIV+	HIV Positive / Infected
HIV-	HIV Negative / Uninfected
CHER Trial	Children with HIV Early Antiretroviral Trial
AR(T)	Antiretroviral (Therapy)
PRESS	Point Resolved Spectroscopy
sMRI	Structural Magnetic Resonance Imaging
DTI	Diffusion Tensor Imaging
RS-fMRI	Resting State Functional MRI
ANOVA	Analysis of Variance
CI	Confidence Interval
CI*	Credibility Interval
LME(M)	Linear Mixed Effect (Model)
CR(M)	Correlated Response (Model)
LV	Latent Variable
FA	Factor Analysis
LF	Latent Factor
GLMM	Generalised Linear (Mixed) Model

Chapter 1: Introduction

1.1 Background:

HIV infection contributes significantly to infant mortality in South Africa. Under current treatment guidelines, Human Immunodeficiency Virus (HIV) infected (HIV+) children initiate antiretroviral therapy (ART) early in life and remain on it lifelong (Violari et al., 2008). However, the long-term impact of ART and HIV on the developing brain is not well documented and longitudinal neuroimaging studies that focus on childhood are rare (Cichocka and Bereś, 2018), especially in developing countries most heavily impacted by HIV/AIDS where access to imaging resources are limited.

The Children with HIV Early Antiretroviral (CHER) trial (Cotton et al., 2013; Violari et al., 2008) was started in 2005 with the aim of investigating the clinical outcomes of different ART initiation strategies in perinatally infected infants in South Africa (two sites located in Cape Town and Soweto). Infants younger than 12 weeks were randomly assigned to receive one of three treatment strategies - immediate limited antiretroviral therapy for 96 weeks, immediate limited antiretroviral therapy for 40 weeks or deferred therapy (ART initiated if CD4% less than 25%). The study concluded that early HIV diagnosis and immediate ART initiation reduced early infant mortality by 76% and HIV progression by 75%. As a consequence of this and similar studies, the current treatment guidelines were formulated, recommending immediate ART in infants testing positive for HIV.

A neurodevelopmental follow up study included the CHER trial participants from Cape Town as well as uninfected control children from an interlinking vaccine trial (Madhi et al., 2010). The longitudinal study used neurocognitive and neuroimaging methods to better understand the long-term consequences of ART and HIV

infection in children aged 5 to 11 years. The neuroimaging component included structural magnetic resonance imaging (sMRI), magnetic resonance spectroscopy (MRS), diffusion tensor imaging (DTI) and resting state functional MRI (RS-fMRI). Few trials have followed HIV+ children who initiated ART in infancy; this follow up study is quite unique as little is known about the influence of ongoing usage of ART on the developing brain.

MRS is a non-invasive technique for measuring specific metabolite levels. In single voxel proton MRS, a spectrum is acquired describing a small region within the brain (defined by the voxel size). On this spectrum, metabolites are identified by their chemical shift (Figure 1.1) and the area under a metabolite peak represents the concentration of that metabolite (Graaf, 2008). The metabolites measured are indicative of localized neuro-metabolism and can be used as a proxy for aspects of brain health. This dissertation focuses on the identification of HIV related changes to the longitudinal trajectories of neuro-metabolite concentrations measured using MRS.

Figure 1.1: Sample MRS Spectra with labelled metabolite peaks (From Rothman et al., 1999).

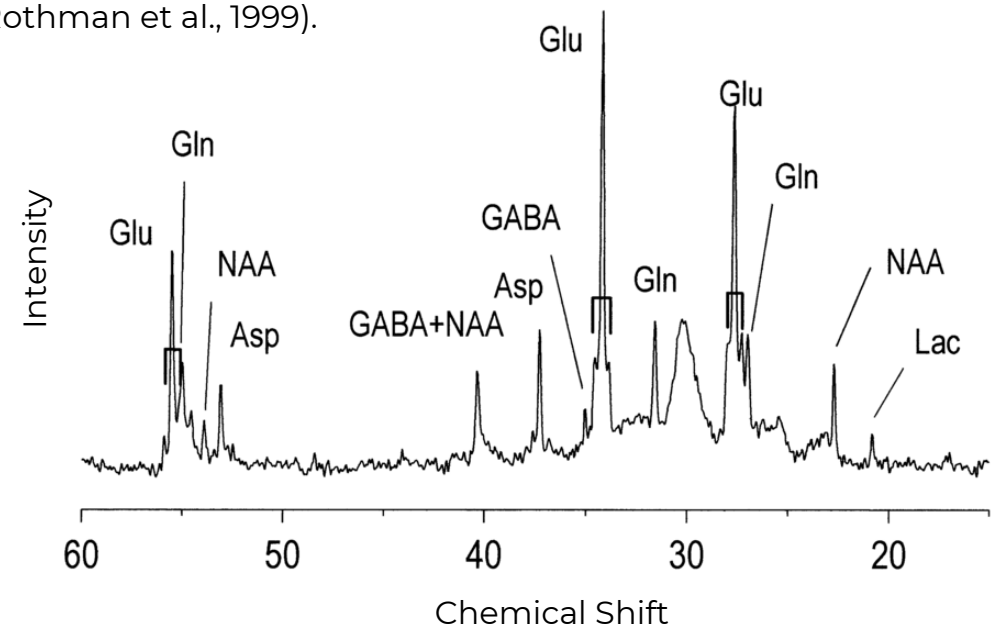

The secondary aim discussed in this dissertation is to address a source of variability introduced by a change in MRI scanner in 2016 during longitudinal data acquisition. During the follow up visits at age 9 the 3T Siemens Allegra MRI scanner that had been used for neuroimaging in the cohort at ages 5 and 7, was decommissioned and replaced by a 3T Siemens Skyra MRI scanner, as illustrated by the design of the study in Figure 1.2. This has introduced another element of variability and this problem, as well as our approaches for resolving this problem, are the focus of chapter two.

Figure 1.2: The design of this longitudinal study.

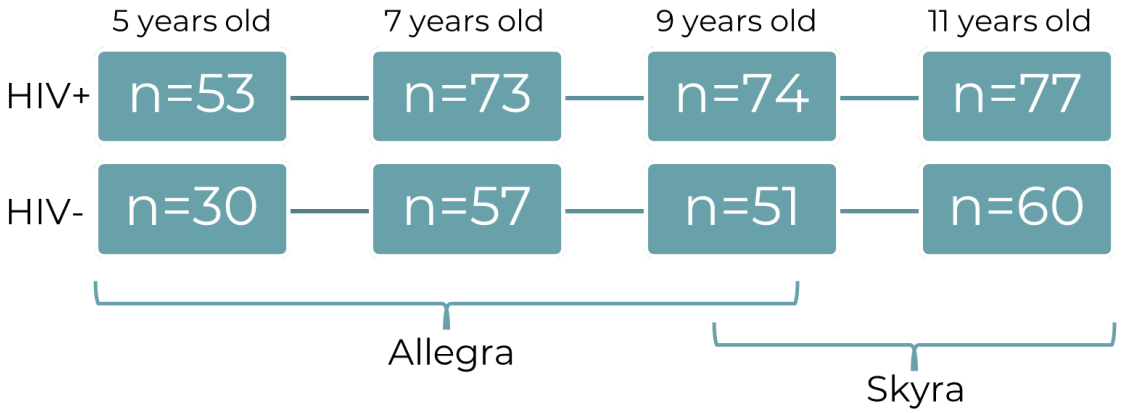

HIV+ children from the CHER trial (Cotton et al., 2013; Violari et al., 2008) and uninfected (HIV-) children were scanned up to 6 times, between the ages of 5 and 11, with a Point Resolved Spectroscopy (PRESS) sequence (voxel size 15 x 15 x 15 mm^3, TR=2000 ms, TE=30ms, 64 averages with CHESS water suppression, 1 without) on 3T Allegra and Skyra scanners (Siemens, Erlangen, Germany). A structural scan was also performed to determine the percentage of various tissue types within the voxels. Absolute metabolite concentrations were calculated using LCmodel (Provencher, 2001) via the water scaling method (Ernst et al., 1993; Kreis et al., 1993).

Our study examines HIV related changes in metabolite level trajectories in three brain regions. The regions of interest are located within the basal ganglia (BG), midfrontal gray matter (MFGM) and peritrigonal white matter (PWM). The BG is often affected early on in HIV infection and without treatment calcification of this region is common (Belman et al., 1986; Govender et al., 2011); MFGM is important in executive functioning and may be sensitive to ongoing HIV related damage as it develops throughout childhood; PWM was previously implicated in paediatric HIV (Flowers et al., 1990; Hoare et al., 2014; Keller et al., 2004). Hence, these are the regions we have focussed on for this study.

Each voxel is likely to be composed of two or three distinct tissue types. Due to the possible effects of operator bias (subjectivity in voxel placement) as well as biological variation among subjects, the amount of white matter (WM), gray matter (GM) and Cerebrospinal fluid (CSF) in each voxel varies. CSF helps maintain homeostasis, is involved in clearing waste from the brain and also serves to protect the brain. CSF has a similar composition to normal blood plasma, but with a much lower concentration of proteins. GM and WM tissue of the brain perform different tasks, GM contains glial and neuronal cell bodies (that control our senses, decision making and muscle control) while WM is made up of myelinated axons that connect GM areas and carry impulses between them.

Because of their different functions and cellular composition, metabolic activity is expected to differ between GM and WM. For example, some metabolites, such as N-acetyl aspartate (NAA), creatine-phosphocreatine (Cr+PCr) and choline

(GPC+PCh) are present in higher concentrations in GM than WM regions of the brain (Wang and Li, 1998). This means that the percentage of GM and WM must be controlled for in the analytical models as the percentage in the voxel scanned will then affect the metabolite concentrations in the specific voxel.

As previously mentioned, metabolite concentrations can be used as a proxy for brain health. The metabolites we present are: glutamate (Glu) and combined Glu+glutamine (Glu+Gln), N-acetyl aspartate (NAA) and combined NAA+N-acetyl-aspartyl-glutamate (NAAG), choline (GPC+PCh) which is a measure of both glycerophosphocholine (GPC) and phosphocholine (PCh), creatine-phosphocreatine (Cr+PCr) and myo-inositol (Ins). NAA and GPC+PCh are markers for neuronal and membrane integrity, respectively, and Cr+PCr, is involved in the Krebs cycle and is a measure of cellular energy levels (Keller et al., 2006; Zhu and Barker, 2011). Ins is a measure of glial proliferation while Glu is an important neurotransmitter (Keller et al., 2006; Zhu and Barker, 2011). GPC+PCh and Ins have been identified in higher levels in HIV+ children which is often associated with inflammation (Chang et al., 2003; Prado et al., 2011; Zahr et al., 2014).

The data used for this longitudinal study has also been analysed cross-sectionally (Mbugua et al., 2016; Robertson et al., 2018). Mbugua et al. (2016) reported on changes seen in the BG region from the first observation period, while Robertson et al. (2018) (and in their unpublished work) reported on results from MFGM and BG data related to the second and third observation periods. In work that is yet to be published, Graham et al., analysed the data at age 11 from all three regions of interest - MFGM, BG and PWM.

Mbugua et al. (2016) found that early antiretroviral (AR) treated HIV+ children had increased concentrations of NAA and GPC+PCh at age 5 in the BG region. This was interesting because lower levels of NAA is something that has been well documented within HIV+ immunosuppressed patients and is thought to indicate a loss of neurons or neuronal dysfunction (Chong et al., 1993).

Robertson et al. (2018) found no differences in NAA concentrations in the BG region at the age of 7, but in contrast at age 9 identified HIV+ children had lower levels of NAA compared to the healthy controls (Robertson et al., 2018). Robertson et al. (2018) also observed a significant decrease in Glu concentrations in HIV+ children at age 9 (Robertson et al., 2018). Previous studies have observed both decreases (Ashby et al., 2015) and increases (Keller et al., 2004; Lu et al., 1996) in GPC+PCh concentrations in the BG region of HIV+ children. Evidently, no clear trends have been observed and often contradicting observations have been recorded. Previous studies that focused on the effect of HIV on metabolite concentrations within the BG, MFGM and PWM and their key findings have been summarised in Table A.1.2 in Appendix A.1.

In unpublished work looking at the MFGM, Robertson found Glu levels to be lower in HIV+ children compared to HIV- children at both 7 and 9 years old. They also found HIV+ children had higher levels of GPC+PCh compared to HIV unexposed

uninfected (HUU) children at age 7 (Robertson et al., unpublished). Analysis of these metabolite concentrations at age 11 has also been performed by Graham and is also currently unpublished. Graham found higher levels of GPC+PCh in the BG region for HIV+ children compared to HIV- controls (Graham et al., Unpublished). They also found reduced concentrations of NAA and Cr+PCr in the PWM region for HIV+ children (Graham et al., Unpublished). Cross-sectional analysis of the data from ages five to nine from the PWM has not yet been performed, and the data acquired at age five from the MFGM has also not been examined.

A longitudinal analysis has also profiled the metabolite concentrations of the control subjects up until the age of 9 (Holmes et al., 2017). This study focused on describing the metabolite levels in healthy children from a low socioeconomic population to allow future comparison for similar populations of diseased children. In the BG they saw a significant increase in the concentrations of Glu, Glu+Gln and NAA+NAAG with age; this may be indicative of subcortical synaptic reorganisation (Holmes et al., 2017). In the PWM they saw related increases in Cr+PCr, NAA, NAA+NAAG, Glu and Glu+Gln that suggest ongoing myelination in this region (Holmes et al., 2017). Finally, in the MFGM they saw Cr+PCr, NAA, NAA+NAAG and Glu+Gln increasing with age, which may be as a result of synaptic activity related to learning (Holmes et al., 2017).

Previous studies have also identified neurodevelopmental differences between HIV- unexposed (HUU) and HIV- exposed (HEU) children (Kerr et al., 2014; Rie et al., 2008). HEU children are born to mothers with HIV, but thanks to mother to child prevention methods do not acquire HIV. Because of the neurodevelopmental variations identified, it is of interest whether other neurological differences, such as neuro-metabolic alterations, are present. Previous studies that focus on changes in metabolite concentrations between these groups have been summarised in Appendix A.1, Table A.1.3. We briefly investigate the effects of exposure to HIV in chapter three, but in the rest of the dissertation focus on the metabolite differences between HIV+ and HIV- children, regardless of exposure status.

1.2 Data Preparation:

1.2.1 Data Cleaning:

As previously mentioned, the MRS procedure produces raw spectra which are then used to compute metabolite concentrations. The program used to calculate metabolite concentrations from the raw spectra is LCModel (Provencher, 2001). LCModel uses a constrained nonlinear least-squares analysis to estimate metabolite concentrations and their uncertainties (Provencher, 1993). The output from this software includes various measures of data certainty, one of these measures is the %SD. The %SD is the estimated standard deviation (from the aforementioned model fitting process) for each measured metabolite expressed as a percent of the estimated concentration. For example, a concentration of 5 with a standard deviation of 1 would give a %SD of 20%. The %SD indicates the reliability of a given metabolite concentration. These estimates are used to quantify the certainty of the measured metabolite and hence a greater %SD would suggest an unreliable measurement, while a small %SD would imply a certain measurement of a concentration. We used a %SD measurement greater than 25 as the cut-off for exclusion from the analysis which was a recommendation from experts that had experience working with MRS data. We found that observations with a %SD greater than 25 usually had a concentration of zero, or something equally as unlikely.

1.2.2 Transforming Covariates:

Age:
In this study, the children's ages range from 5 to 11 years. The ages used for the modelling process were the ages observed with 5 subtracted so that the age effect measured is from the start of the observation period and not from birth.

HIV Exposure:
The HIV uninfected children are subdivided into two categories: (1) HIV unexposed uninfected (HUU) and (2) HIV exposed uninfected (HEU) children. The HEU children were born to HIV positive mothers with HIV. The HEU group has been exposed to HIV but is uninfected, while the HUU group has never been exposed to HIV.

Relative GM / WM%:
CSF is predominantly made up of water with small traces of nutrients and minerals. As a result, we assume that it contains none (or at least undetectable amounts) of the metabolites we are interested in measuring. Thus, we use the percentage of GM or WM tissue as a proportion of the total tissue measured excluding CSF.

Figure 1.3 shows the box-and-whisker plots representing the range of percentages of GM, WM and CSF present in the MFGM voxel during imaging for each subject. Here we can see that the CSF values vary between 0% and up to almost 50% in one case. As a result of this we are using relative GM % (and relative WM% for the PWM region) where we use the percentage of GM or WM that is tissue and not CSF. Thus, we take the percentage from 100-CSF. We do see a fair amount of variability in this

percentage of GM in the voxel. Because of this variability in GM% for each subject, we have included this as a covariate in the linear models that follow as an effort to reduce variability relating to the scanning procedure.

Figure 1.3: Box and Whisker plots of WM, GM and CSF Voxel percentage during imaging of the Mid Frontal Gray Matter Region for all time points.

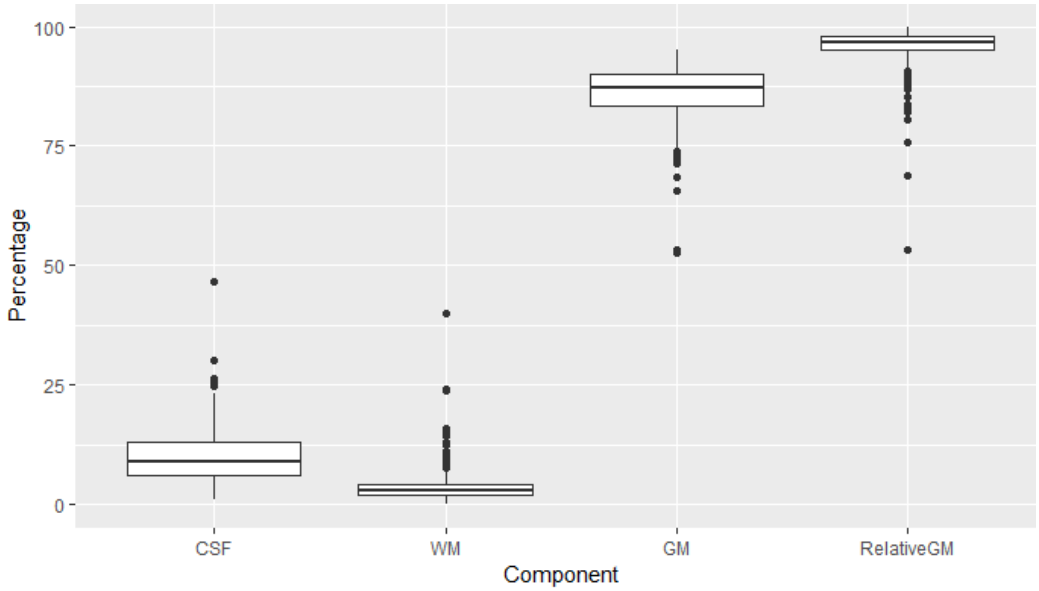

The relative tissue percentage is calculated as follows:

$$Relative\ GM\% = \frac{\%GM}{100 - \%CSF} \tag{1.1}$$

$$Relative\ WM\% = \frac{\%WM}{100 - \%CSF}$$

When analysing the concentrations from the BG and MFGM regions relative GM% was used as a covariate, while when looking at PWM we used the relative WM% measurement. Later, when exploring the data in a multivariate setting, relative GM% was used for all three regions.

Gender and Race:
In Table 1.1 we present the summary statistics describing the cohort of children involved in this study.

Table 1.1: The summary statistics of all subjects included in this longitudinal study.

	HIV +	**HIV -**	**Total**
Number of Subjects	89	85	174
Percentage Unexposed	-	50.59	24.71
Percentage African	88.76	81.18	85.06
Percentage Males	48.31	58.82	53.45
Average number of visits	3.25	2.36	2.88

The cohort is made up of 174 children that were predominantly of African ethnicity with a relatively even split of males and females (Table 1.1). The HIV- group comprises of almost half HIV exposed children and a little over half were unexposed to HIV. Few children were present at all follow-up visits and we saw a higher average number of follow-up visits in the HIV+ group compared to the controls (Table 1.1).

Table 1.2 describes all the covariates incorporated into this study to clarify the different variables we considered that may have an effect on metabolite concentrations within the brain.

Table 1.2: Covariates that were measured or documented in this data.

Covariate	**Definition**	**Variable Type**
Age	The age of the child with the youngest scan age as baseline.	Continuous
Status	HIV status of child. HIV positive or negative.	Categorical
Relative WM/GM %	The percentage of GM or WM in the voxel relative to the total amount of GM+WM in the voxel (see equation above).	Continuous
Race	Race of the child, either of mixed ancestry or African.	Categorical
Exposure	The exposure status of the child w.r.t HIV. They are either HIV positive (and thus HIV exposed and infected), HIV negative unexposed or HIV negative exposed. The exposed but uninfected children were born to mothers with HIV, but these children were not infected with HIV.	Categorical
Gender	Either male or female.	Categorical
Scanner	The MRI machine used to measure the metabolite levels at a given time point, either the Allegra or Skyra scanner.	Categorical
Time Between Scans	The time between the two scans taken at the nine year old follow-up on the two different MRI scanners.	Continuous

1.3 Objectives:

The overarching goal of this study is to model metabolite profiles from 5 to 11 years to determine if HIV status effects age-related changes in metabolite concentrations in three regions of the brain. With respect to clinical objectives, this dissertation focuses on the identification of possible covariates that may affect brain metabolite concentrations with a specific focus on the effects of HIV Status. Profiling these metabolite concentrations over time is also key. We also aim to investigate these metabolite concentrations in a multivariate setting to identify any effects on concentration due to changes in other metabolites or due to regions the concentrations are measured in.

The statistical approach had to take into account:

1. The repeated measures over time,
2. The multivariate nature of the data due to the multiple responses,
3. The bias due to the change of scanners.

This dissertation will present two main approaches to deal with the above data features, namely hierarchical mixed effect models (chapter 4) and multivariate correlated response models (chapter 4) while the calibration of scanners is discussed in chapter 2.

Chapter 2: Calibration of MRS Data

2.1 Background:

There are four key sources of variation when looking at MRI and MRS data (Biberacher et al., 2016). In brief, these are i) scanner related factors that cause variation between observations from one scanner (intra-scanner effects) and the differences between scanners (inter-scanner effects), ii) factors that relate to the scanning procedure (eg. position and motion), iii) physiological factors (such as hydration status) and iv) factors related to data acquisition and processing (Biberacher et al., 2016; Minati et al., 2010). We are focussing on investigating the first source of variability and quantifying the inter- and intra-scanner variation present within our dataset.

As previously mentioned, the Allegra MRI scanner initially used to acquire MRS data from our cohort at ages 5-9 was decommissioned in 2016 and replaced by a Skyra MRI scanner. The Skyra scanner has been shown to be more reliable than the Allegra scanner – the uncertainty of metabolites as illustrated by the %SD measured is much lower than that from the Allegra scanner (Figure 2.1). This is the first inconsistency between the output from these two scanners.

Few studies exist that investigate the effect of inter-scanner effects with respect to different types of MRS scanners. Barreto et al. (2014), Lee et al. (2003) and Sacktor et al. (2005) have investigated the feasibility of multicentre studies and compared inter-scanner effects using the same MRI model and strength across various research sites. While Lee and Baretto found no site-specific differences in metabolite concentrations (using a Sigma 1.5T and 3T Philips Achieva scanners respectively) Sacktor (who also used a Sigma 1.5T scanner) did observe some significant site-specific concentrations for CR+PCr and NAA (Barreto et al., 2014; Lee et al., 2003; Sacktor et al., 2005). The general consensus when using the same scanner and same protocol across multiple sites, is that the data is reliable, and an

effect of scanner/site does not need to be considered. However, we see that this is not always the case with the results from Sacktor, where the same MRI scanner model and strength was used as the Lee study.

Figure 2.1: Box and Whisker plots of standard deviation for the various metabolites measured in the (A) MFGM and (B) BG regions at age 9.

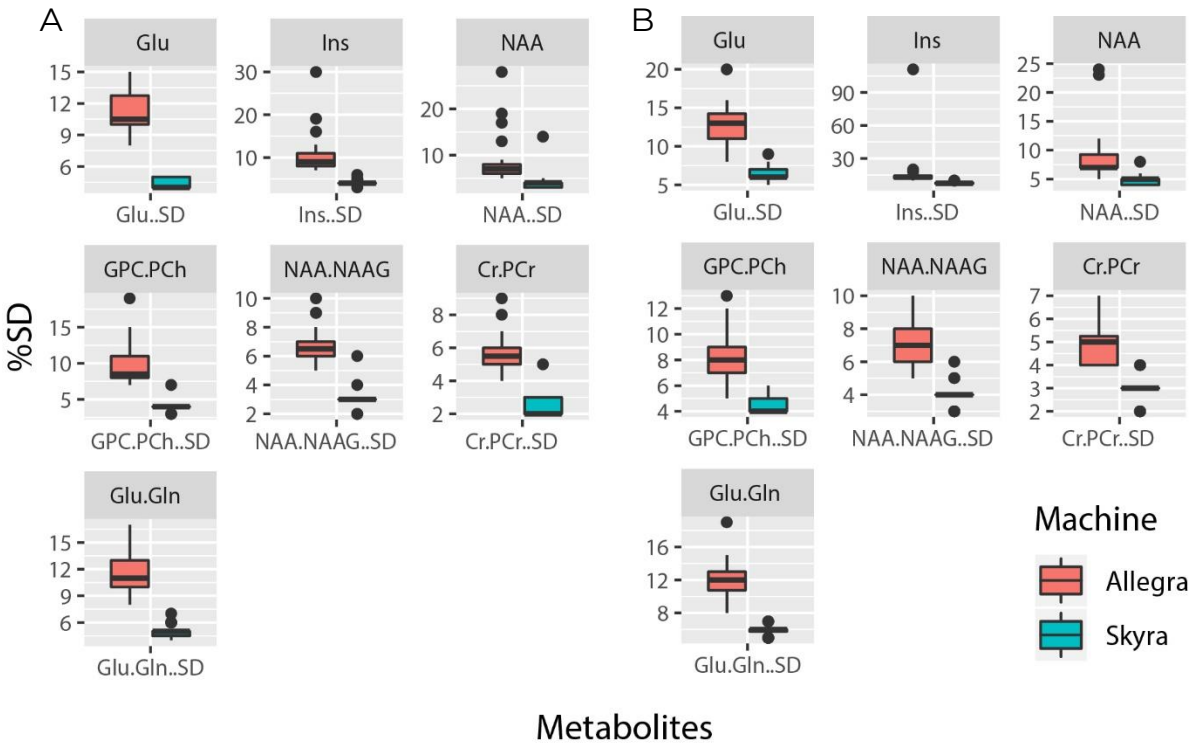

On the other hand, the use of multiple different scanners in MRS studies has also been investigated which is more relevant to our analysis as the Allegra and Skyra machines are different models both produced by Siemens. Kang et al. (2011), compared Proton Density Fat Fractions (PDFF) measured in the liver using a 1.5T and a 3T scanner. These scanners gave significantly different results, they illustrated this using a Bland-Altman plot that will be discussed in detail later. They observed a clear bias between these two modalities, however they did not give any recommendations on how to proceed with analysis of this data and how to address the bias (Kang et al., 2011).

Jessen et al. (2009) also completed an MRS study with four different 1.5T MRS scanners. They used an Analysis of Variance (ANOVA) approach to investigate the scanner effect among controls only and found this effect to be significant (Jessen et al., 2009). Biberacher et al., (2016), concluded that when combining multi-centre data using different scanner types, the effect of these scanners must be considered (Biberacher et al., 2016). As there does not appear to be a clear agreement on whether multicentre/scanner data can be combined without accounting for the scanner effect, we have set out to investigate this effect within our dataset. Following this we aim to test some approaches for calibrating this data. In any data set there are two types of error that may be present: i) random error and ii)

systematic error. The use of two different MRI scanners may have introduced the latter into our data set.

No clear approach has been described for dealing with inter-scanner variability. Jessen et al. (2009) used control data to identify the mean and standard deviation specific to each scanner and used these values to normalise their data with respect to each scanner. This approach may reduce the observed systematic difference between scanners, however it is not a feasible approach as we will not identify the longitudinal trends present in the data if we perform longitudinal analysis on normalised data. Two strategies for addressing the scanner/site specific effects recommended by Sacktor et al. (2005) include i) expressing patient metabolite concentrations relative to scanner/site specific controls and ii) including site/scanner as a factor in multivariate statistical analysis.

Figure 2.2: Box and Whisker plots of absolute concentration for the various metabolites measured in the (A) MFGM and (B) BG regions at age 9.

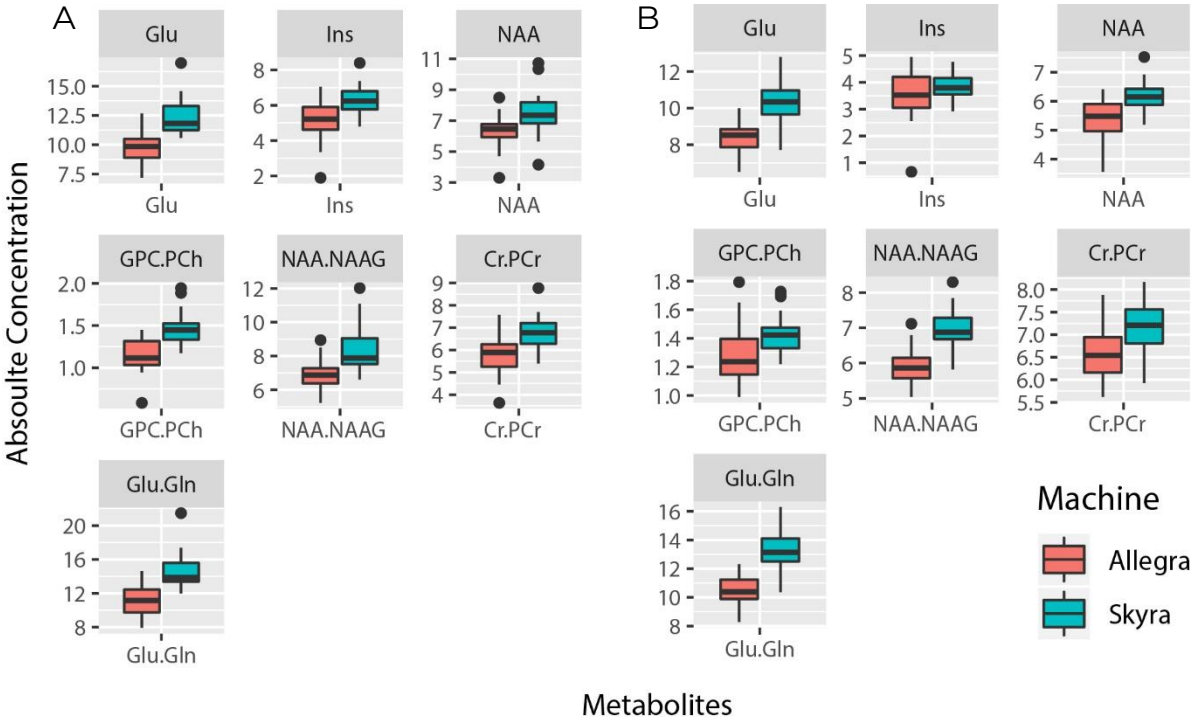

The boxplots in Figure 2.2 show the distribution of absolute concentrations measured at the age 9 follow-up period on the two different MRI scanners. We can see a general trend for the measurements taken on the Skyra scanner to have a greater concentration than those taken on the Allegra scanner. However, these measurements were not taken on the two scanners on the same day. The Allegra scanner was decommissioned during the follow-up period and when the Skyra scanner was in operation the children initially scanned using the Allegra scanner were brought back for a second scan on the new machine. This means that while we compare these observations as if they are from the same follow up period, these measurements were actually taken on average 10.8 months apart with an average

age of 9.15 for the first scan and 9.97 for the second scan using the new machine. As we know from previous studies, age results in an increase in brain metabolite concentrations in these regions (Holmes et al., 2017). Thus, it is difficult to identify if this general increase seen between these observations at age 9 are due to the time between these scans and normal increases of concentrations with age, or if it is as a result of the change is MRI scanner. Hence, there is an element of confounding here due to age and scanner.

2.2 Methods:

2.2.1 Comparing Intra-scanner- and Inter-scanner variation:

At the age of five 22 children were scanned twice using the Allegra MRI scanner. Using these repeated measures from the same MRI instrument the intra-scanner variability present when using the Allegra scanner can be identified. At the age of nine 24 children were also scanned twice, but instead on two different scanners - the Allegra and Skyra MRI machines. Using these measurements, the inter-scanner variability can be identified.

We identified the intra- and inter-scanner variabilities respectively by finding the absolute difference between the repeated measurements for each subject. The intra- and inter-scanner variability was then compared using a Students t-test to identify if the size of this variation was significantly different. This analysis was performed using the *t.test* function from the *stats* package in R (RStudio Team, 2018).

2.2.2 Simple Linear Regression Approach:

The aim of the simple linear regression model is to identify the relationship between metabolite concentrations obtained using the Allegra and the Skyra MRI scanners. The intention is to identify if a systematic difference between the two scanners can be observed across the metabolites and brain regions. Below is the formulated linear model:

$$Y = \beta_0 + \beta_1 X_1 + \varepsilon \qquad (2.1)$$

where:

Y = metabolite concentration measured using the Allegra scanner,
X_1 = metabolite concentration measured using the Skyra scanner,
$\varepsilon \sim N(0, \sigma^2)$.

This is a general model formulation where 'Allegra Concentrations' and 'Skyra Concentrations' refers to the concentration of the various metabolites measured in the respective brain regions. Hence, as there are three regions and seven metabolites, 21 independent linear models were created according to this model formulation. β_0 and β_1 refer to the intercept and slope that describe the linear

relationship between MRS measurements taken using the Allegra and Skyra MRI scanners. β_0 would thus represent the shift in overall scale between the two scanners, while β_1 will capture the equivalent unit change in measurements from the two scanners.

2.2.3 Linear Regression Approach with covariates:

The aim of the following model is to account for variability seen in the previous simple model using covariates such as 'Time Between Scans', HIV Status and the 'Allegra/ Skyra GM%'. These covariates are not constant between the subjects and hence need to be investigated as they may influence metabolite levels measured using the Allegra and Skyra scanners and thus confound the relationship between the measurements from the two scanners.

The multivariable regression model is:

$$Y = \beta_0 + \beta_1 X_1 + \beta_2 X_2 + \beta_3 X_3 + \beta_4 X_4 + \beta_5 X_5 + \varepsilon \quad (2.2)$$

where:

Y = metabolite concentration measured using the Allegra scanner,
X_1 = metabolite concentration measured using the Skyra scanner.
X_2 = time (in months) between scans,
X_3 = relative percentage of GM or WM measured from the Allegra scan,
X_4 = relative percentage of GM or WM measured from the Skyra scan,
X_5 = HIV Status (=1 for positive, =0 for negative).
$\varepsilon \sim N(0, \sigma^2)$

This model again generalises the measurements taken across different regions for different metabolites using 'Allegra' and 'Skyra' in the formula. Hence, again, 21 different models are created here to look at the effect of these covariates on metabolite concentrations in different regions of the brain. The β_i values measure the size of the effect on the metabolite concentration measured using the Allegra MRI while β_0 measures the baseline concentration given all other covariates are equal to zero.

All linear regression was performed using the *lm* function from the *stats* package in R (RStudio Team, 2018).

2.2.4 Bland-Altman Analysis:

Bland-Altman analysis is a technique used to compare two measurements of the same variable (Altman and Bland, 1983). Hence, it is a useful technique when assessing the reproducibility of a measurement system. The Bland-Altman plot is created by plotting the differences between two repeated observations from the same individual from two different measurement techniques against the mean of those two observations from the same individual thus allowing for the detection of an association between bias and scale.

Three lines are also drawn onto the plot to aid interpretation; a horizontal line that represents the bias drawn at the mean difference ($\bar{d}$) between the two measurements and two horizontal lines drawn at $\bar{d} \pm 1.96\ S_d$ to represent 95% limits, where S_d represents the standard deviation of these differences. This method allows one to identify the difference (the bias) between two measurement techniques and to subsequently identify an interval where 95% of these differences fall. Hence, this technique can be used to identify the range of differences obtained from inter- and intra-scanner measurements, which we can subsequently use to identify the inter- and intra-scanner effects.

Using the *BlandAltmanLeh* package in R (RStudio Team, 2018), Bland-Altman plots were created to compare the inter- and intra-scanner bias and 95% ranges. Separate plots were created for repeated measures at five years old and nine years old for each of the metabolites measured in the three regions of the brain.

2.3 Results:

As the analysis of each metabolite in each region is rather repetitive, the figures and tables for the exploration and findings of the PWM and BG can be found in the Appendix (A.2), with the figures and findings for the MFGM present here to illustrate the general trends present in these results.

2.3.1 Repeated subjects:

Table 2.1: Summary Statistics and Demographics of the group of individuals used to identify the intra- and inter-scanner variability, and to perform calibration of scanner effects.

	In 5 year old rescanned group	**In 9 year old rescanned group**
Number Scanned Twice	11	24
% HIV Positive	100	29.17
% Exposed of HIV-	-	47.06
Mean Age at first scan (years)	5.18	9.15
Mean Time Between Scans (months)	7.60	10.83
African (%)	100	58.33
Male (%)	36.36	66.67

Fewer children were rescanned at age 5 compared to age 9, and we see only HIV+ children in the rescanned group at age 5 while the age 9 group was predominantly made up if HIV- controls. The relatively large lapse in time between repeated measurements, especially for nominal age 9, necessitates including time between scans into the regression model to eliminate the confounding.

2.3.2 Intra-scanner Effects:

To look at the variability within observations taken at the same time point (nominal age 5) using the same scanner (the intra-scanner variability), we compared the variability within the observations from the first and second scans taken at age 5. These scans were both performed using the Allegra MRI scanner and the variability was visualised using box-and-whisker plots (Figure 2.3).

Figure 2.3: Box and Whisker plots of Repeated Scans at Five years old in the MFGM illustrating the intra-scanner variability present.

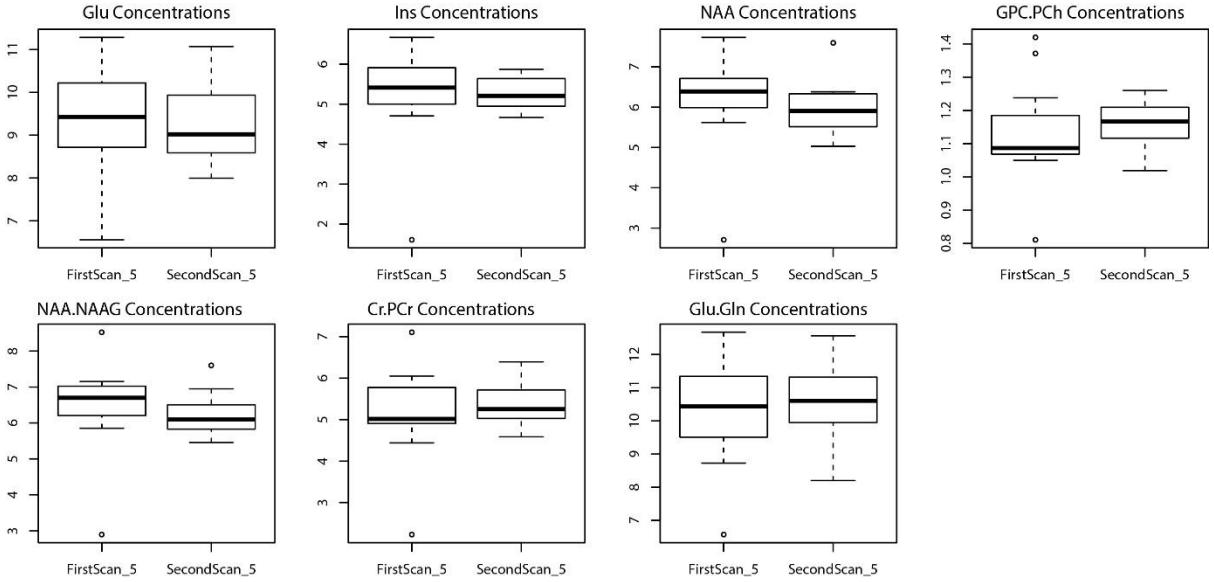

The ranges of observations from the two scans taken at age five using the Allegra scanner show no obvious shift between repeated measurements (Figure 2.3). The ranges do vary between metabolites, but there is a large degree of overlap and the median values all fall within the range of the other.

Another means of investigating this intra-scanner variability is by looking at the correlation between the observations from the same individuals at these two follow-up visits within the same time point.

Table 2.2: Correlation between repeated metabolite observations at 'five' years old for all three brain regions.

Metabolite	BG (n=11)	MFGM (n=11)	PWM (n=11)
Glu	0.122	0.500	0.419
Ins	0.007	0.059	0.786
NAA	0.391	0.258	0.597
GPC	0.559	0.190	0.252
NAA.NAAG	0.176	0.311	0.668
Cr.PCr	0.611	0.194	0.678
Glu.Gln	-0.095	0.128	0.270

The strength of the correlation between repeated observations taken at age five using the same scanner varies significantly between metabolites. The highest correlation is seen for Ins in the PWM region (Table 2.2). These correlations do seem

to suggest that some of the measurements are repeatable and the concentrations are consistent for the few metabolites with high correlations. However, there are also many concentrations that have not been measured consistently and this has resulted in low correlations – indicating a possible lack of reliability in these measurements or a source of variability that must be considered. This is likely due to the time between observations.

2.3.3 Inter-scanner Effects:

To visualise the inter-scanner variability within the observations taken at age 'nine', box-and-whisker plots were used to illustrate and compare the distributions of measurements taken from the two scanners. This allows us to observe the scanner effect on the median of the observations and the variability as illustrated by interquartile and full ranges.

Figure 2.4: Box and Whisker plots of Repeated Scans at 'nine' years old in the MFGM illustrating the inter-scanner variability present.

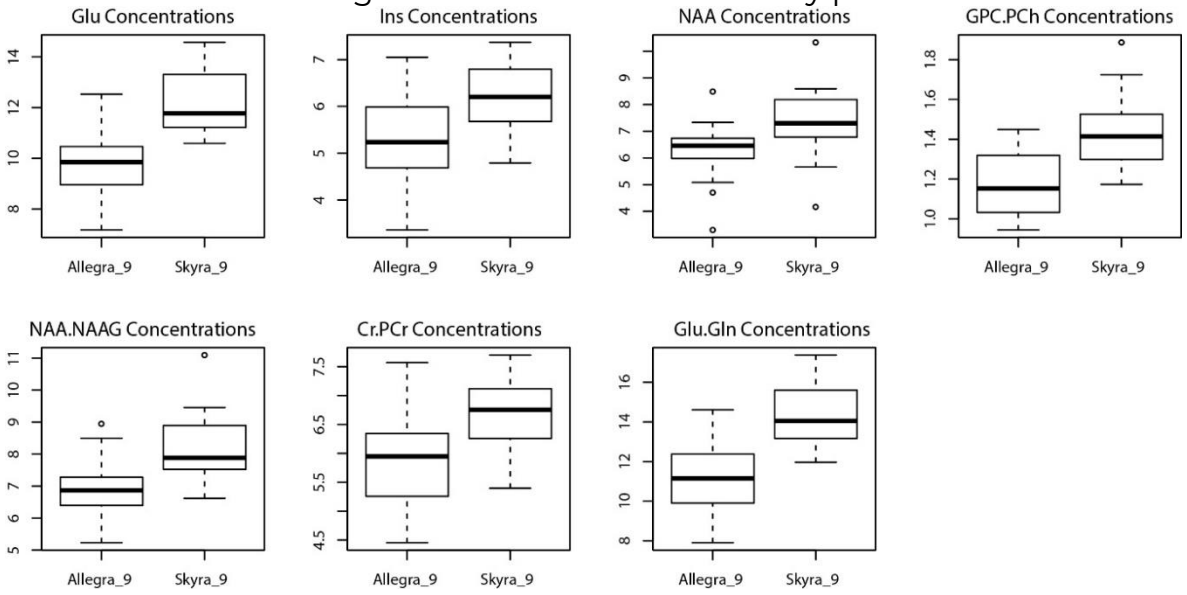

The box and whisker plots of repeated observations taken at nominal age nine show a general trend of a higher metabolite concentration measured using the Skyra MRI machine (Figure 2.4). This does suggest a scanner effect; however, it cannot be ruled out that the increase is as a result of age due to the longer time interval between the two repeated scans.

Table 2.3: Correlation between repeated metabolite observations at' nine' years old for all three brain regions.

Metabolite	BG (n=24)	MFGM (n=24)	PWM (n=6)
Glu	0.239	-0.111	0.439
Ins	0.135	0.138	0.387
NAA	0.181	0.010	0.891
GPC	0.255	0.250	0.086
NAA.NAAG	-0.030	-0.194	0.906
Cr.PCr	0.057	-0.186	0.425
Glu.Gln	-0.012	-0.131	-0.205

The correlations of observations taken at age nine on the two different scanners are generally lower than the correlations seen from the repeated observations at age 5 (Table 2.2, Table 2.3). The correlations between observations from the PWM are quite high, however as only six subjects were scanned twice these are not very reliable (Table 2.3).

To contrast this intra- and inter-scanner variability the differences between the two observations at each time point was calculated and also summarised using box-and-whisker plots (Figure 2.5). We also performed t-tests to compare these differences and the p-values from these tests are show in figure 2.5.

Figure 2.5: Box and Whisker plots of the difference between metabolite concentrations within the MFGM region from repeated scans taken at ages five and nine with the significance of t-tests comparing these differences.

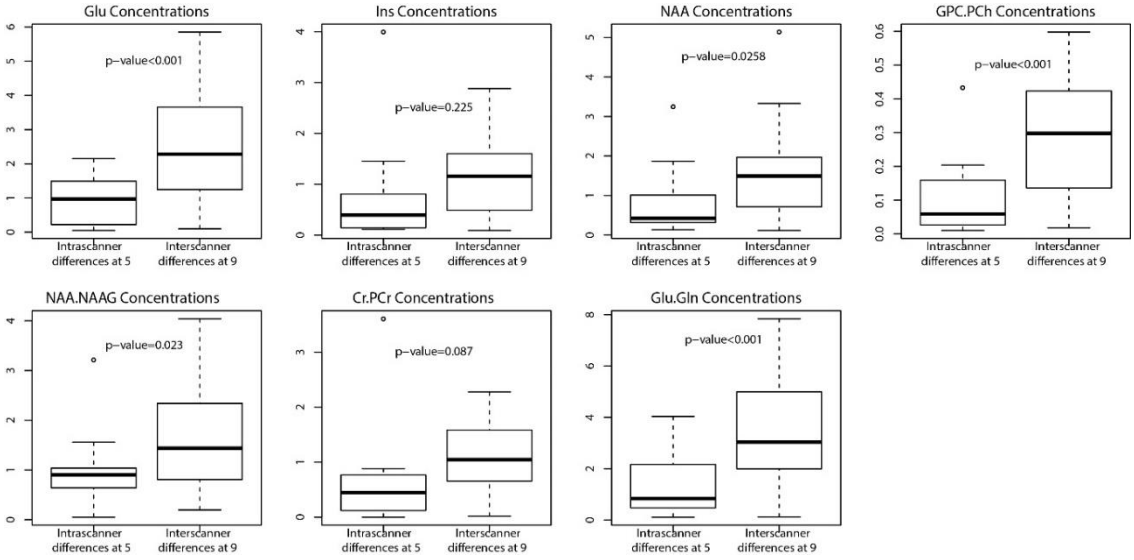

From the boxplots comparing inter- and intra-scanner differences we see the inter-scanner differences are greater than intra-scanner across all metabolites (Figure 2.5). Hence, we see evidence of some bias present in the nine-year-old data. The bias is significantly greater for observations taken on the two different scanners for all metabolites except for Ins and Cr+PCr in the MFGM, Glu in the BG and Ins, Cr+PCr and Glu in the PWM. Hence, inter-scanner differences are greater than intra-scanner differences and needs to be controlled for during the longitudinal modelling process.

2.3.4 Linear Regression Approach to Calibration:

Figure 2.6 shows scatter plots of metabolite measurements taken on the two scanners with a linear regression trend superimposed. The plots show the shift in absolute value of measurements taken on the Skyra scanner compared to the Allegra scanner. However, there does not appear to be a clear trend present in the data since the figures present a random scatter of points around the regression lines.

Figure 2.6: The relationship between the various concentrations measured within the MFGM using the Allegra and Skyra scanners.

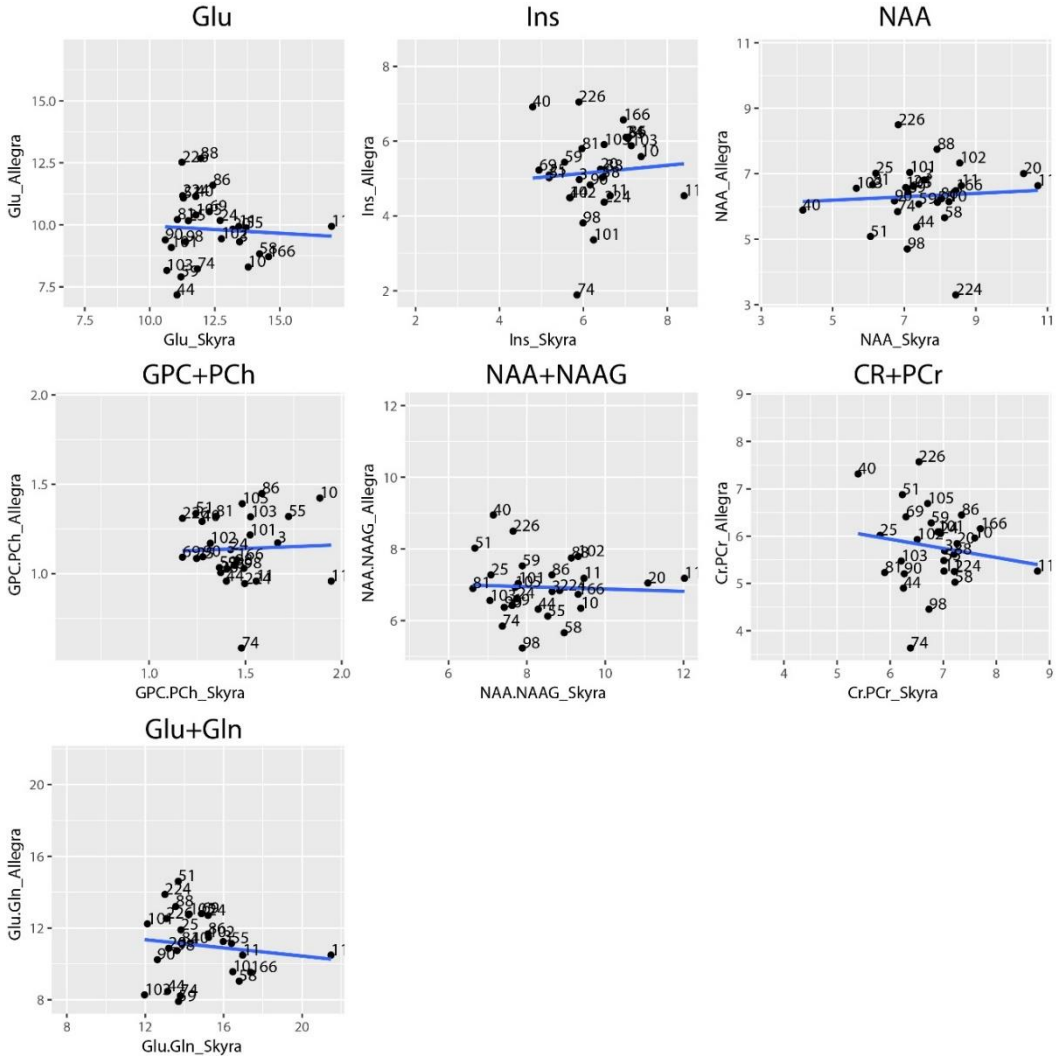

Table 2.4: Intercepts and slope coefficients for separate linear models of Allegra Concentration ~ Skyra Concentration of each metabolite in the MFGM region.

Metabolites		Estimate	Standard error	P-value
Glu	(Intercept)	10.555	2.259	0.0001
	Slope	-0.060	0.182	0.7458
Ins	(Intercept)	4.502	1.691	0.0134
	Slope	0.107	0.268	0.6945
NAA	(Intercept)	5.933	1.116	<0.0001
	Slope	0.052	0.147	0.7263
GPC	(Intercept)	1.078	0.295	0.0012
	Slope	0.042	0.202	0.8367
NAA.NAAG	(Intercept)	7.202	1.103	<0.0001
	Slope	-0.032	0.131	0.8085
Cr.PCr	(Intercept)	7.096	1.662	0.0002
	Slope	-0.194	0.244	0.4346
Glu.Gln	(Intercept)	12.723	2.554	<0.0001
	Slope	-0.114	0.173	0.5142

For all simple linear models looking at the relationship between the metabolite concentrations measured on the Allegra and Skyra scanners (Table 2.4) we see a significant intercept term, however none of the slope coefficients are significant. This means that any unit change in the concentration of metabolite measured using the Skyra scanner will have no consistent effect on the concentration measured by the Allegra scanner. As the concentrations measured on the Skyra scanner increase, we don't see a proportional increase or decrease in the concentrations measured using the Allegra scanner. Hence, the lack of significance for the slope coefficients indicate that the per-unit change in measurements for the two scanners are not related. The significant intercept terms indicate a significant overall shift in scale of measurements. Very similar results are seen for the PWM and BG regions of the brain (seen in Appendix A.2 - Tables A.2.1, A.2.3).

Table 2.5 contains the parameter estimates of the linear models explaining the relationship between the concentration of metabolites measured using the Allegra and Skyra scanners with added covariates.

Table 2.5: Intercepts and slope coefficients for separate linear models of Allegra Concentration ~ Skyra Concentration of each metabolite with various covariates in the MFGM region.

Metabolite		Estimate	Standard Error	P-value
Cr.PCr	Intercept	20.958	13.126	0.1278
	Slope	-0.211	0.295	0.4839
	Allegra GM%	-0.068	0.101	0.5100
	Skyra GM%	-0.044	0.071	0.5415
	Time Between Scans	1.31	1.826	0.4822
	HIV Status (HIV)	0.111	0.926	0.9062
GPC+PCh	Intercept	4.746	8.535	0.5850
	Slope	-0.189	0.268	0.4887
	Allegra GM%	-0.071	0.063	0.2717
	Skyra GM%	0.071	0.039	0.0894
	Time Between Scans	2.289	1.107	0.0533
	HIV Status (HIV)	0.445	0.567	0.4426
NAA	Intercept	17.303	11.536	0.1510
	Slope	-0.222	0.216	0.3177
	Allegra GM%	-0.061	0.082	0.4644
	Skyra GM%	-0.05	0.057	0.3926
	Time Between Scans	0.309	1.422	0.8302
	HIV Status (HIV)	0.245	0.746	0.7469
NAA.NAAG	Intercept	4.317	1.814	0.0286
	Slope	-0.242	0.225	0.2968
	Allegra GM%	-0.026	0.012	0.0525
	Skyra GM%	-0.007	0.008	0.4136
	Time Between Scans	0.076	0.206	0.7153
	HIV Status (HIV)	0.066	0.109	0.5544
Ins	Intercept	23.816	9.078	0.0172
	Slope	-0.095	0.225	0.6778
	Allegra GM%	-0.126	0.061	0.0533
	Skyra GM%	-0.059	0.049	0.2438
	Time Between Scans	0.312	1.075	0.7748
	HIV Status (HIV)	-0.303	0.572	0.6033
Glu	Intercept	23.233	8.193	0.0110
	Slope	-0.025	0.295	0.9344
	Allegra GM%	-0.155	0.055	0.0112
	Skyra GM%	-0.038	0.036	0.3088
	Time Between Scans	0.004	0.924	0.9966
	HIV Status (HIV)	-0.281	0.487	0.5714
Glu.Gln	Intercept	42.068	17.36	0.0261
	Slope	-0.081	0.275	0.7708
	Allegra GM%	-0.193	0.135	0.1689
	Skyra GM%	-0.131	0.088	0.1569
	Time Between Scans	-1.231	2.443	0.6204
	HIV Status (HIV)	-0.936	1.235	0.4585

The time between repeated scans does not appear to have a significant effect on the measured metabolites, with the exception of GPC+PCh. The Skyra GM% and Allegra GM% don't appear to have a large effect on measured concentrations, however the % GM measured for the Allegra observations did significantly affect the concentration of Glu measured (Table 2.5). Thus, this covariate should be included in later multivariate and longitudinal models to identify if any greater effect due to GM% can be detected. Across all metabolites measured HIV status had no detectable effect on the reading taken from the two scanners (Table 2.5).

Similar to the previous simpler linear models, the intercept terms remain significant while the Skyra Concentration slope does not (Table 2.5), except for the concentrations of NAA, Cr+PCr and GPC+PCh. Again, this shows that even while we have controlled for the relative GM%'s and the time between these scans, there still does not appear to be a consistent relationship between an increasing or decreasing concentration measured on the Allegra and Skyra scanners. However, the baseline values for four of the seven concentrations measured on the two scanners remains different. Again, these results are similar to those seen in the PWM and BG regions (seen in Appendix A.2 – Tables A.2.2, A.2.4).

2.3.5 Bland-Altman Analysis:

The Bland-Altman analysis allows one to investigate the relationship between the differences and the mean of two repeated observations. Hence, if an increasing or decreasing difference was related to an increasing mean, this would be apparent on the Bland-Altman plot.

Figure 2.7: Bland-Altman output for inter- and intra-scanner repeated observations in the MFGM region. These Bland-Altman plots show an average difference between observations (the bias) and a 95% CI around this difference, along with the actual differences seen.

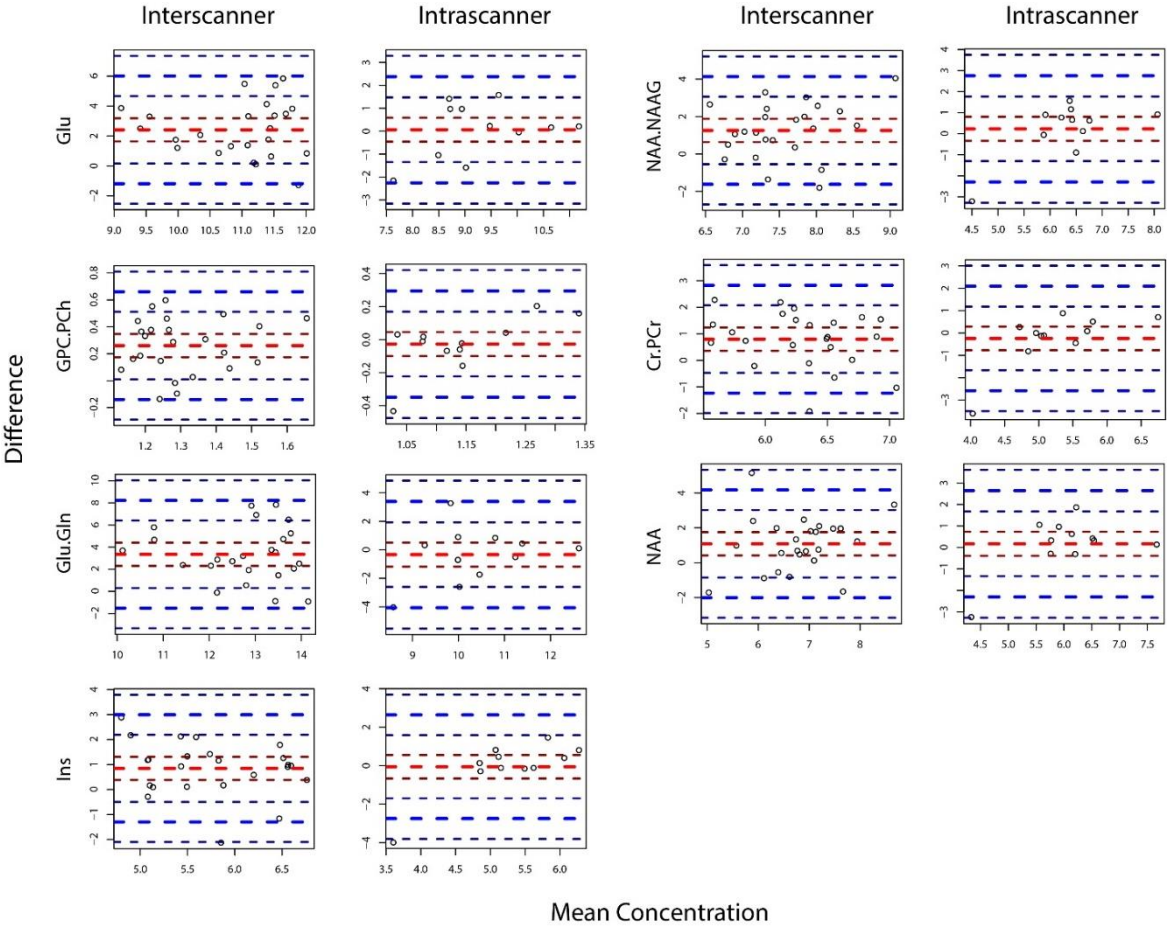

Figure 2.7 summarises the Bland-Altman analysis and shows that the differences between the observations don't appear to have any relationship with the mean concentrations of metabolites. Across all metabolites for both the inter- and intra-scanner differences appear random and hence we don't see a trend relating the values of the measured concentrations to the differences between the observations. This is also seen in the Bland-Altman plots for intra- and inter-scanner differences in the PWM and BG regions (Figures A.2.5 and A.2.10 in Appendix A.2).

2.3.6 Isolating scanner from age effects:

As previously mentioned, the average time between observations taken using the Allegra and Skyra machines at the age nine follow-up visit was 10.8 months. As brain metabolite concentrations have been shown to increase during development, the increase in concentrations seen across these two observations (Allegra at 'age 9' and Skyra at 'age 9') may be due to normal increases with age or may be due to the change in scanner.

Entirely separating these effects is difficult. One approach to visualise the scanner effect without the confounding due to age-related increases is described below. To remove the age effect from the data one must:

1. Using data from the 'age 9' follow-up visit regress:
$$Concentration_{Allegra} \sim Age$$
$$Concentration_{Skyra} \sim Age$$
2. Extract residuals from these models ($residuals_{Allegra}$ and $residuals_{Skyra}$ respectively),
3. Plot these residuals against one another to visualise the trends present within the data once the age effect has been removed.

Figure 2.8: The relationship between residuals from age adjusted concentrations (from the MFGM region) measured using the Allegra and Skyra machines at age nine.

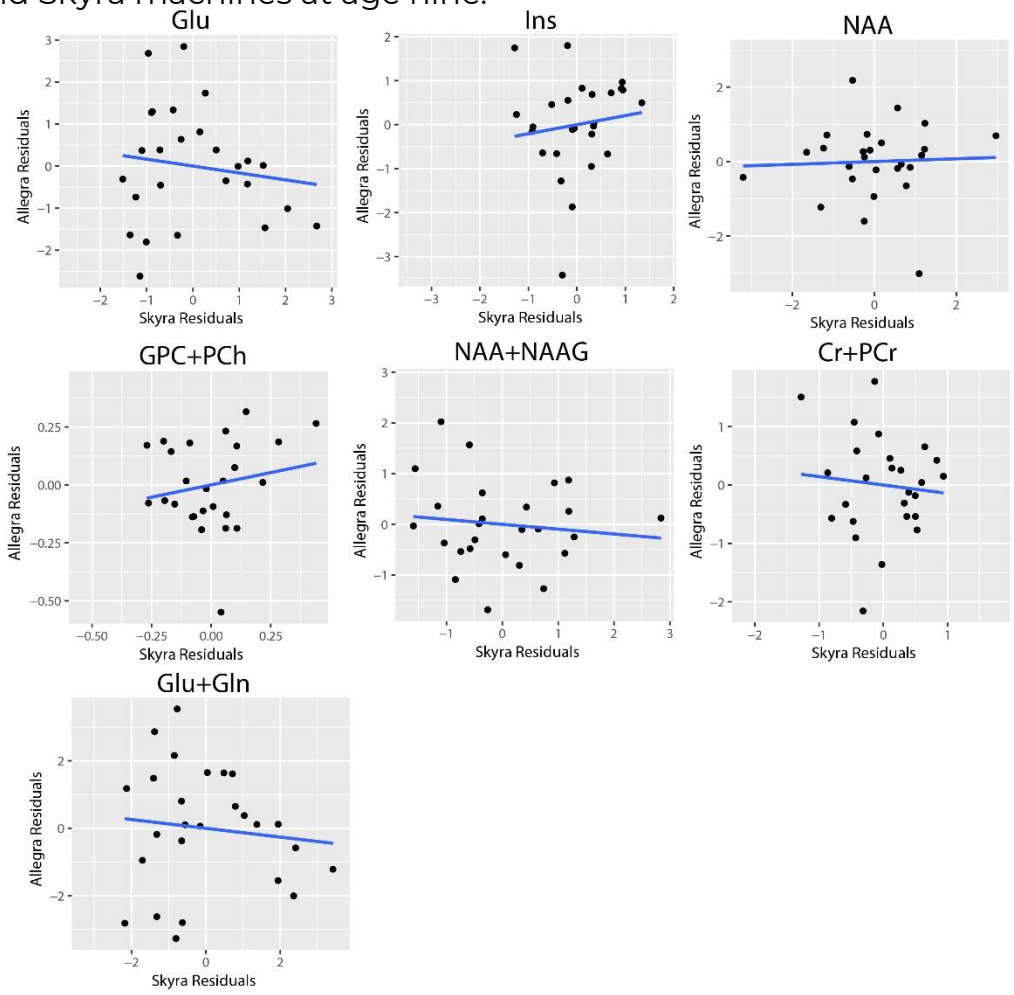

Figure 2.8 shows the plots of 'age-effect' removed residuals for Allegra against Skyra. For all metabolites we see a scatter about zero, with different scales for the Skyra and Allegra residuals. This shows that while the age effect definitely plays a role in the shift between observations taken across the two scanners at 'age 9', there is still a scanner effect present. Thus, in further analyses we will include a scanner effect covariate to ensure the scanner effect is adjusted for age and the age effect is adjusted for scanner.

2.4 Discussion:

The analysis presented in this chapter confirmed that there is clearly some variation present in the measured concentrations due to scanner. There is clearly a 'scanner effect' that must be accounted for in the proceeding longitudinal analyses to allow a fair profiling of the metabolite profiles over time. The weak relationship, or lack of significant relationship between unit changes in concentrations measured on the two scanners is of concern. However, at the very least future models will adjust for the difference in scale.

In addition, the analysis showed that the relative percentage of gray matter and white matter in each voxel should be included as a confounder as it appears to effect metabolite concentrations.

There are various approaches, one may employ to try compensate for the scanner effect, as mentioned in the introduction to this chapter. These approaches are summarised below and the final approach, the inclusion of scanner as a fixed effect in the linear mixed effect models, will be discussed further and implemented in the next chapter.

Approaches one may use when handling data from two different scanners:

A. <u>Use only data from the Allegra scanner:</u>
   You may choose to longitudinally analyse only the data from the first three time points and discard any data recorded using the Skyra scanner. Illustrated in Figure 2.9A, this approach is an easy solution to this problem, however it limits the analysis to changes between the ages of 5 and 9 and all information beyond this point is lost. The mixed effect model formulation of this approach would look like this:

$$Y_{\text{Allegra}_{ij}} = \beta_0 + \beta_1 \text{age}_{ij} + b_{0i} + \varepsilon_{ij}$$

   where:

   $Y_{\text{Allegra}_{ij}}$= the concentrations (from one metabolite within one region) measured using the Allegra scanner for subject i at time j,
   age_{ij} = the age of the child at the time the measurements were taken,
   b_{0i} = subject-specific random effect; $b_{0i} \sim N(0, {\sigma_b}^2)$,
   ε_{ij} = within subject error; $\varepsilon_{ij} \sim N(0, {\sigma_e}^2)$.

B. Use the data from the two scanners in two separate longitudinal analyses:
Another option is to perform two separate longitudinal analyses, one using the data acquired using the Allegra scanner and another using data recorded using the Skyra scanner (Figure 2.9B). This approach allows for separate inference in two age intervals, but form no formal comparison across age intervals. The formulation of this approach is as follows:

$$Ages\ 5-9: Y_{\text{Allegra}_{ij}} = \beta_0 + \beta_1 \text{age}_{ij} + b_{0i} + \varepsilon_{ij}$$

$$Ages\ 9-11: Y_{\text{Skyra}_{ij}} = \beta_0 + \beta_1 \text{age}_{ij} + b_{0i} + \varepsilon_{ij}$$

where:

$Y_{\text{Allegra}_{ij}}$ = the concentrations (from one metabolite within one region) measured using the Allegra scanner.

$Y_{\text{Skyra}_{ij}}$ = the concentrations (from one metabolite within one region) measured using the Skyra scanner.

C. Use either Allegra or Skyra scans at age 9:
Depicted in Figure 2.9C, one may also choose to only use the data acquired at age nine from one of the two scanners. This would assume any differences seen between the scanner change are entirely due to the age differences between these scans – which, based on our findings in this chapter, is not an entirely valid assumption to make. This may change the slope of the fit line as it is affected by the higher Skyra or lower Allegra measurements at age 9. We would need to appropriately decide whether to use the observations at age nine from the Skyra or Allegra scanner.

D. Use an average of the two scans at age 9:
An option is to take the observations at nominal age nine from the two different scanners and to average them, this is illustrated in Figure 2.9D. Hence, someone who has measurements from both scanners at age nine could have these two observations averaged to represent one measurement at age 9. This approach raises a few questions, such as: i) should observations from children at age 9 that were not repeated be kept in this model, or should all other observations at age 9 be discarded? ii) Should these average observations be assigned to an average age (an average of the ages from the first and second scans) and would this be a valid choice to make? Additionlly, this approach may resolve the problem of scanner effects at age nine, however the observations at age 11 will still have a bias present due to the scanner change.

E. Standardise the data using the mean and standard deviation from the control subjects:
Previous multi-centre studies mentioned using the mean and standard deviation from the control data (in this case the metabolite concentrations from HIV- subjects) to standardise the data at each time point. While this approach would remove the scanner effect from the data, it would also

remove any age effects which we are interested in observing (Figure 2.9E). The interpretation of models created using this standardised data would not be very useful as trends would be removed and effect sizes would be with respect to the standardised scale, not the observed metabolite concentration scales.

F. Include the scanner effect as a fixed effect in linear mixed effect models:
The final approach for resolving the bias due to scanner within the data, is to use the scanner as a fixed effect within the univariate and multivariate models. This approach is further described in chapter 3, but the key advantage is that it allows us to quantify and control for the scanner effect within each of the response variables, this is illustrated in Figure 2.9F. This method also allows all the data collected to be used in the modelling process. The formulation of this model is as follows:

$$Y_{ij} = \beta_0 + \beta_1 \text{age}_{ij} + \beta_3 \text{Scanner}_{ij} + b_{0i} + \varepsilon_{ij}$$

where:

Y_{ij} = the concentrations (from one metabolite within one region) measured,

Scanner_{ij} = the scanner used for the respective measurement (=0 for Allegra, =1 for Skyra).

Figure 2.8F illustrates the jump in scale due to the change in scanners at and immediately after age 9. The inclusion of the scanner effect does imply that the effect of age and HIV status will now be independent of the scanner effect. Should one wish to allow for different effects of age and HIV on concentrations for measurements taken on different scanners, it can be done through the inclusion of interaction terms.

Figure 2.9: Illustrations of the various approaches one may use to resolve scanner bias.

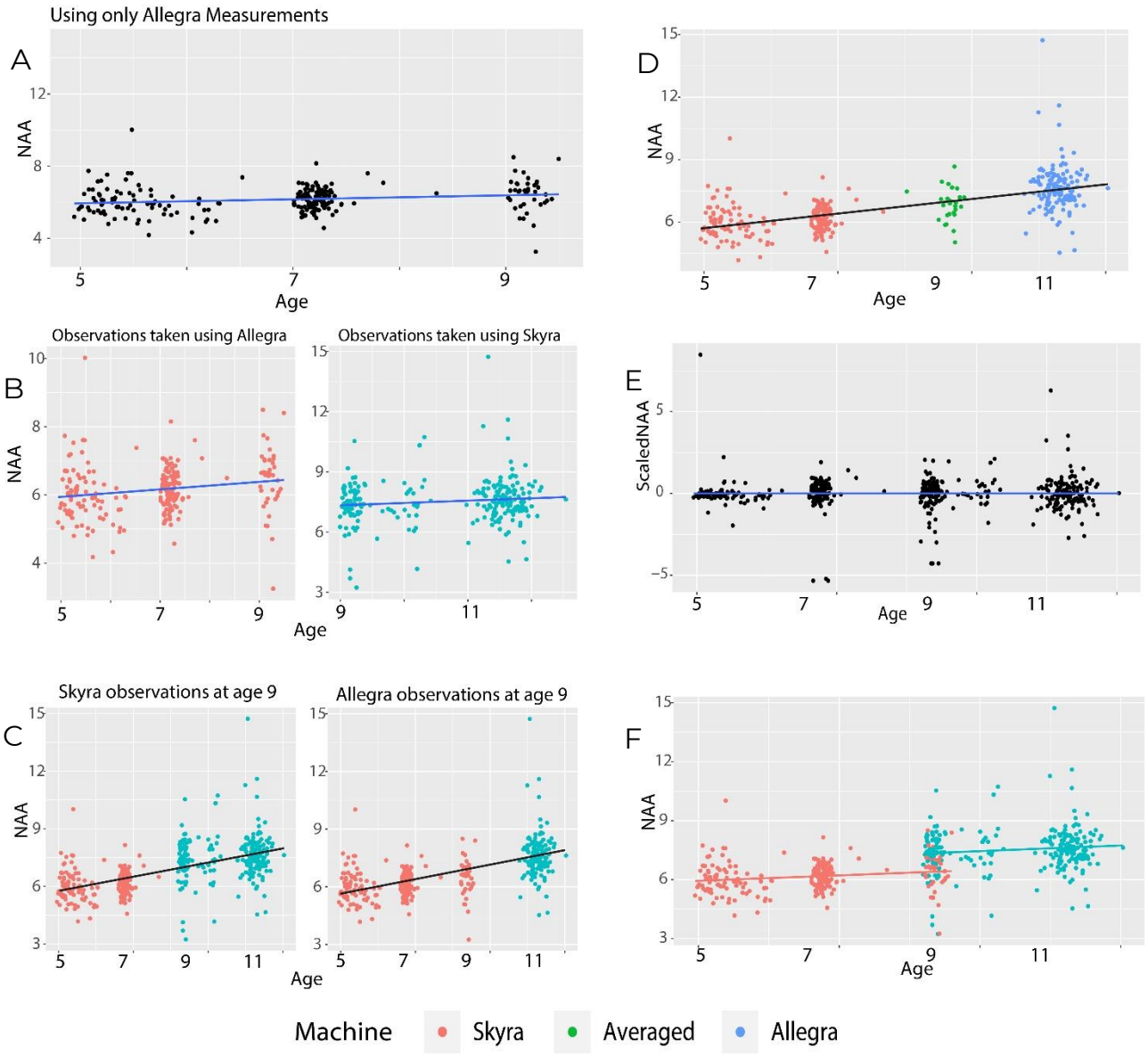

Chapter 3: Univariate Longitudinal Data Analysis

3.1 Background:

The principal goal of this dissertation is to determine longitudinal trends of seven metabolites within three regions of the brain, and to subsequently identify any effects the combination of HIV and antiretroviral treatment may have on these metabolites. We will not include any information on ART regimen within our analysis, however all HIV+ children are receiving treatment and thus what we refer to as 'HIV effects' are in fact differences between children who are HIV- and those that are HIV+ and subsequently are taking AR treatment.

Because our data contains repeated measurements from the same individuals, we do not have independent observations and hence, regular parametric analysis techniques are no longer valid. An option for analysing dependent repeated measures data is through the use of Mixed Effect Models (Pinheiro and Bates, 2006).

The key characteristic of Mixed Effect Models, and the means of accounting for the dependence between repeated observations from the same individual, is the inclusion of subject-specific random effects into the model. These random effects capture a subject's individual trend over time and hence the model can be used to observe subject-specific changes over time instead of only identifying population level changes. The inclusion of subject specific random effects also induces the correlation present in the repeated measures data, and will also describe the degree of variation present in the chosen population (Hedeker and Gibbons, 2006).

Figure 3.1: The hierarchical nature of our problem. Each subject has been scanned in three regions of their brain, at each scan the concentration of seven metabolites were recorded and this process was repeated at up to six different times at different ages or using different scanners.
* at these ages some children were scanned twice.

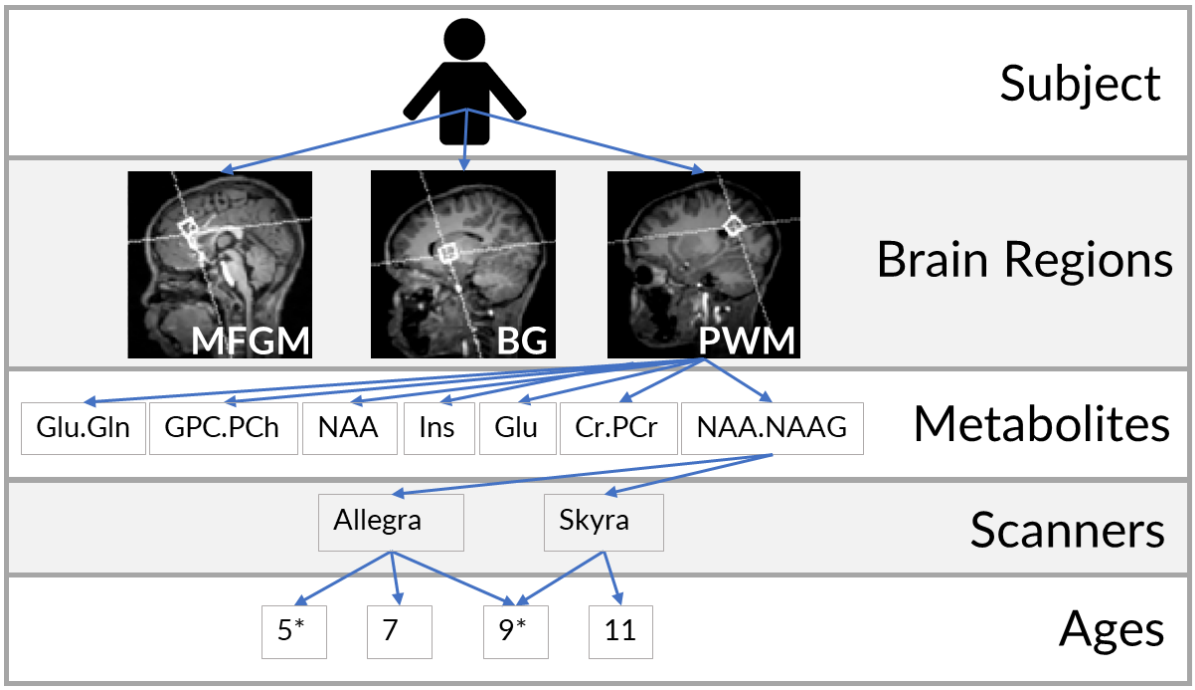

3.2 Methods:

A simple mixed effect formulation is as follows (Pinheiro and Bates, 2006):

$$y_{ij} = \mu + a_i + \varepsilon_{ij} \tag{3.1}$$

where:

$y_{ij} =$ response for subject i at measurement occasion j,
$\mu =$ overall mean,
$a_i =$ subject specific random effect, where $a_i \sim N(0; {\sigma_a}^2)$,
$\varepsilon_{ij} =$ within-subject error, where $\varepsilon_{ij} \sim N(0; {\sigma_e}^2)$,

and ε_{ij} and a_i are assumed to be independent.

This model formulation allows for an overall mean, subject specific deviations from the mean and occasion-specific deviations from the subject-specific mean as illustrated in Figure 3.2.

The inclusion of random effects means that for any factor that has repeated observations (in our case subject), a mean will be calculated for each element (for each subject) within that factor as illustrated in Figure 3.2. Hence, if multiple subjects have repeated measures of the same variable taken over time, those subjects will have their own subject specific mean variable response (this is displayed using the blue arrows below). The repeated measurements for each subject will have their own pattern of variation around the subject specific mean

(displayed with the smaller arrows that are colour specific to each subject). These subject specific means will then surround the true overall mean response for a factor.

Figure 3.2: Concept of Mixed Effect Models; inclusion of Random Effects for subjects results in individual means and population level means being identified. The observations are denoted using x_{ij} for each subject.

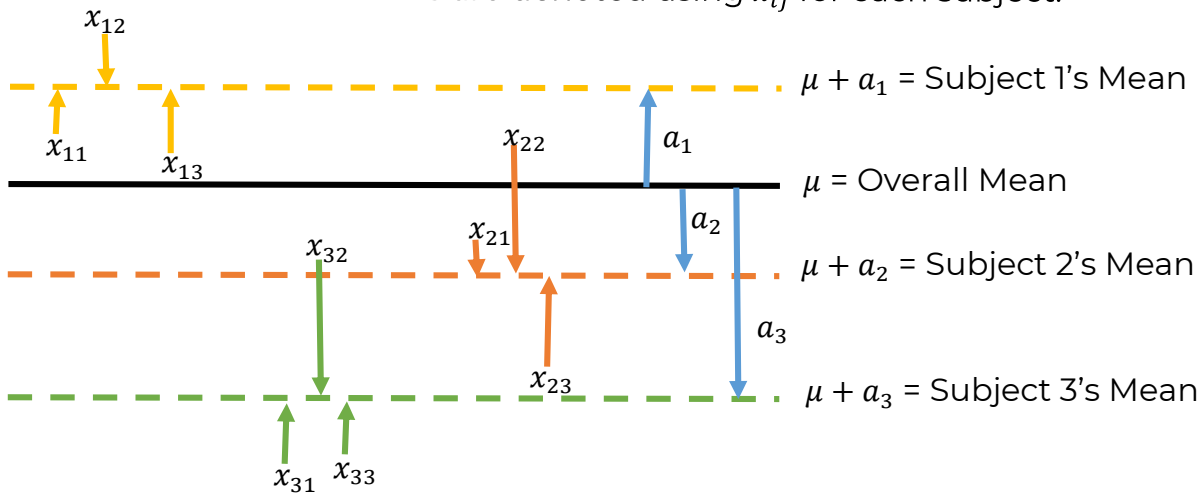

An advantage of mixed effect models is that subjects are not assumed to be measured at the same time points. This allows the use of actual ages instead of nominal ages at each observation and this means that subjects that were not observed at all time points of interest may be included in the analysis, thereby increasing the power of the study (Hedeker and Gibbons, 2006). This is a particularly useful characteristic in our case, as follow up has not been very consistent and only a two children have been scanned at all six scan times. Table 3.1 shows the number of children that were scanned between one and six times, we see a quarter of the children were only scanned once, with almost half of the children scanned three or four times. These children that were scanned six times were scanned twice at age five, once at age seven, twice at age nine and once at age eleven.

Table 3.1: Percentage of children followed up between one and six times.

Number Of Visits	Number	Percentage
1	44	25.29
2	20	11.49
3	37	21.26
4	42	24.14
5	29	16.67
6	2	1.15

3.2.1 Two Level Model for Longitudinal Data:

The more general mixed effect formulation is:

$$\boldsymbol{y}_i = \boldsymbol{X}_i\beta + \boldsymbol{Z}_i v_i + \varepsilon_i \quad (3.2)$$

$i = 1 \ldots . N$ individuals,
$j = 1 \ldots . n_i$ observations for individual i,

where:

$\boldsymbol{y}_i = [y_{ij}] = n_i \times 1$ response vector for individual *i*,
$\boldsymbol{X}_i = [x_{ij}] = n_i \times p$ design matrix for the fixed effects,
$\beta = p \times 1$ vector of unknown fixed parameters,
$\boldsymbol{Z}_i = [z_{ij}] = n_i \times r$ design matrix for the random effects,
$v_i = r \times 1$ vector of unknown random effects $\sim N(0, \boldsymbol{\Sigma}_v)$,
$\varepsilon_i = n_i \times 1$ error vector $\sim N(0, \sigma^2 \boldsymbol{I}_{n_i})$.

The mixed effect model can be formulated as a two-stage model that includes a between- and a within-subject model.

Within-Subjects Model (Level One):

The within-subject model describes the structure of the longitudinal profile structure of the responses. For example, for a linear trend:

$$y_{ij} = b_{0i} + x_{ij} b_{1i} + \varepsilon_{ij} \quad (3.3)$$

where both the intercept and slope is allowed to be subject-specific (Hedeker and Gibbons, 2006).

Between-Subjects Model (Level Two):

The between subject model further decomposes the level one model parameters into population average and subject specific components. For example:

$$\begin{aligned} b_{0i} &= \beta_0 + v_{0i} \\ b_{1i} &= \beta_1 \end{aligned} \quad (3.4)$$

This model shows that the *i*'th individual's initial concentration level b_{0i} is made up of two elements: i) the starting level for the population (β_0, the average for the population) and ii) the unique subject specific contribution, v_{0i}. In the above model we see that for all individuals' the effect size of x (the slope) is the same, all are equal to β_1. This is not always the case, we may also have a random effect added to this level and consider different slopes for each individual; the effect of which is illustrated in Figure 3.3 (Hedeker and Gibbons, 2006).

Figure 3.3: The theoretical expected relationships from (a) random intercepts model and (b) random intercept and slope model.

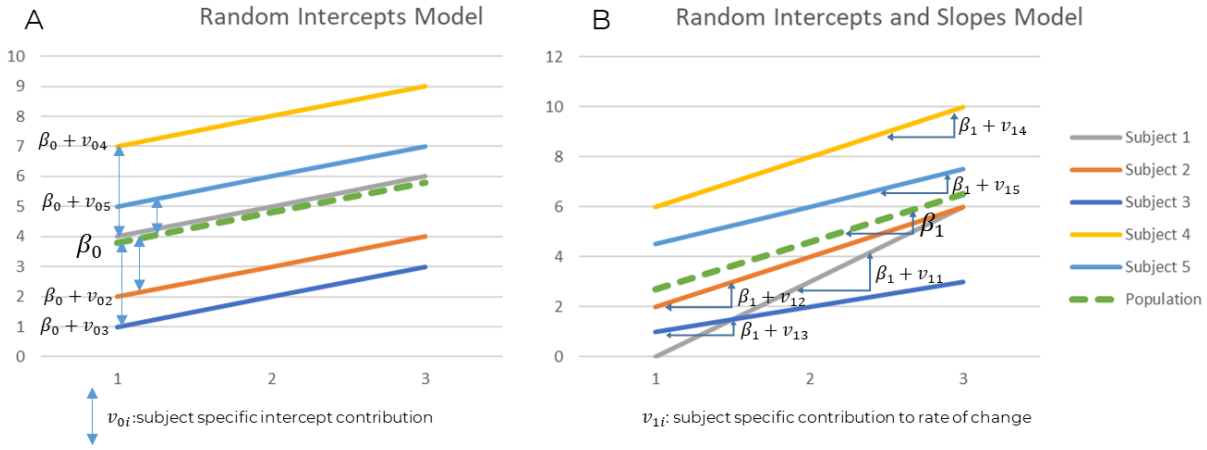

With the random intercepts model all subjects may have different starting levels of the response but the same rate of change of that response (Figure 3.3A). In contrast, the random intercepts and slope model allows subjects to have different starting levels as well as different rates of change (Figure 3.3B).

While we can allow for different intercepts and slopes across the different subjects, we can also allow these effects to vary by subject and occasion specific covariate values,

$$\begin{aligned} \beta_0 &= \alpha_{00} + \alpha_{01}X_1 + \alpha_{02}X_2 + \cdots + \alpha_{0p}X_p \\ \beta_1 &= \alpha_{10} + \alpha_{11}X_1 + \alpha_{12}X_2 + \cdots + \alpha_{1p}X_p \end{aligned} \tag{3.5}$$

where X_1 to X_p refer to the covariates chosen.

Fixed effects from model formulation 3.1 are modelled using:

$$\mu = \beta_0 + \beta_1 x_1 + \cdots + \beta_p x_p \tag{3.6}$$

This structure results in the estimates of:

$$E(y_{ij}) = \mu\,, \tag{3.7}$$

$$cov(y_{ij}, y_{ik}) = {\sigma_a}^2, \tag{3.8}$$

which is the covariance between observations from one subject. This is equal to ${\sigma_a}^2$ as the inclusion of random effects imposes a nonzero covariance between observations from the same subject.

In constrast the covariance of observations between individuals:

$$cov(y_{ij}, y_{mj}) = 0, \tag{3.9}$$

these observations are independent and hence the covariance is zero.

Thus,

$$var(y_{ij}) = {\sigma_a}^2 + {\sigma_e}^2 \tag{3.10}$$

and finally, the within subject covariance matrix is:

$$var(y_{ij}) = \begin{bmatrix} {\sigma_a}^2 + {\sigma_e}^2 & {\sigma_a}^2 & {\sigma_a}^2 \\ {\sigma_a}^2 & {\sigma_a}^2 + {\sigma_e}^2 & {\sigma_a}^2 \\ {\sigma_a}^2 & {\sigma_a}^2 & {\sigma_a}^2 + {\sigma_e}^2 \end{bmatrix}. \quad (3.11)$$

Hence, the inclusion of random effect terms within a mixed effect model imposes an exchangeable (constant nonzero) correlation structure on y_{ij}.

The basic linear mixed effect model thus imposes the exchangeable correlation structure and further assumes the within group errors are identically distributed random variables with a mean of zero and constant variance (Pinheiro and Bates, 2006). However, we often encounter data that contains heteroscedasticity (unequal variance) or within group correlation that differs from an exchangeable structure (Pinheiro and Bates, 2006). The basic model can be extended to allow for a different covariance or correlation structure of these within-group errors. Initially the within-group errors followed the $\varepsilon_i \sim N(0, \sigma^2 I_{n_i})$ distribution (i.i.d.) but we can relax this to $\varepsilon_i \sim N(0, \sigma^2 \boldsymbol{\Lambda_i})$ where $\boldsymbol{\Lambda_i}$ is a positive definite matrix defining the imposed structure.

The $\boldsymbol{\Lambda_i}$ can be decomposed into three parts:

$$\boldsymbol{\Lambda_i} = \boldsymbol{V_i C_i V_i}\ , \quad (3.12)$$

where $\boldsymbol{C_i}$ is a correlation matrix with all diagonal elements equal to one and $\boldsymbol{V_i}$ is a diagonal matrix that is not uniquely defined (any of its rows may be multiplied by -1 and the same decomposition will be obtained).

It can be shown that:

$$\begin{aligned} \text{Var}\ (\varepsilon_{ij}) &= \sigma^2\ [\text{V}_i]_{jj} \\ \text{cor}\ (\varepsilon_{ij}, \varepsilon_{jk}) &= [\text{C}_i]_{jk} \end{aligned} \quad (3.13)$$

Hence, $\boldsymbol{V_i}$ describes the variance and $\boldsymbol{C_i}$ describes the correlation of the within-group errors. This decomposition allows us to easily define these structures and account for the patterns in within-group error (Pinheiro and Bates, 2006).

3.2.2 Multiple Testing:

The nature of our data structure results in the creation of 21 separate linear mixed effect models that investigate metabolites changes in the seven different metabolites in each of the three regions separately (structure seen in Figure 3.1). Each model has on average five covariates that are being tested for significance and we have 21 models, this resulting in 105 hypothesis tests in this section alone. We know this is a problem as the more tests we complete the more likely we are to include Type I errors in the subsequent analysis. We need to use an adjustment method to correct for these multiple comparisons and we have chosen to use the Holm adjustment. This method is also known as the Holm's Sequential Bonferroni Procedure and involves adjusting the alpha value for each test depending on the

rank of the p-values (Holm, 1979). The steps to perform the Holm adjustment are as follows:

1. Rank all p-values from smallest to largest.
2. Use the formula $h = \frac{\alpha}{n-r+1}$ (where n is the number of tests, r is the rank of that value and α is the significance value) to calculate a new significance cut-off value (*h*).
3. If the p-value is smaller than *h*, then reject the null hypothesis for that test and move on to the next ranked p-value.
4. Repeat the above steps changing r for each new p-value.
5. Once the p-value is greater than *h*, accept the null hypothesis for that specific test and all subsequent tests with a lower ranked p-value.

Thus, instead of comparing all tests to the standard significance value of 0.05, we use adjusted significance values specific to the rank of each p-value. This means the new significance values will be $\frac{\alpha}{n}, \frac{\alpha}{n-1}, \frac{\alpha}{n-2}, \ldots, \frac{\alpha}{1}$ for the respectively ranked p-values (Holm, 1979).

From this approach it follows that instead of adjusting α one may adjust the p-values, which is what we have chosen to do. This is done using the following formula:

$$q_i = (n - r + 1)p_j \tag{3.14}$$

q_i is then compared to the chosen unadjusted level of α (Aickin and Gensler, 1996; Wright, 1992). This is also done sequentially (starting with the smallest p-values) and when a non-significant result is found the procedure ends. Hence, not all p-values will be adjusted, for example those that were non-significant to start with will be unchanged (Wright, 1992).

The *p.adjust* function with the "*Holm*" method from the *stats* package in R (RStudio Team, 2018) was used to calculate these adjusted p-values.

3.2.3 Possible Covariates of Interest:

Equation 3.5 suggests the inclusion of various covariates to help understand the factors effecting metabolite concentrations within the brain. Previous studies involving the brain development of HIV+ children have also looked at the effects of exposure to HIV (Kerr et al., 2014; Rie et al., 2008; Robertson et al., 2018). We have selected to focus on comparing HIV+ to HIV- children. This was chosen as comparing the three groups of HIV+, HEU and HUU requires the use of dummy variables and a reference category must be appropriately chosen. This complicates interpretation slightly. We also avoided this approach as it also causes the control group to be subsetted into even smaller groups. While we focus on comparing HIV+ and HIV- children, we have also included a brief investigation of the effects of the exposure groups on metabolite concentrations.

Other covariates considered in previous MRS studies include race and gender (Harezlak et al., 2011; Holmes et al., 2017; Robertson et al., 2018). Our cohort is predominantly made up with children that are Mixed-Race and Black Africans. The proportions of these groups are not entirely even across the control and HIV+ groups (Table 3.2). Hence, it is important to investigate potential confounding due to race and gender. Accordingly, we have chosen to explore the effect of these groups on the metabolite concentrations we have recorded and these results are presented in Appendix A.3.

Table 3.2: Summary statistics of additional potential confounding variables.

	Overall	**HIV + (n=89)**	**HIV – (Exposed) (n=42)**	**HIV – (Unexposed) (n=43)**
Race (% African)	85.06	88.76	97.62	65.12
Gender (% Female)	46.55	51.69	38.10	44.19

We can summarise all possible covariates we considered including in the univariate models:

- Age,
- HIV Status,
  - HIV+ vs HIV- OR
  - HIV+ vs HIV- exposed (HEU) vs HIV- unexposed (HUU).
- Relative GM% or -WM%,
- Scanner,
- Race,
- Gender.

3.2.4 Model Selection:

As previously mentioned, this chapter focuses on the univariate modelling approach whereby a separate model is created for each metabolite measured in each region. The aim of these models is to identify any relationship between the respective brain metabolite level and HIV status in children over time, and to account for any confounding variables.

The mixed effect models were initially constructed with the most basic model. This model includes the key covariate we are interested in: HIV status, scanner to ensure the scanner effect is considered and age to identify the time between the repeated metabolite measurements. These covariates were included as fixed effects and we also incorporated subject specific random effects. Individual models were created for each region of the brain and each metabolite, hence 21 models were created and investigated.

The basic starting model is defined as:

$$Y_{ij} = \beta_0 + X_i^T \beta_j + b_{0i} + \varepsilon_{ij} \quad (3.15)$$

where:

Y_{ij} = metabolite concentration from subject i at occasion j,

$X_i^T \beta_j = \beta_1 X_{1ij} + \beta_2 X_{2ij} + \beta_3 X_{3i}$

where:

X_{1ij} = the age of child i at occasion j,

X_{2ij} = the scanner the measurement was taken on,

X_{3i} = the HIV status of the child.

$b_{0i} \sim N(0; {\sigma_b}^2)$,

$\varepsilon_{ij} \sim N(0; {\sigma_e}^2)$.

Using the forward stepwise model building procedure we looked at the effect of including the relative GM% or -WM%, race, gender and various interaction terms. With this approach, we started with the basic model containing HIV status and age as covariates as these are key factors we know we want included within our models. One by one potential covariates were added to the model and using AIC values model fit was assessed. If a covariate improved model fit and had a significant effect on the metabolite concentration it was incorporated into the model. If not, the next covariate was considered for inclusion.

We consistently saw relative GM% or -WM% to have a significant effect and accordingly it was introduced into each of the models. Including race or gender did not improve the any model fit and hence was not introduced into the model (effect sizes and significance can be seen in Appendix A.3). The age*HIV status and age*scanner interaction terms were included into some of the models where we saw improvements in model fit.

The final model below was found to best describe most metabolites, with a few deviations depending on model fit:

$$Y_{ij} = \beta_0 + X_i^T \beta_j + b_{0i} + \varepsilon_{ij} \quad (3.16)$$

where:

Y_{ij} = the metabolite concentration from subject i at occasion j,

$X_i^T \beta_j = \beta_1 X_{1ij} + \beta_2 X_{2ij} + \beta_3 X_{3i} + \beta_4 X_{4ij} + \beta_5 X_{1ij} * X_{3i} + \beta_6 X_{1ij} * X_{2ij}$

where:

X_{1ij} = the age of child i at occasion j,

X_{2ij} = the scanner the measurement was taken on,

X_{3i} = the HIV status of the child,

X_{4ij} = the relative percentage of GM or WM in the voxel for each measurement,

β_5 = the interaction effect between age at each scan and HIV status,

β_6 = the interaction effect between age at each scan and the scanner used for concentration measurement.

$b_{0i} \sim N(0; {\sigma_b}^2)$,

$\varepsilon_{ij} \sim N(0; {\sigma_e}^2)$.

The model with the lowest AIC that also included the key variables (age, and HIV status) was chosen as the best fitting model and was subsequently validated. Model validation involved ensuring that both within and between subject residuals followed a normal distribution and any outlying observations were identified. The residuals were also plotted against the fitted values and any abnormal structures were identified and used as an indication to define variance and correlation structures for the model.

The model building approach was repeated separately for each metabolite in each region of the brain. Following the model building procedure, the Holm adjustment was used to adjust the p-values for multiple testing.

All mixed effect models were fit using the *lme* function from the *nlme* (Pinheiro et al., 2019) package in R (RStudio Team, 2018).

3.2.5 HIV Exposure Models:

To briefly explore the effects of HIV exposure on the relative metabolite concentrations, we used the final models from the previous section but incorporated the HIV effect as a three-level categorical variable, modelled using two dummy variables.

This model is the same as 3.9, however HIV status has been replaced with HIV exposure:

$$Y_{ij} = \beta_0 + X_i^T \beta_j + b_{0i} + \varepsilon_{ij} \quad (3.17)$$

where:

Y_{ij} = the metabolite concentration from subject i at occasion j,

$X_i^T \beta_j = \beta_1 X_{1ij} + \beta_2 X_{2ij} + \beta_3 X_{3i} + \beta_4 X_{4i} + \beta_5 X_{5ij} + \beta_6 X_{1ij} * X_{3i} + \beta_7 X_{1ij} * X_{4i} + \beta_8 X_{1ij} * X_{2ij}$

where:

X_{1ij} = the age of child i at occasion j,

X_{2ij} = the scanner the measurement was taken on,

X_{3i} = HIV- vs HIV+ unexposed (HUU) (0=HIV+, 1=HUU),

X_{4i} = HIV- vs HIV+ exposed (HEU) (0=HIV+, 1=HEU),

X_{5ij} = the relative percentage of GM or WM in the voxel for each measurement,

β_6 = the interaction effect between age at each scan and HIV+ vs HUU,

β_7 = the interaction effect between age at each scan and HIV+ vs HEU,

β_8 = the interaction effect between age at each scan and the scanner used for concentration measurement.

$b_{0i} \sim N(0; {\sigma_b}^2)$,

$\varepsilon_{ij} \sim N(0; {\sigma_e}^2)$.

The exposure variables are categorical, accordingly dummy variables are used during this modelling process, with respect to HIV positive as the reference category. However, we did repeat this with HEU as the reference to identify the effects of HEU vs HUU.

3.3 Results:

3.3.1 Exploratory Analysis:

Figure 3.4 illustrates the difference in measurement scales across the different metabolites. These metabolites are present in different concentrations because of the variations in efficacy and activity of each of these metabolites in each of these regions.

Figure 3.4: Ranges of metabolite concentration over the entire observation period in the MFGM region.

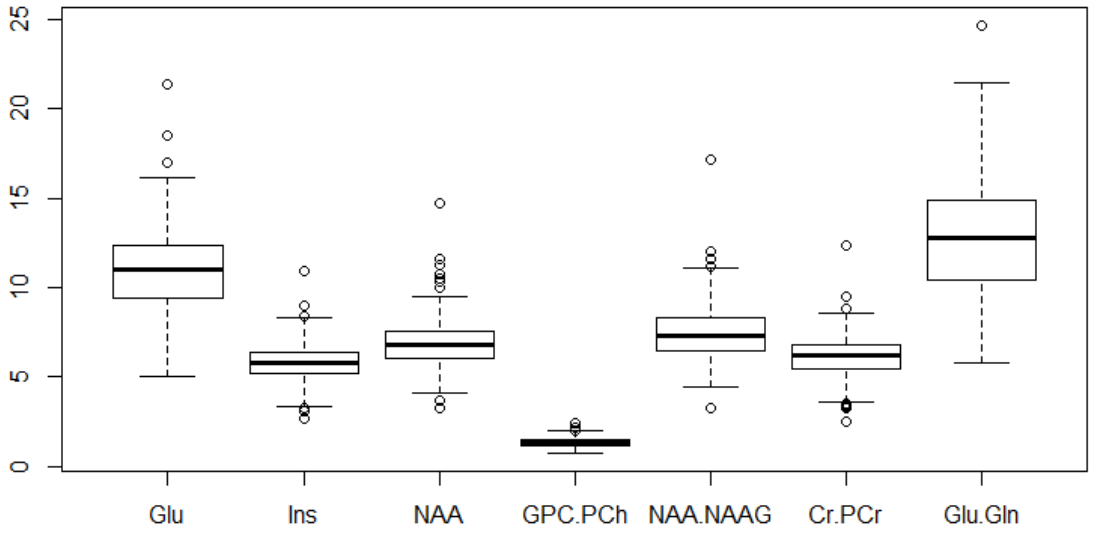

These metabolite concentrations were not standardised as a key focus of this research is the longitudinal profiling of these metabolites. If we had standardised these concentrations, we would not be able to interpret the direct effect sizes of the covariates, but instead it would be interpreted as some effect on the standardised concentration, which is not very intuitive and is less useful.

Figure 3.5 – 3.7 show scatterplots of the metabolite concentrations versus age with linear trends stratified by HIV status superimposed for the three different regions respectively.

Figure 3.5: The concentrations of individual metabolites measured over time in the peritrigonal white matter voxel of the brain coded by HIV status (pink = HIV negative; blue = HIV positive).

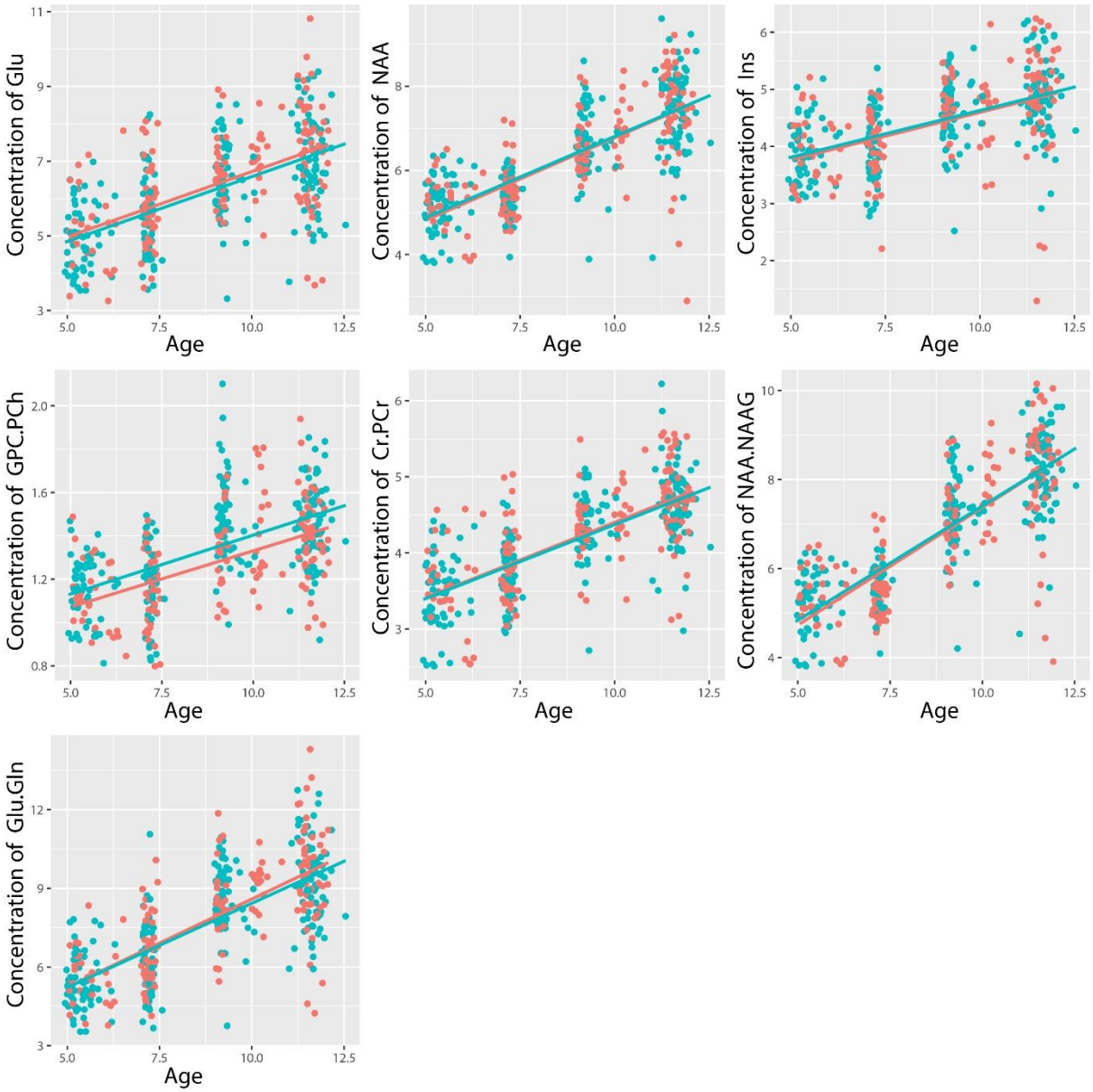

From Figure 3.5 we can see that in the PWM there is no obvious effect of HIV status on the Glu, Ins, NAA, NAA+NAAG, Cr+PCr and Glu+Gln metabolite levels. We do however see that GPC+PCh appears to have a group difference between the HIV status groups, where HIV positive subjects have a greater level of GPC+PCh compared to the HIV negative controls. We see reasonably large variability in the metabolite concentration levels at each age point for each metabolite. This further supports the fact that there is a large amount of inter-subject variability. The range of concentrations at age eleven appears to be greater than most other ages for every metabolite.

Figure 3.6: The concentrations of metabolites measured over time in the Mid-Frontal Gray Matter Region of the brain separated by HIV status (pink = HIV negative; blue = HIV positive).

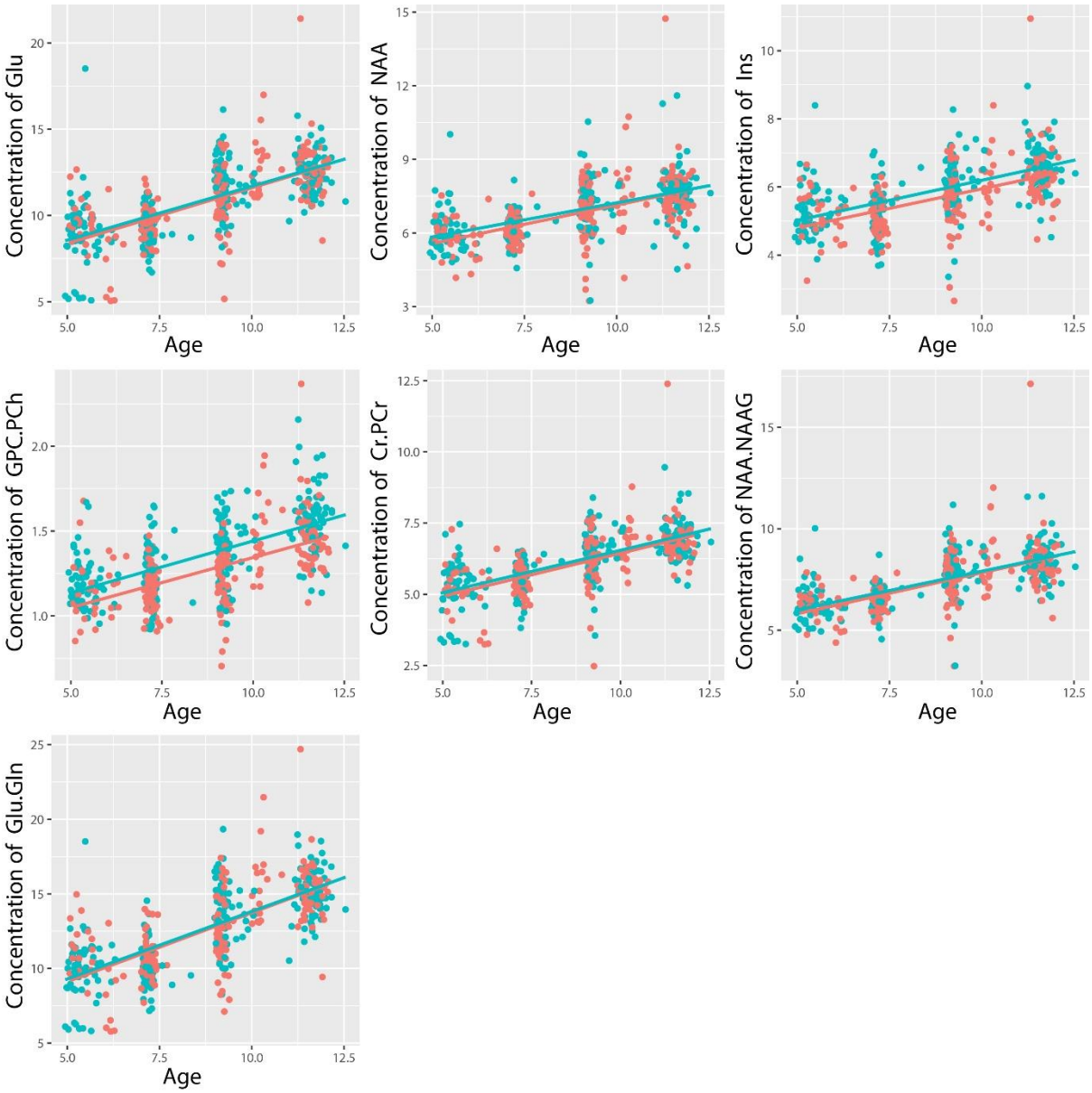

Figure 3.6 shows similar results where most metabolite concentrations appear to be unaffected by HIV status in the MFGM, except for Ins and GPC+PCh which appear to have some group effect. For both Ins and GPC+PCh the HIV positive group appears to have a greater metabolite concentration compared to the HIV negative subjects. The variability of metabolite concentrations around these four observation periods appears to be smaller than the variability seen in the PWM region. Here the values appear to be somewhat more clustered around the mean concentration than the observations from the other two regions. The recorded %SD for the metabolites measured within this region is also slightly smaller than that of the other two regions.

Figure 3.7: The concentrations of metabolites measured over time in the Basal Ganglia Region of the brain separated by HIV status (pink = HIV negative; blue = HIV positive).

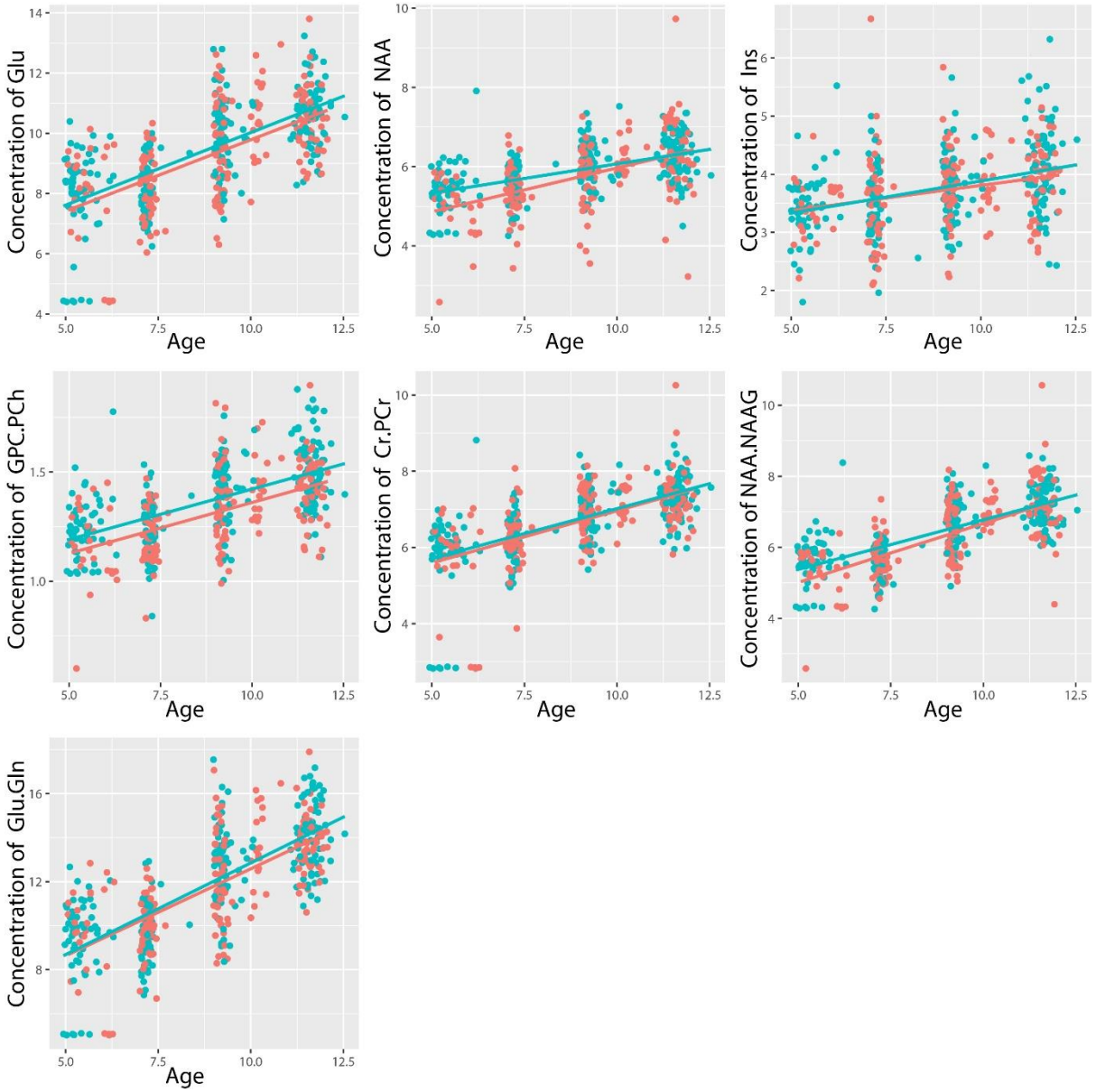

In the BG region we see the first possible group- time effect in the concentration of NAA (Figure 3.7). Again, there appears to be a group effect for the concentration of GPC+PCh. An increased concentration of GPC+PCh in HIV positive subjects appears to be conserved across all regions of the brain. Again we see a smaller amount of variability about the mean concentration when compared to observations from the PWM region, but a greater variability than observations from the MFGM region of the brain. The decreased variability in these regions will translate to increased power in analysis thereof.

3.3.2 Univariate Longitudinal Mixed Effect Models:

This section presents the results for the univariate models for each metabolite within each region. All of the models were created using the same approach: a forward stepwise building procedure, starting with the key covariates and adding in those that improve model fit or were significantly effecting the response variable. In most cases we see that the relative GM or WM percentage has a significant effect on the response variable, which we can understand as these different regions have different activities and hence different metabolite concentrations. We also saw that the interaction between HIV status and age seldom improved model fit and hence, was seldom included in the final models. The Age*Machine interaction term was significant for some metabolites which allows a different slope for metabolite level increases over time given the two different scanners (Figure 3.8). Almost all metabolites showed an increase over time and were significantly affected by the change in scanner. The fixed effect estimates are shown in tables 3.3 to 3.5 and estimates of the variance components are given in table 3.6.

A large effect on Glu levels in the MFGM comes from the relative percentage of GM which has an effect size of 6.77, thus the greater the concentration of GM% in the voxel the greater the concentration of Glu. This is supported by the effect size of -5.34 in the PWM for relative % of white matter. Hence, an increase in white matter (and thus a decrease of gray matter) in the voxel causes a decrease in Glu concentration. We see this again in the BG region and a one-unit increase in relative GM % leads to a 5.9 increase in the concentration of Glu. Another large effect on Glu concentrations was that of scanner where we see in all three regions the Skyra scanner lead to about a 2 unit increase in metabolite concentration, compared to the Allegra scanner.

An increase in one unit of % GM leads to a 1.4 unit increase in Ins concentration in the MFGM, a 3.2 unit increase in the BG and the increase of WM% leads to a 0.5 decrease in the PWM concentration of Ins. In the MFGM we also see a significant effect of HIV on Ins levels, HIV positive children have on average a 0.21 increase in Ins compared to HIV negative controls. This relationship was not conserved in the PWM and BG regions.

NAA concentration is also significantly affected by the Relative GM%, where a one unit increase leads to a 5.1 unit increase in NAA concentrations in the MFGM, but a 0.1 decrease in the NAA concentration in the BG and an increase in white matter leads to a 2.8 unit decrease in NAA concentration in the PWM region. Hence, here we don't see a clear positive or negative relationship with GM% in the voxel and NAA concentration as with the Glu and Ins concentrations.

In the BG region we see that HIV status and the HIV Status*Age interaction both have significant effects on NAA concentration, showing a larger concentration at younger ages for the HIV positive children with lower concentration of NAA after age 11 on average.

Table 3.3: Final Mixed effect models for each metabolite measured in the Peritrgonal White Matter region.

Metabolite		Estimate	Standard Error	P-value	Adjusted P-value
Glu	Intercept	9.399	0.367	<0.0001	<0.0001
	Age	0.238	0.065	0.0003	0.0167
	Machine (Skyra vs Allegra)	1.733	0.319	<0.0001	<0.0001
	Status (HIV+ vs HIV-)	-0.168	0.100	0.0938	1.0000
	Relative WM %	-5.335	0.415	<0.0001	<0.0001
	Age*Machine	-0.191	0.082	0.0203	0.7325
Ins	Intercept	4.278	0.242	<0.0001	<0.0001
	Age	0.050	0.025	0.0409	1.0000
	Machine (Skyra vs Allegra)	0.609	0.114	<0.0001	<0.0001
	Status (HIV+ vs HIV-)	0.023	0.079	0.7728	1.0000
	Relative WM %	-0.499	0.276	0.0722	1.0000
NAA	Intercept	7.261	0.284	<0.0001	<0.0001
	Age	0.211	0.031	<0.0001	<0.0001
	Machine (Skyra vs Allegra)	0.901	0.144	<0.0001	<0.0001
	Status (HIV+ vs HIV-)	0.018	0.081	0.8299	1.0000
	Relative WM %	-2.785	0.324	<0.0001	<0.0001
GPC.PCh	Intercept	0.777	0.065	<0.0001	<0.0001
	Age	0.004	0.007	0.5648	1.0000
	Machine (Skyra vs Allegra)	0.273	0.031	<0.0001	<0.0001
	Status (HIV+ vs HIV-)	0.059	0.022	0.0072	0.3143
	Relative WM %	0.406	0.075	<0.0001	<0.0001
NAA.NAAG	Intercept	7.281	0.306	<0.0001	<0.0001
	Age	0.156	0.053	0.0035	0.1740
	Machine (Skyra vs Allegra)	0.786	0.261	0.0029	0.1490
	Status (HIV+ vs HIV-)	-0.005	0.085	0.9542	1.0000
	Relative WM %	-2.579	0.345	<0.0001	<0.0001
	Age*Machine	0.172	0.067	0.0107	0.4158
Cr.PCr	Intercept	5.457	0.156	<0.0001	<0.0001
	Age	0.125	0.027	<0.0001	0.0003
	Machine (Skyra vs Allegra)	0.744	0.130	<0.0001	<0.0001
	Status (HIV+ vs HIV-)	-0.036	0.045	0.4243	1.0000
	Relative WM %	-2.432	0.176	<0.0001	<0.0001
	Age*Machine	-0.065	0.033	0.0549	1.0000
Glu.Gln	Intercept	10.448	0.487	<0.0001	<0.0001
	Age	0.365	0.087	<0.0001	0.0021
	Machine (Skyra vs Allegra)	3.125	0.428	<0.0001	<0.0001
	Status (HIV+ vs HIV-)	-0.234	0.130	0.0726	1.0000
	Relative WM %	-6.010	0.549	<0.0001	<0.0001
	Age*Machine	-0.265	0.110	0.0161	0.5988

Table 3.4: Final Mixed effect models for each metabolite measured in the Mid-Frontal Gray Matter.

Metabolite		Estimate	Standard Error	P-value	Adjusted P-value
Glu	Intercept	2.724	1.722	0.1146	1.0000
	Age	0.125	0.057	0.0285	0.9675
	Machine (Skyra vs Allegra)	2.487	0.248	<0.0001	<0.0001
	Status (HIV+ vs HIV-)	-0.115	0.140	0.4133	1.0000
	Relative GM %	6.770	1.829	0.0003	0.0148
Ins	Intercept	3.707	0.862	<0.0001	0.0015
	Age	0.040	0.037	0.2752	1.0000
	Machine (Skyra vs Allegra)	0.242	0.248	0.3290	1.0000
	Status (HIV+ vs HIV-)	0.213	0.078	<0.0001	0.3103
	Relative GM %	1.415	0.914	0.1225	1.0000
	Age*Machine	0.116	0.053	0.0296	0.9783
NAA	Intercept	1.078	1.129	0.3405	1.0000
	Age	0.085	0.037	0.0231	0.8083
	Machine (Skyra vs Allegra)	0.999	0.161	<0.0001	<0.0001
	Status (HIV+ vs HIV-)	0.073	0.095	0.4446	1.0000
	Relative GM %	5.105	1.199	<0.0001	0.0017
GPC.PCh	Intercept	1.082	0.188	<0.0001	<0.0001
	Age	-0.001	0.008	0.8708	1.0000
	Machine (Skyra vs Allegra)	-0.029	0.052	0.5759	1.0000
	Status (HIV+ vs HIV-)	0.092	0.020	<0.0001	0.0007
	Relative GM %	0.057	0.200	0.7763	1.0000
	Age*Machine	0.055	0.011	<0.0001	0.0001
NAA.NAAG	Intercept	3.058	1.150	0.0082	0.3368
	Age	0.109	0.038	0.0046	0.2251
	Machine (Skyra vs Allegra)	1.401	0.166	<0.0001	<0.0001
	Status (HIV+ vs HIV-)	0.002	0.092	0.9797	1.0000
	Relative GM %	3.360	1.221	0.0063	0.2948
Cr.PCr	Intercept	2.680	0.867	0.0022	0.1176
	Age	0.142	0.029	<0.0001	0.0001
	Machine (Skyra vs Allegra)	0.770	0.125	<0.0001	<0.0001
	Status (HIV+ vs HIV-)	0.046	0.071	0.5192	1.0000
	Relative GM %	2.606	0.921	0.0050	0.2383
Glu.Gln	Intercept	3.801	2.100	0.0713	1.0000
	Age	0.212	0.069	0.0022	0.1177
	Machine (Skyra vs Allegra)	3.509	0.299	<0.0001	<0.0001
	Status (HIV+ vs HIV-)	-0.200	0.180	0.2680	1.0000
	Relative GM %	6.677	2.231	0.0030	0.1525

Table 3.5: Final Mixed effect models for each metabolite measured in the Basal Ganglia.

Metabolite		Estimate	Standard Error	P-value	Adjusted P-value
Glu	Intercept	4.299	0.587	<0.0001	<0.0001
	Age	0.106	0.052	0.0414	1.0000
	Machine (Skyra vs Allegra)	2.100	0.228	<0.0001	<0.0001
	Status (HIV+ vs HIV-)	0.029	0.134	0.8316	1.0000
	Relative GM %	5.934	0.891	<0.0001	<0.0001
Ins	Intercept	1.311	0.284	<0.0001	0.0004
	Age	0.102	0.024	<0.0001	0.0015
	Machine (Skyra vs Allegra)	0.098	0.105	0.3518	1.0000
	Status (HIV+ vs HIV-)	0.053	0.074	0.4753	1.0000
	Relative GM %	3.245	0.431	<0.0001	<0.0001
NAA	Intercept	5.146	0.304	<0.0001	<0.0001
	Age	0.083	0.032	0.0104	0.4148
	Machine (Skyra vs Allegra)	0.681	0.114	<0.0001	<0.0001
	Status (HIV+ vs HIV-)	0.425	0.133	0.0017	0.0954
	Relative GM %	-0.112	0.445	0.8018	1.0000
	Age*Status	-0.078	0.029	0.0071	0.3143
GPC.PCh	Intercept	0.773	0.073	<0.0001	<0.0001
	Age	0.019	0.006	0.0019	0.1058
	Machine (Skyra vs Allegra)	0.153	0.027	<0.0001	<0.0001
	Status (HIV+ vs HIV-)	0.052	0.019	0.0077	0.3226
	Relative GM %	0.643	0.111	<0.0001	<0.0001
NAA.NAAG	Intercept	5.510	0.082	<0.0001	<0.0001
	Age	0.063	0.026	0.0158	0.5988
	Machine (Skyra vs Allegra)	1.176	0.115	<0.0001	<0.0001
	Status (HIV+ vs HIV-)	0.041	0.065	0.5304	1.0000
Cr.PCr	Intercept	3.716	0.344	<0.0001	<0.0001
	Age	0.257	0.039	<0.0001	<0.0001
	Machine (Skyra vs Allegra)	1.142	0.264	<0.0001	0.0013
	Status (HIV+ vs HIV-)	0.026	0.076	0.7304	1.0000
	Relative GM %	3.036	0.507	<0.0001	<0.0001
	Age*Machine	-0.157	0.057	0.0064	0.2948
Glu.Gln	Intercept	4.674	0.763	<0.0001	<0.0001
	Age	0.262	0.067	0.0001	0.0066
	Machine (Skyra vs Allegra)	3.080	0.296	<0.0001	<0.0001
	Status (HIV+ vs HIV-)	-0.080	0.175	0.6480	1.0000
	Relative GM %	7.567	1.159	<0.0001	<0.0001

In all three regions we see an increase of relative GM % or relative WM% leads to an increase in GPC+PCh concentration, again showing no consistent increase or decrease related to GM% or WM%, an increase in either results in an increase in GPC+PCh concentration. We also see that HIV status has a significant effect on GPC+PCh concentrations across all three of these regions. These effect sizes appear small, but since GPC+PCh is on the smallest scale, with a minimum of 0.7 and a maximum of 2.4 they are relatively large.

The effects on NAA+NAAG are similar to that of NAA, where in the PWM and MFGM the relative GM or WM% has a large effect on concentration while in the BG no effect was seen. HIV also had no substantial effect on NAA+NAAG levels in the BG region.

Cr+PCr concentration was consistently increased by the relative GM% by 2.6 units in the MFGM and 3 units in the BG with a one-unit increase in relative GM%. We see a 2.4-unit decrease in the PWM with a relative increase in WM%. Thus, we observe another situation where an increase in gray matter leads to an increase in metabolite concentration.

The Glu+Gln results are similar to that of Glu; relative GM% leads to a 6.7-unit increase in Glu+Gln in the MFGM, 7.5 unit increase in the BG and a 6-unit decrease is expected in the PWM with an increase in relative WM%. We also see at least a three-unit increase in Glu+Gln concentration as a result of the Skyra scanner in all three regions.

The inclusion of a scanner-age interaction effect in the mixed effect models allows for the rate of concentration change, with respect to age, to be different for the two scanners. Figure 3.8 illustrates the impact on the association between metabolite levels depending on whether the means include just a scanner main effect or additionally an interaction between scanner and age.

Figure 3.8: Theoretical Model structure given different components.

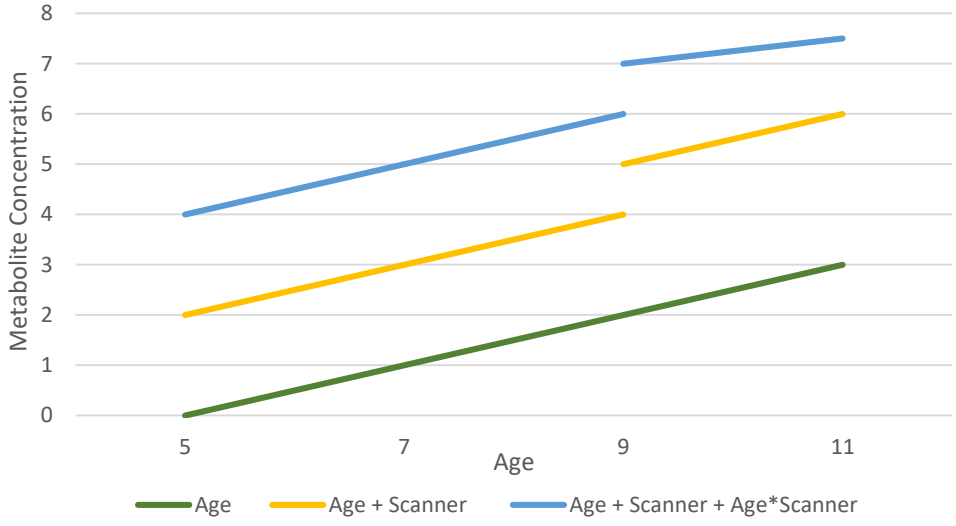

Essentially this results in a different scale or a different scale and slope on either side of age 9 (the age at which the scanners were changed).

This is illustrated by the following model decomposition:

$$Y_{ij} = \beta_0 + \beta_1 age_{ij} + \beta_2 scanner_{ij} + \beta_3 age_{ij} * scanner_{ij}$$

$$\equiv Y_{ij} = \beta_0 + \beta_1 age_{ij} \text{ for scanner 1 (Allegra).}$$

$$\equiv Y_{ij} = (\beta_0 + \beta_2 scanner_{ij}) + (\beta_1 + \beta_3) age_{ij} \text{ for scanner 2 (Skyra).}$$

Because the scanners are different before and after the ages of 9 (approximately) this is equivalent to:

$$\equiv Y_{ij} = \beta_0 + \beta_1 age[5\ to\ 9] + (\beta_1 + \beta_3) age[9\ to\ 11] \text{ for scanner 2 (Skyra).}$$

We can illustrate this effect using the Cr+PCr metabolite in the BG region. In this model we see a significant Age*Machine interaction. This means the rate of change of metabolite concentration over time is different before and after the scanner change.

For observations taken using the Allegra scanner (age 5-9) the age effect on Cr+PCr concentration in the BG is (using estimates reported in Table 3.5):

$$0.257,$$

while the age effect after age 9 (when using the Skyra scanner) is:

$$0.257 - 0.157\,.$$

This means the Cr+PCr – BG region model (adjusted for HIV status and relative GM%) for the Allegra scanner is:

$$3.716 + 0.257\ Age$$

and the same model for the Skyra scanner is:

$$(3.716 + 1.142) + (0.257 - 0.157)\ Age.$$

To summarise, the main objective of this section is to compare age profiles of HIV+ to HIV- children. The key results, based on unadjusted p-values, are with respect to the consistent differences seen in the different regions for GPC+PCh concentrations across the different regions and for the age-group effect seen for NAA concentrations in the BG region.

For NAA:
the age effect among HIV- children is: $0.083,$
while, the age effect among HIV+ children is: $0.083 - 0.078.$

Hence, for HIV-, the NAA model (adjusted for machine and relative GM%) is:

$$5.146 + 0.083\ Age.$$

While for HIV+, the NAA model is:

$$(5.146 + 0.425) + (0.083 - 0.078)\ Age$$

Thus, we see a stronger positive slope among the HIV negative children which is significantly decreased for HIV positive children. This also shows that while HIV positive children start with a greater concentration of NAA at age five compared to HIV negative children. There is some mechanism of action causing these children to have lower NAA at later ages.

The mixed effect model formulation produces estimates for both σ_e and σ_b. The within subject error is described by σ_e. This represents the random variability present within our data, which is the variability of observations for each subject around the subject specific mean ($\beta_0 + b_{0i}$). The between subject variability, σ_b , is the variation between the different subjects and this is the variability of the subject specific means ($\beta_0 + b_{0i}$) about the population mean (β_0).

Table 3.6: The estimates of σ_e, the standard deviation for the within group error and σ_b, the standard deviation for the subject-specific random effects from the respective LME Models.

Region	**Metabolite**	σ_e	σ_b
WM	Glu	0.877	0.285
	Ins	0.517	0.365
	NAA	0.662	0.286
	GPC+PCh	0.138	0.102
	NAA+NAAG	0.714	0.281
	Cr+PCr	0.355	0.167
	Glu+Gln	1.180	0.322
GM	Glu	1.444	0.175
	Ins	0.689	0.253
	NAA	0.930	0.213
	GPC+PCh	0.143	0.092
	NAA+NAAG	0.970	0.043
	Cr+PCr	0.723	0.112
	Glu+Gln	1.719	0.451
BG	Glu	1.313	0.260
	Ins	0.589	0.284
	NAA	0.658	0.119
	GPC+PCh	0.150	0.078
	NAA+NAAG	0.672	<0.0001
	Cr+PCr	0.743	0.140
	Glu+Gln	1.704	0.357

The within subject variability is larger than between subject variability, this shows that a large proportion of random variation is still present within our data (Table 3.6). However, as the observations of σ_b are not zero, the inclusion of the random effect terms has reduced the random variability and explained some of the variation present.

Glu and Glu+Gln showed the greatest variation, while GPC+PCh had the least (Table 3.6). This lower variability leads to greater power, which may be why we are able to identify the effects of HIV on GPC+PCh concentration.

3.3.3 Multiple Testing Correction:

Tables 3.3 to 3.5 include adjusted p-values calculated using the Holm method. This did lead to different results in terms of significance. However, this being an exploratory analysis, we still see something of interest in these variables and metabolites compared to the others and hence they should still be investigated in future for playing some role in the brain throughout HIV infection.

When we rank these p-values, we see the most significant effects for the relative WM% in the PWM region, followed by the effect of age, machine and then HIV status. In the BG and MFGM region the most significant effects are from the machine covariate, then relative GM%, age and finally HIV status.

3.3.4 Exposure to HIV:

HIV status was replaced with the HIV exposure variable in each of the final models. The full ouput from these models can be found in Appendix A.3. To illutsrate the effects of these different exposure groups on metabolite concentration we extracted the effect sizes with 95% confidence intervals from each of the separate models and illustrated these values in Figure 3.9.

The metabolite levels for exposed HIV- and unexposed HIV- patients were compared to HIV+ children and very similar results were seen which leads us to believe that exposure to HIV has no observable effect on brain metabolite concentrations (Figure 3.9A). The results were identical apart from the concentration of Ins in the BG and MFGM regions which was significantly lower for HIV- unexposed controls compared to HIV+ children (Figure 3.9B). Using exposure as well as HIV status did not improve model fit at all, showing the use of status instead of exposure groups is sufficient.

Comparing the metabolite concentrations among the controls, between the HIV exposed and HIV unexposed children we see no significant metabolite differences across all metabolites and regions (Figure 3.9C). Again, supporting the observation that exposure to HIV does not affect brain metabolite levels in the BG, PWM and MFGM regions of the brain. Figure 3.9 illustrates the consistent effect of HIV status on NAA and GPC+PCh concentration when comparing HIV+ to either the HEU or HUU groups.

Figure 3.9: The β estimates with 95% CI for the effect of (A) HIV- exposed (HEU) compared to HIV+, (B) HIV- unexposed (HUU) compared to HIV+ and (C) HIV- exposed (HEU) compared to HIV- unexposed (HUU) on metabolite concentrations.

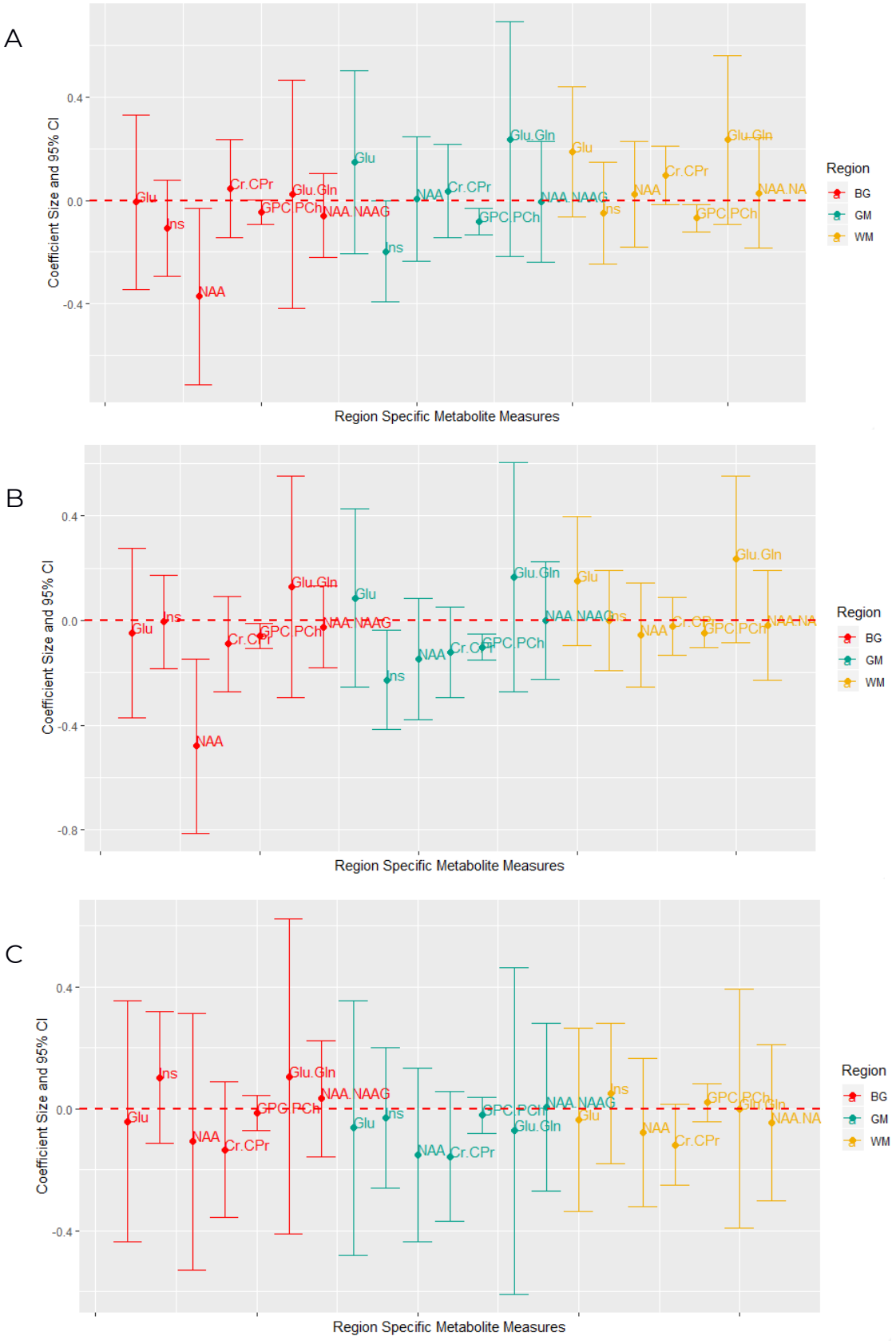

3.3.5 Model Validation:

Figure 3.10 shows histograms and scatter plots of the residuals for a selection of all models validated. We only illustrate four examples here as all 21 models had very similar residual plots and hence this subset is representative of all models validated. The scatter plots of residuals against fitted values for both the between and within subject residuals show no evidence of heteroscedasticity. The grouping of residuals in terms of fitted values reflects the different predicted values for measurements taken on different scanners. The histograms of residuals show that the distribution of residuals did not differ significantly from the normal distribution, though they may have thinner tails due to some outlying observations.

Figure 3.10: Between and within subject residuals represented using histograms and scatter plots for the univariate mixed effects models created to describe the concentrations of (A) Cr+PCr, (B) GPC+PCh, (C) NAA and (D) Glu in the MFGM region.

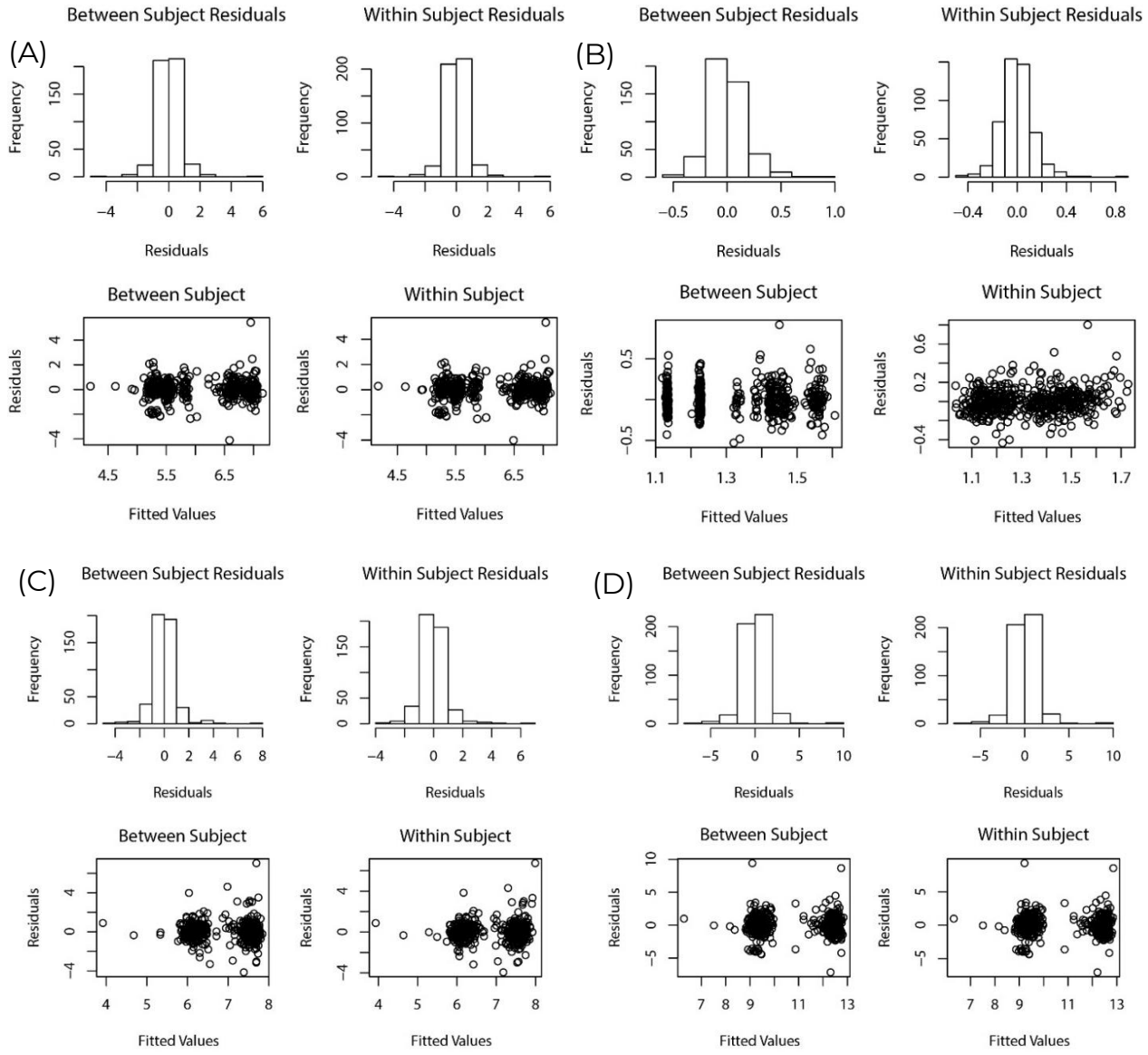

3.4 Discussion:

Ins is a compound found most commonly in the glial cells, which are the cells that surround neurons and protect them. In these cells Ins functions as an osmolyte. Osmolytes are compounds that regulate the properties of fluids, such as intracellular fluids, and accordingly effect all metabolic processes within those systems. Cell integrity and activity can be affected if there is an imbalance in the osmoregulation of a cell. Elevated Ins levels have been caused by increased membrane turnover or damage to myelin sheets (Haris et al., 2011). GPC+PCh is an important metabolite involved in many biochemical processes. In the body, GPC+PCh is involved in many different processes (Zeisel and da Costa, 2009) and is generally considered to be a marker of inflammation if elevated in conjunction with Ins (Harezlak et al., 2011).

We observed increased concentrations of Ins in HIV+ children within the MFGM and across the three regions investigated we observed increased mean GPC+PCh levels in HIV positive children compared to HIV negative children from 5 to 11 years. The elevation of both Ins and GPC+PCh within the MFGM region suggests that HIV+ children are exhibiting an inflammatory response within this region, and as GPC+PCh is also elevated within the BG and PWM regions we can hypothesise that some inflammation may also be present there. Inflammation is a natural response to any harmful substance, stimulus or damage to the body and this observation suggests that while these children are taking treatment, there is still some sort of damage or harmful substance present in these regions of the brain.

In the BG region we saw elevated levels of NAA within HIV+ children at younger ages, with a reduction in this elevation as time progressed. NAA is an indicator of neuronal health and integrity, low levels of NAA may indicate neuronal or axonal loss or compromised neuronal metabolism (Moffett et al., 2007). Past studies have found NAA to be reduced by HIV associated encephalopathy and have speculated that with the introduction of ART this reduction would no longer be seen (Moffett et al., 2007; Paley et al., 1996). Interestingly, in contrast to the previous findings, we see initially elevated levels of NAA in the HIV positive group with a decrease in this difference over time.

Effectively, these findings show that while these HIV+ children included in our cohort have started ART at birth and present as healthy, we still see evidence of altered brain chemistry and metabolism from the age 5 to 11. We cannot make assumptions whether these differences are beneficial or damaging, but we can see that they are present and that these children are experiencing some effects that may be due to HIV or ART itself.

When looking at the differences between HIV+ vs HEU and HIV+ vs HUU children we saw identical results: i) lower BG-NAA for HEU and HUU children, ii) lower GPC+PCh across all three regions for HEU and HUU children and iii) lower Ins in the MFGM for HEU and HUU children. Thus, these results show identical findings

irrespective of exposure to HIV during gestation. We also observe no significant difference between metabolite concentrations between HEU and HUU children.

We saw increases in most metabolite concentrations with increasing age. Within the BG this may be a symptom of subcortical synaptic reorganisation (Holmes et al., 2017). Increases seen in the PWM suggests that these metabolites may be involved in ongoing myelination within this region (Holmes et al., 2017). In the MFGM region this may be an indication of synaptic activity due to learning (Holmes et al., 2017).

We saw consistent increases in metabolite concentrations measured using the Skyra MRI scanner, which again validates the need to consider the scanner effect on concentrations measured in longitudinal or multicentre studies. The relative GM% / WM% also had a significant effect on most concentrations measured, Generally the relative WM% had a negative effect on concentrations measured and relative GM% had a positive effect, suggesting that for the metabolites we investigated here more GM tissue within a voxel resulted in greater metabolite concentrations.

Previous studies have also explored gender and race as possible covariates that may affect metabolite concentrations within the brain. We have found that the final models for each of these response variables does not require the addition of gender as a covariate to explain effects on metabolite concentration (see the Appendix A.3 for these results). Race did not improve model fit or significantly affect the metabolite concentrations for any metabolites except for the concentration of Cr+PCr the BG region (see the Appendix A.3 for these results). However, this conclusion may be biased as the distribution of races within our data was not even, African children made up over 80% of all children in our study.

A possible concern with the linear mixed effect modelling approach is the assumption of linearity in the trend of metabolite concentrations over time. Looking at the metabolite concentrations over time, seen in Figures 3.5-3.7, it is clear they generally appear to follow a linear trend. However, for some metabolites the profile may be better suited to a non-linear model. For example, the Glu+Gln concentration in the PWM region could potentially be better fit by a broken stick model – a linear spline with a knot at age 10. This allows for two linear models that have different slopes between the ages of 5-10 and 10-12, which may be better suited to this profile. This was investigated and the results are given in Table 3.7 and Figure 3.11 illustrates the change in model formulation.

This new model formulation results in different effect size estimates for the age and intercept covariates (as expected), but has little effect on the HIV and Relative WM% effect sizes (Table 3.7). The above age 10 model does not have a scanner effect as all measurements above the age of 10 were taken using the Skyra scanner. The linear approach to modelling this data appears to be adequate when considering our goal which is to identify the effect of HIV on metabolite concentrations.

By allowing for an age*machine interaction term within our LME models we account for, non-linearly, the change in scanner (which was around age 10 for most children). The age*machine interaction allows observations taken using the Allegra scanner to have a different age slope than observations taken using the Skyra scanner, which should adequately capture any non-linear relationships present due to the scanner change.

Figure 3.11: The concentration of Glu+Gln measured over time, fit with two discrete models before and after age 10.

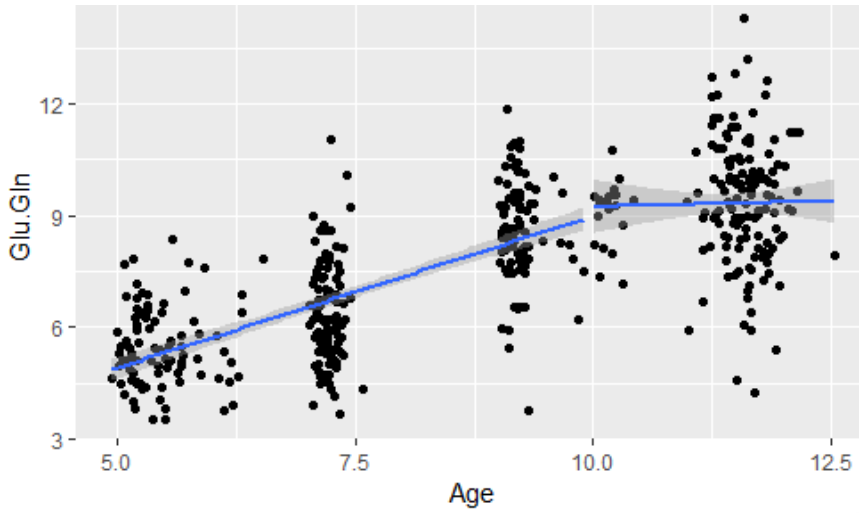

Table 3.7: The model parameters for a LMEM fit to Glu+Gln data before age 10, after age 10 and using all ages.

		Value	Standard Error	P-value
Below Age 10	Intercept	10.358	0.568	<0.0001
	Age	0.353	0.076	<0.0001
	Machine (Skyra)	2.012	0.256	<0.0001
	Status (HIV)	-0.256	0.153	0.0970
	Relative WM %	-5.873	0.656	<0.0001
Above Age 10	Intercept	13.538	1.600	<0.0001
	Age	0.147	0.222	0.5151
	Status (HIV)	-0.267	0.238	0.2652
	Relative WM %	-6.33	0.957	<0.0001
All Ages	Intercept	10.649	0.483	<0.0001
	Age	0.201	0.055	0.0003
	Machine (Skyra)	2.292	0.256	<0.0001
	Status (HIV)	-0.247	0.129	0.0573
	Relative WM %	-5.938	0.550	<0.0001

A disadvantage to the univariate modelling approach is the number of parameters that need to be estimated and the time involved in creating and performing the model building procedure for 21 separate models. These models are also entirely separate and assume an independence between the metabolite concentrations and brain regions. Hence, a multivariate approach to analysing these metabolite concentrations together will be informative and this will be explored in chapter four.

Chapter 4: Multivariate Approaches

4.1 Background:

This chapter refers to methods for analysing multiple responses and compares hierarchical linear mixed effect models to a multivariate regression model with a latent component to capture the correlation among the many responses. Emphasis is put on the ease of interpretation of results from the different models.

Univariate mixed effect modelling approaches may be used to analyse this data, however this involves the creation and interpretation of 21 separate models that will not give any insight to the interactions between metabolite concentrations and regions of the brain. As we know the body is a connected system that always tends toward homeostasis, we cannot assume these factors are independent and hence, they must be analysed together in a multivariate setting.

Four of the responses previously being investigated NAA, NAA+NAAG and Glu, Glu+Gln have highly correlated measurements as they measure NAA and its derivatives and Glu and its derivatives respectively. Hence, in this chapter we only investigate changes in NAA and Glu and accordingly analyse five metabolites (Glu, NAA, Ins, Cr+PCr, GPC+PCh) within each region instead of the initial seven.

The previous chapter focused on models to cope with repeated observations from the same subjects over a period of time. In this chapter, we have repeated measures across time (within subjects) but since we wish to model the different metabolites in the different regions simultaneously, we also have repeated observations each time point. This creates another level of correlation within the data that must be accounted for by the modelling process (Bandyopadhyay et al., 2011).

One approach to analysing the fifteen responses simultaneously is the use of a univariate multilevel mixed effect model that creates a long response vector of all metabolite levels and model them as a function of metabolite type and brain region, plus their interactions with HIV status and age. Within subject correlation due to multiple responses and repeated time measurements will be captured through modelling the effects of region and metabolite as fixed effects. However, the interpretation of the two- and three-way interactions can be complex.

An alternative multivariate approach, traditionally applied to ecological data is the Correlated Response Model (Hui, 2016). The Correlated Response Models involve adding a latent factor component to a generalised linear mixed model (GLMM). Correlated Response Models (CRM) have a similar model formulation as the mixed effect models, however a key difference is the addition of a latent factor (LF) component which performs a factor analysis (FA) on the residuals of the model (Hui, 2016). This is essentially equivalent to adding a latent variable that quantifies all unmeasured covariates and hence accounts for the correlation between the response variables (Hui, 2016).

Verbeke et al., (2014) discuss the use of latent variables as a means to impose a correlation structure between observations when dealing with multivariate longitudinal data (Verbeke et al., 2014). They focus on reducing the dimensionality of the data by representing the response variables using one or more latent variables. This may allow the identification of some latent factors, such as region, metabolite or activity factors, which are then regressed against the covariates of interest (Verbeke et al., 2014). A key disadvantage to this approach is the fact that the relationship between the covariates and the response are not in terms of the initially observed response but instead a latent construct representing these response variables.

The CRM is different as it allows the incorporation of the latent factor component to impose this correlation structure between the response variables, however it also conserves the fixed effects component of this model allowing interpretation of the effect of covariates on the response variables directly, instead of a latent variables representing the responses.

4.2 Methods:

4.2.1 Multilevel Mixed Effect Model:

The multilevel mixed effect model approach is based on changing the multivariate response design into a univariate response by forming a long response that contains all metabolite concentrations in all regions taken at all occasions for each subject. This multilevel design is illustrated in Figure 3.1 of the previous chapter. More specifically the multivariate response vector,

$$(Y_{11}, \dots, Y_{15,} Y_{21}, \dots, Y_{25}, Y_{31}, \dots, Y_{35})$$

with

$Y_{jk} = [Y_{it}] = n \times n_i$ vector of concentrations for n subjects taken at n_i time points.

is replaced by a univariate response vector,

$$Y = [Y_{ijkt}],$$

i = subject index (from 1 to n),
j = region index (from 1 to 3),
k = metabolite index (from 1 to 5),
t = occasion index (from 1 to n_i).

One can reflect the nested structure of the design (time nested in metabolite nested in region nested in subject) through the inclusion of metabolite-specific, region-specific and subject-specific random effects.

For example,

$$Y_{ijkt} = \mu + b_i + b_{j,i} + b_{k,ji} + \varepsilon_{ijk}$$

with

$b_i \sim N(0, {\sigma_{b_i}}^2)$ the subject specific random effect,

$b_{j,i} \sim N(0, {\sigma_{b_{j,i}}}^2)$ the region within subject specific random effect,

$b_{k,ji} \sim N(0, {\sigma_{b_{k,ji}}}^2)$ the metabolite within region within subject specific random effect,

$\varepsilon_{ijk} \sim N(0, {\sigma_{e_{ijk}}}^2)$.

However, we chose to incorporate the metabolite and region effects as fixed effects in the models, still include the subject-specific random effect to capture the repeated measures and impose an equal and exchangeable correlation among all measurements across time, metabolite and region for each subject, and then allowed different variances for the different region-metabolite groups through a stratified variance specification,

$$Var(Y) = {\sigma_e}^2 + {\sigma_b}^2 = {\sigma_{jk}}^2 + {\sigma_b}^2,$$

$$cov(Y) = {\sigma_b}^2 .$$

Within the basic model we require β_0, age, HIV status and the HIV status*age interaction to explore the focus of this research which is the effects of age and HIV status on the respective metabolite concentrations within three brain regions.

This basic model is:

$$Concentration = \beta_0 + \beta_1 * age + \beta_2 * HIV + \beta_3 * age * HIV$$

Because of the variability seen in metabolite concentrations both within and across the regions, we wish to let these variables vary with respect to:

i) Metabolite (across regions),
ii) Region (across metabolites),
iii) Metabolite within region.

This means we must include the following terms within our model:

	Metabolite	Region	Metabolite within Region
β_0	+ Metabolite	+ Region	+ Metabolite*Region
β_1	+ age*Metabolite	+ age*Region	+ age*Metabolite*Region
β_2	+ HIV*Metabolite	+ HIV*Region	+ HIV*Metabolite*Region
β_3	+ HIV*age*Metabolite	+ HIV*age*Region	+HIV*age*Metabolite*Region

This is also required for the other covariates of interest:

for the scanner variable:
β_4 + scanner*Metabolite +scanner* Region + scanner*Metabolite*Region

for the relative %GM variable:
β_5 + %GM*Metabolite +%GM * Region

(as relative GM% is a minor covariate and to save complexity, we think it is sufficient to omit a three-way interaction between metabolite and region).

The full model thus becomes:

$$Y_{ijkt} = \beta_0 + X_{it}^T \beta_j + b_{0i} + \varepsilon_{ijkt} \quad (4.1)$$

$$i = subject,\ j = region,\ k = metabolite,\ t = occasion$$

where:
Y_{ijkt} = metabolite concentration for metabolite *k* in region *j* taken on occasion *t* for subject *i*,
β_0= the baseline metabolite concentration for the reference metabolite and region,

$$X_{it}^{T}\beta_j = \tag{4.2}$$

$$\beta_1 X_{1it} + \beta_2 X_{3i} + \beta_3 X_{3i} * X_{1it}$$
(basic model focus)

$$+\beta_4 X_{2it} + \beta_5 X_{4ijt}$$
(other covariates)

$$+\beta_{6j} X_{5ij} + \beta_{7k} X_{6ijk} + \beta_{8jk} X_{6ijk} * X_{5ijk}$$
(region and metabolite specification and interaction)

$$+\beta_{9k} X_{4ijt} * X_{6ijk} + \beta_{10j} X_{4i} * X_{5ijk}$$
(different GM% effects by region and metabolite)

$$+\beta_{11k} X_{2it} * X_{6ijk} + \beta_{12j} X_{2it} * X_{5ijk} + \beta_{13jk} X_{2it} * X_{6ijk} * X_{5ijk}$$
(modified scanner effects by region, metabolite and region*metabolite)

$$+\beta_{14k} X_{3i} * X_{6ijk} + \beta_{15k} X_{1it} * X_{6ijk} + \beta_{16k} X_{3i} * X_{1it} * X_{6ijk}$$
(for modification of age and HIV and age*HIV by metabolite)

$$+\beta_{17j} X_{3i} * X_{5ijk} + \beta_{18j} X_{1it} * X_{5ijk} + \beta_{19j} X_{3i} * X_{1it} * X_{5ijk}$$
(for modification of age and HIV and age*HIV by region)

$$+\beta_{20jk} X_{3i} * X_{6ijk} * X_{5ijk} + \beta_{21jk} X_{1it} * X_{6ijk} * X_{5ijk} + \beta_{22jk} X_{3i} * X_{1it} * X_{6ijk} * X_{5ijk}$$
(for modification of age and HIV and age*HIV by region and metabolite)

where:
X_{1it} = age of the children at each scan occasion,
X_{2it} = scanner the measurement was taken on,
X_{3i} = HIV status of the child,
X_{4ijt} = relative percentage of GM or WM in the voxel for each measurement,
X_{5ij} = region the concentration was measured for,
X_{6ijk} = metabolite that was measured,

b_{0i} = subject specific random effect $\sim N(0; {\sigma_{b_{0i}}}^2)$, $\varepsilon_{ijkt} \sim N(0; {\sigma_{jk}}^2)$. The stratified variance function allowing region and metabolite variables to have different residual within subject variances has the following form:

$$Var(\varepsilon_{ijkt}) = {\sigma_{jk}}^2 = \sigma^2 {\delta_{S_{jk}}}^2 \tag{4.3}$$

where:
${\delta_{S_{jk}}}^2$ = the stratum specific adjustments to σ^2.

As can be seen in (4.2), this model contains multiple higher-order interaction terms and each of these terms included are described in the list below:

β_1 = Age effect,
β_2 = HIV Status effect (HIV+ vs HIV-),
β_3 = HIV modification of Age effect,
β_4 = Machine effect (Skyra vs Allegra),
β_5 = Relative GM% effect,

β_{6j} = Region effect (j=2 to 3),
β_{7k} = Metabolite effect (k=2 to 5),
β_{8jk} = Metabolite modification of region effect (j=2 to 3, k=2 to 5),

β_{9k} = Metabolite modification of **Relative GM%** effect (k=2 to 5),
β_{10j} = Region modification of **Relative GM%** effect (j=2 to 3),

β_{11k} = Metabolite modification of **Machine** effect (k=2 to 5),
β_{12j} = Region modification of **Machine** effect (j=2 to 3),
β_{13jk} =Region and metabolite interaction modification of **Machine** effect (j=2 to 3, k=2 to 5),

β_{14k} = Metabolite modification of **HIV** effect (k=2 to 5),
β_{15k} = Metabolite modification of **Age** effect (k=2 to 5),
β_{16k} = Metabolite and **HIV** modification of **Age** effect (k=2 to 5),

β_{17j} = Region modification of **HIV** effect (j=2 to 3),
β_{18j} = Region modification of **Age** effect (j=2 to 3),
β_{19j} = Region and **HIV** modification of **Age** effect (j=2 to 3).

β_{20jk} = Region and metabolite interaction modification of **HIV** effect (j=2 to 3, k=2 to 5),
β_{21jk} = Region and metabolite interaction modification of **Age** effect (j=2 to 3, k=2 to 5),
β_{22jk} = Region and metabolite and **HIV** interaction modification of **Age** effect (j=2 to 3, k=2 to 5),

Model fit was assessed by looking at the AIC values for the respective models with the different random effect and fixed effect specifications. The model validity was determined by using qq-plots to test normality and analysing plots of residuals versus fitted values to identify data structures unaccounted for by the model.

Multilevel LME models were fit using the *lme* function from the *nlme* package (Pinheiro et al., 2019) in R (RStudio Team, 2018).

4.2.2 Correlated Response Model:

This model fits separate GLMs to each column of the multivariate vector response and allows for residual correlation between these columns through the latent variables (Hui and Blanchard, 2018). Similar to the multilevel models, subject specific random effects account for the correlation induced by the repeated measurements over time for each subject.

As previously mentioned, this multivariate model deals with the correlation between multiple variables (in this case five metabolite measures in each of the three regions) through the addition of a latent component. Again, here we jointly fit a GLM with a FA component which results in a FA of residuals, which is different to a FA alone which would produce an analysis of the multivariate response Y. To decide the number of latent factors to incorporate in the model, factor analysis was performed using the response variables and assessed for the best choice of the number of factors.

The model formulation is as follows:

$$E(Y_{ijt}) = \beta_{0j} + X_{it}^T \beta_j + z_i^T \theta_j + u_i \quad (4.4)$$

where:

Y_{ijt} =the concentration in (mM) for metabolite-region combination j (=1 to 15) at scan t (=1 to 4) for subject i (=1 to 163),

β_{0j} =response-specific offset to account for different scales,

$$X_{it}^T \beta_j = \beta_{j1} X_{1it} + \beta_{j2} X_{2it} + \beta_{j3} X_{3i} + \beta_{j4} X_{4i} + \beta_{j5} X_{5i} + \beta_{j6} X_{6i} + \beta_{j7} X_{1it} * X_{3i} \quad (4.5)$$

where

X_{1it} =the age of the children at each scan,

X_{2it} =the scanner the measurements were taken on (0=Allegra, 1=Skyra),

X_{3i} = the HIV status of the child (1=HIV+, 0=HIV-),

X_{4i}, X_{5i}, X_{6i} =the relative percentage of GM in the voxel for each measurement in the BG, PWM and MFGM respectively (as voxel placement does not give exactly identical tissue proportions for each child, and the type of tissue effects activity and hence metabolite concentrations),

$X_{1it} * X_{3i}$ = interaction between HIV status and age,

u_i =the random effect term for repeated subject observations, and is assumed to follow a $N(0; \sigma)$ distribution,

$\boldsymbol{z_i}$ $(\boldsymbol{n} \times \boldsymbol{k})$ = the k latent variables included in the model, induced by the between response associations,

$\boldsymbol{\theta_j}$ $(\boldsymbol{k} \times \mathbf{15})$ = refers to the loadings of the measured variables on the k latent constructs.

Correlated Response Traits Model:

Traits refer to response variable characteristics rather than the characteristics of the samples (or subjects). The inclusion of traits into the CRM allows one to investigate the differences in grouped response variables due to the covariates (Hui, 2016; Hui and Blanchard, 2018). Marginal effects can be investigated (using the Traits-CRM) as well as metabolite-region specific effects using the original CRM model. Our 15 response concentrations can be differentiated depending on which metabolite from which region they were measured.

Metabolite and regions can thus be treated as variable traits and can be incorporated in the model to allow for interaction with the subject specific covariates. This is done by treating the coefficients $\boldsymbol{\beta}_j$ and $\boldsymbol{\beta}_{0j}$ as random effects taken from a normal distribution which has a mean depending on the given traits. Hence, there will be region and metabolite specific means and the coefficients are sampled from this distribution:

$$\begin{aligned} \beta_{0j} &\sim N(\boldsymbol{t}_j{}^T \boldsymbol{\kappa}_0,\ \sigma^2{}_0) \\ \beta_{jk} &\sim N(\boldsymbol{t}_j{}^T \boldsymbol{\kappa}_k,\ \sigma^2{}_k) \end{aligned} \tag{4.6}$$

where

$\boldsymbol{t}_j$ is the vector of observed traits indicating to which group the response variable belongs,

β_{jk} is the k^{th} regression coefficient for $\boldsymbol{\beta}_j$,

$\boldsymbol{\kappa}_k$ relates the variable traits to the intercept and regression coefficients.

To fit the CRM models we used the *boral* package in R (Hui, 2016; Hui and Blanchard, 2018) which uses Bayesian estimation procedures as opposed to a maximum likelihood approach used in all previous model fitting procedures. Thus, within the CRM result section CI refers not to confidence intervals, but instead credibility intervals which we will refer to using CI*.

Model validity was assessed by looking at a normal quantile plot to assess the normality of the data. The Dunn-Smyth residuals were plotted against linear predictors, column index and row index to identify any structures in the data that would question the validity of the model.

Model fit was assessed by looking at the residual correlation from each model and the relative reduction in residual correlation due to model changes. The following formula was used to compare one model to another:

$$\begin{aligned} x &= Trace\ of\ the\ Residual\ Correlation\ of\ Model\ 1 \\ y &= Trace\ of\ the\ Residual\ Correlation\ of\ Model\ 2 \\ &\frac{x-y}{y} \end{aligned} \tag{4.7}$$

A positive value indicates a decrease in residuals and hence an improved model fit.

4.3 Results:

4.3.1 Multilevel Approach:

The multilevel model formulation, from which the results in this section were obtained is presented by equations 4.1, 4.2 and 4.3. With this model, by adding the interaction terms, we have allowed the effect of HIV, age, relative percentage of GM and the scanner effect to vary with metabolite and region. From the previous univariate models, we observed that these covariates had different effects across the different regions and for different metabolite concentrations. Hence, the inclusion of these interaction terms is key. As a result of this and the numerous dummy variables describing the metabolite and region covariates, we have extremely complicated model output with 82 estimated parameters (seen in Table 4.1 & Figure 4.1). This is difficult to interpret as the use of a reference metabolite and region means one would be required to constantly compare effects relative to another region and metabolite. To identify the overall effect of one covariate for a different region or metabolite than the reference used you would be required to sum up the effects of numerous different factors. The interpretation of the three- and four-way interaction terms is particularly complicated.

Figure 4.1 and Table 4.1 show the number of parameters estimated from this one multilevel model. Figure 4.1 is useful as we are able to immediately see the variables with larger effect sizes and with significant effect sizes based on a 95% confidence. However, we are unable to see exact estimate sizes as there are simply too many variables presented. For example, the clear effects identified are that of region, metabolite and region*metabolite differences. The machine effects, relative GM% and interactions thereof have significant effects. This further justifies the need for different estimates of covariate effects on the concentrations measured within different regions, and hence the importance of the interaction terms (Figure 4.1).

Figure 4.1: The coefficient estimates with 95% CI from the multi-level mixed effect model with Cr+PCr as the reference metabolite and BG as the reference region.

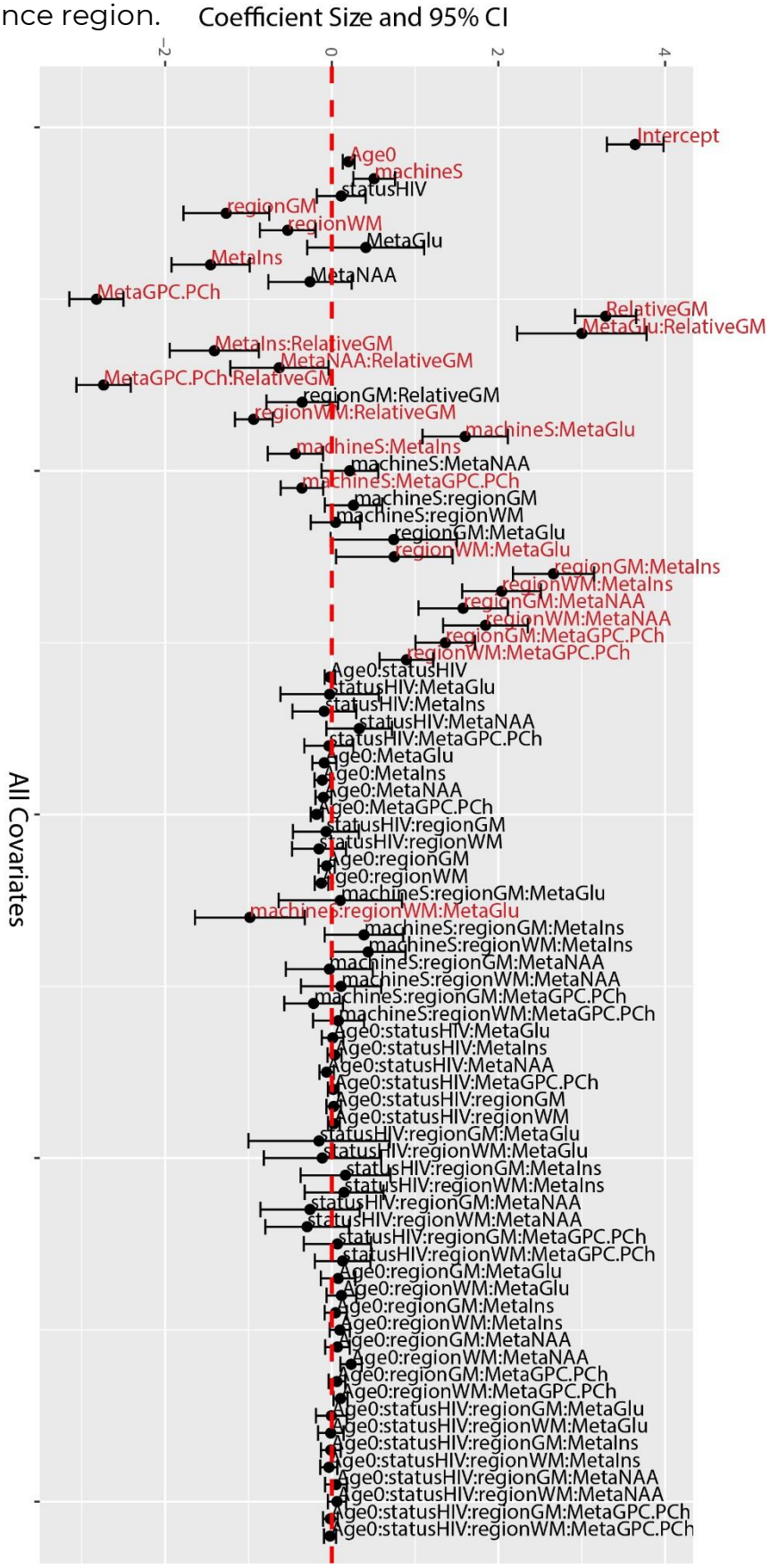

Table 4.1: Model output from the HLMEM with Cr.PCr and BG as the reference metabolite and region respectively.

Interaction Variable	Effect Variable	Estimate	Standard Error	P-value	Inference
	Intercept	3.641	0.173	<0.0001	Concentration of BG-Cr+PCr at age 5 for HIV- children.
	Age	0.202	0.036	<0.0001	Effect of age on BG-Cr+PCr concentration.
	Machine(Skyra)	0.509	0.128	0.0001	Increase in BG-Cr+PCr concentration due to use of the Skyra scanner.
	Status (HIV)	0.113	0.148	0.4469	Effect of HIV on BG-Cr+PCr concentration at age 5.
	Region (GM)	-1.265	0.263	<0.0001	Reflects the different scales of Cr+PCr within the different regions.
	Region (WM)	-0.528	0.172	0.0021	
	Meta (Glu)	0.407	0.358	0.2557	
	Meta (Ins)	-1.454	0.240	<0.0001	Reflects the different scales of metabolite measurement with reference to Cr+PCr.
	Meta (NAA)	-0.262	0.256	0.3062	
	Meta (GPC.PCh)	-2.824	0.166	<0.0001	
	Relative GM%	3.286	0.187	<0.0001	Effect of increasing GM% on BG-Cr+PCr concentration.
Meta (Glu)	**RelativeGM%**	3.001	0.396	<0.0001	The modification of the effect of GM% for metabolites relative to the modification on Cr+PCr.
Meta (Ins)		-1.41	0.273	<0.0001	
Meta (NAA)		-0.629	0.301	0.0365	
Meta (GPC.PCh)		-2.738	0.166	<0.0001	
Region(GM)		-0.354	0.218	0.1046	The modification of the effect of GM% for within different regions relative to the modification on the BG measurements.
Region (WM)		-0.936	0.116	<0.0001	
Meta (Glu)	**Machine (Skyra)**	1.601	0.261	<0.0001	The modification of the scanner effect for metabolites relative to Cr+PCr.
Meta (Ins)		-0.436	0.169	0.0099	
Meta (NAA)		0.218	0.174	0.2104	
Meta (GPC.PCh)		-0.358	0.130	0.0060	
Region(GM)		0.26	0.176	0.1392	The modification of the scanner effect within different regions, relative to BG.
Region (WM)		0.044	0.151	0.7713	
Meta (Glu)	**Region(GM)**	0.742	0.386	0.0544	Shows different relative levels of metabolite with respect to BG-Cr+PCr within different regions.
Meta (Ins)		2.66	0.248	<0.0001	
Meta (NAA)		1.576	0.274	<0.0001	
Meta (GPC.PCh)		1.362	0.182	<0.0001	
Meta (Glu)	**Region(WM)**	0.751	0.357	0.0352	
Meta (Ins)		2.037	0.241	<0.0001	
Meta (NAA)		1.844	0.259	<0.0001	
Meta (GPC.PCh)		0.896	0.164	<0.0001	
Age	**HIV Status (HIV+)**	-0.023	0.032	0.4746	HIV effect on BG-Cr+PCr doesn't change with age.
Meta (Glu)		-0.026	0.301	0.9313	No significant differences in HIV effect on other metabolites relative to Cr+PCr.
Meta (Ins)		-0.09	0.195	0.6460	
Meta (NAA)		0.329	0.201	0.1014	
Meta (GPC.PCh)		-0.036	0.150	0.8113	
Region(GM)		-0.07	0.201	0.7276	No significant differences in HIV effect on Cr+PCr across respective regions.
Region (WM)		-0.153	0.165	0.3538	
Meta (Glu)	**Age**	-0.089	0.073	0.2239	Differences in age profiles for respective metabolites relative to Cr+PCr.
Meta (Ins)		-0.113	0.048	0.0175	
Meta (NAA)		-0.1	0.049	0.0415	
Meta (GPC.PCh)		-0.181	0.037	<0.0001	
Region(GM)		-0.062	0.049	0.2075	Differences in age profiles for different regions relative to BG.
Region (WM)		-0.123	0.041	0.0028	
Region(GM)* **Meta (Glu)**	**Machine**	0.103	0.377	0.7844	Differences in effect of machine on other metabolites and in different regions relative to BG-Cr+PCr.
Meta (Ins)		0.385	0.241	0.1095	
Meta (NAA)		-0.029	0.266	0.9127	
Meta (GPC.PCh)		-0.218	0.180	0.2241	
Region(WM)* **Meta (Glu)**	**Machine**	-0.983	0.336	0.0035	
Meta (Ins)		0.437	0.228	0.0556	
Meta (NAA)		0.111	0.245	0.6519	
Meta (GPC.PCh)		0.081	0.156	0.6017	
Meta (Glu)	**Age*HIV Status**	0.01	0.066	0.8764	Modification of the age*HIV interaction for metabolites relative to that of BG-Cr+PCr.
Meta (Ins)		0.033	0.043	0.4358	
Meta (NAA)		-0.061	0.044	0.1629	
Meta (GPC.PCh)		0.018	0.033	0.5830	
Region(GM)		0.024	0.044	0.5889	Modification of the age*HIV interaction for measurements from regions relative to that of BG-Cr+PCr.
Region (WM)		0.026	0.036	0.4686	
Region(GM)* **Meta (Glu)**	**HIV status**	-0.153	0.431	0.7234	Modification of the HIV effect on metabolites and regions relative to that of BG-Cr+PCr.
Meta (Ins)		0.166	0.275	0.5468	
Meta (NAA)		-0.261	0.304	0.3908	
Meta (GPC.PCh)		0.069	0.206	0.7378	

Region(WM)*	**Meta (Glu)**	**HIV status**	-0.112	0.359	0.7556	
	Meta (Ins)		0.148	0.241	0.5390	
	Meta (NAA)		-0.296	0.256	0.2481	
	Meta (GPC.PCh)		0.131	0.170	0.4414	
Region(GM)*	**Meta (Glu)**	**Age**	0.076	0.106	0.4745	Modification of the age effect within metabolites and regions relative to that of BG-Cr+PCr.
	Meta (Ins)		0.047	0.068	0.4892	
	Meta (NAA)		0.068	0.075	0.3621	
	Meta (GPC.PCh)		0.062	0.050	0.2222	
Region(WM)*	**Meta (Glu)**	**Age**	0.117	0.091	0.1991	
	Meta (Ins)		0.096	0.061	0.1189	
	Meta (NAA)		0.231	0.066	0.0004	
	Meta (GPC.PCh)		0.105	0.043	0.0141	
Region (GM)*	**Meta (Glu)**	**Age*HIV Status**	-0.005	0.095	0.9613	Modification of the age*HIV effect for metabolites and regions relative to that of BG-Cr+PCr.
	Meta (Ins)		-0.012	0.060	0.8445	
	Meta (NAA)		0.051	0.067	0.4444	
	Meta (GPC.PCh)		-0.016	0.045	0.7191	
Region (WM)*	**Meta (Glu)**	**Age*HIV Status**	-0.011	0.078	0.8865	
	Meta (Ins)		-0.035	0.052	0.5003	
	Meta (NAA)		0.063	0.056	0.2598	
	Meta (GPC.PCh)		-0.021	0.037	0.5772	

As we imposed a stratified variance structure within this model, we have estimates of σ^2 and ${\sigma_{b_{0i}}}^2$ as well as estimates of the adjustment to σ^2, which is ${\delta_{S_{jk}}}^2$. These estimates obtained from the multilevel model were:

$\sigma^2 = 1.435$
${\sigma_{b_{0i}}}^2 = 0.100$

Table 4.2: Estimates of ${\delta_{S_{jk}}}^2$ for the various strata from the multilevel LMEM.

	Glu	**NAA**	**Ins**	**GPC+PCh**	**Cr+PCr**
MFGM	1.000	0.659	0.495	0.111	0.495
PWM	0.645	0.503	0.428	0.103	0.264
BG	0.922	0.477	0.450	0.100	0.518

The estimate of σ^2 represents the within subject (random) error, while ${\sigma_{b_{0i}}}^2$ represents the between subject error. We see the inclusion of the subject-specific random effects has explained some of the variability within the data, validating our choice to include this term.

From Table 4.2 it is evident that the variability within region and metabolite is not equal. This confirms that the use of a stratified variance structure was correct. The largest variability is seen for the measurements of MFGM-Glu followed by BG-Glu. The smallest variability was that of GPC+PCh which was smallest in all three regions measured. Again, this shows that GPC+PCh has greater power than Glu, which may be why we are able to identify the HIV effects on GPC+PCh.

To aid in the interpretation of this model, instead of calculating the different effect sizes of each covariate for the different metabolites in the different regions manually using the interaction terms from one model output, we changed the reference category and refitted the model to obtain output with each possible region-metabolite combination as the baseline. This means that effect sizes from each of these models will give the effects of Age, HIV Status, GM% and machine for the reference region-metabolite combination. This change of reference was

repeated and the key variables of interest were extracted. These effect sizes as well as the 95% CI around these estimates are illustrated in the Figures 4.2-4.6 and the effect sizes of interest are summarised in Tables 4.3 -4.7.

The results given are predominantly from the multilevel model without the Age*Machine and HIV Status*Age interaction terms as this model had a lower AIC and hence a better model fit. However, the effect of HIV Status*Age on the HIV Status effect is shown in Figure 4.4 and the Age*Machine effects can be found in the Appendix.

The metabolite concentrations at age 5 in the three different regions is represented in Figure 4.2 and Table 4.3. We do not see a consistent region that always has greater concentrations of all measured metabolites, which supports the fact that as the regions differ, so do the activities they perform and accordingly, so does the metabolic environment. We see the highest concentration of NAA, Ins and GPC+PCh in the WM region. Cr+PCr and Glu are most abundant in the BG region.

Figure 4.2: Baseline concentrations (intercept estimates) for the respective metabolites given different regions along with 95% confidence bands.

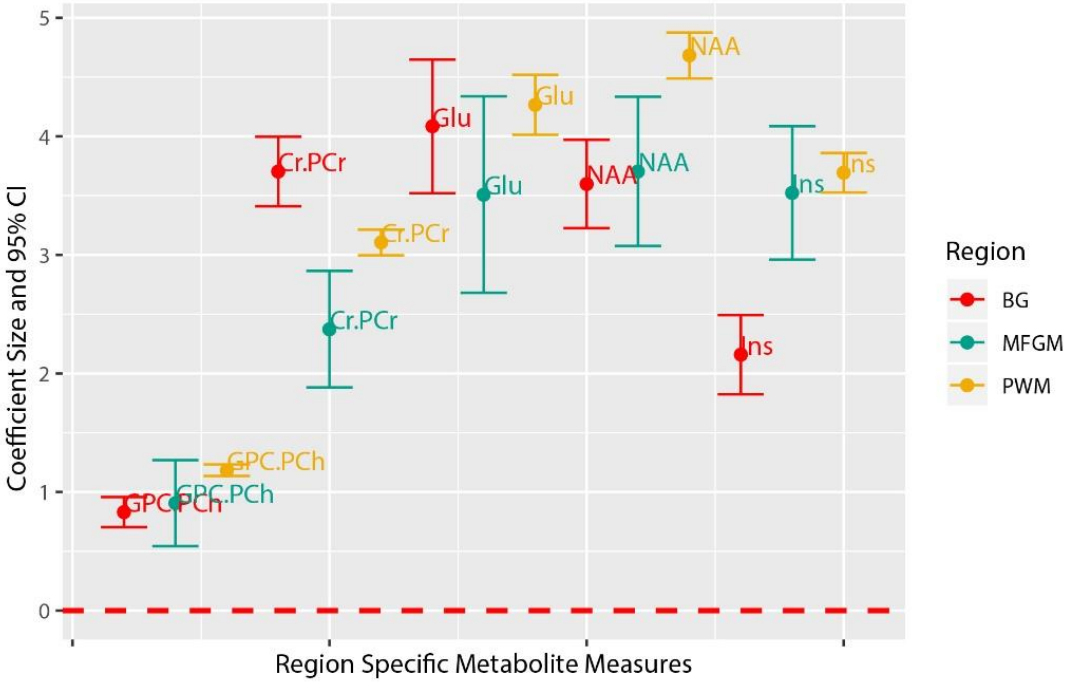

Table 4.3: The intercept estimates from the multilevel mixed effect model (without an age*status interaction) with different metabolite-region references.

Reference Region	Reference Metabolite	β estimate	Standard Error	P-value
BG	Cr.PCr	3.703	0.149	<0.0001
	Glu	4.083	0.288	<0.0001
	Ins	2.159	0.170	<0.0001
	NAA	3.598	0.190	<0.0001
	GPC.PCh	0.832	0.065	<0.0001
WM	Cr.PCr	3.105	0.055	<0.0001
	Glu	4.266	0.129	<0.0001
	Ins	3.693	0.085	<0.0001
	NAA	4.682	0.099	<0.0001
	GPC.PCh	1.184	0.025	<0.0001
GM	Cr.PCr	2.374	0.251	<0.0001
	Glu	3.509	0.423	<0.0001
	Ins	3.522	0.287	<0.0001
	NAA	3.705	0.321	<0.0001
	GPC.PCh	0.907	0.185	<0.0001

For most metabolites we see an increasing concentration with time (Figure 4.3 and Table 4.4). The only metabolite that did not show significant increases over time was GPC+PCh in the PWM. Though the CI for NAA in the BG region includes zero, it is predominantly positive. Across all three regions GPC+PCh had the smallest increase over time, while Cr+PCr had the largest increase in the MFGM and BG regions and NAA had the largest increase in the PWM region (Table 4.4, Figure 4.3).

Figure 4.3: Age effects (from the model without age*HIV Status interactions) for the respective metabolites given different regions along with 95% confidence bands.

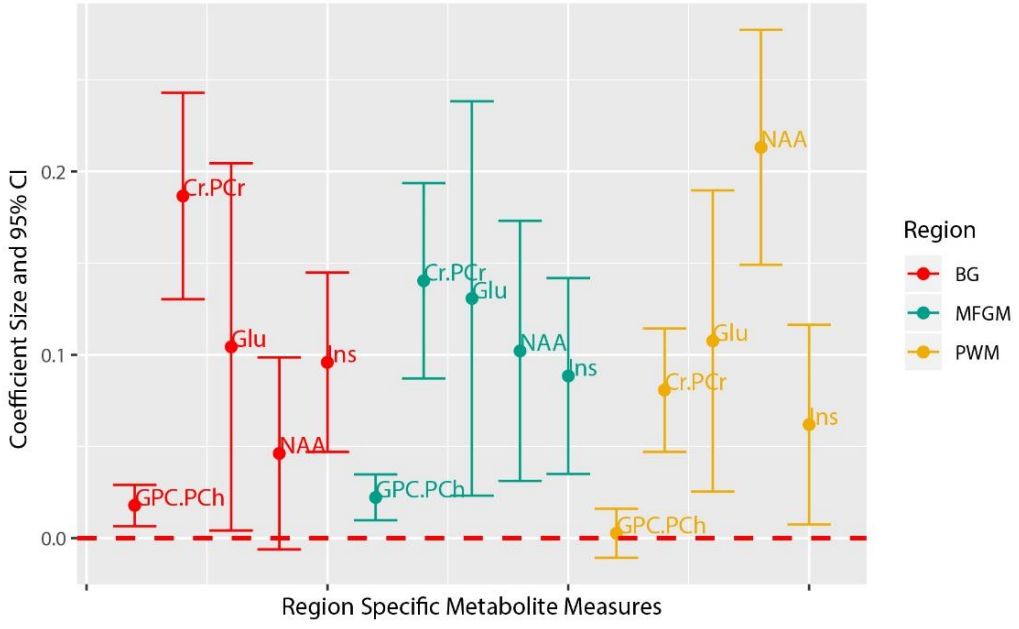

Table 4.4: The estimates of Age effect size from the multilevel mixed effect model (without an age*status interaction) with different metabolite-region references.

Reference Region	Reference Metabolite	β estimate	Standard Error	P-value
BG	Cr.PCr	0.187	0.029	<0.0001
	Glu	0.104	0.051	0.0412
	Ins	0.096	0.025	0.0001
	NAA	0.046	0.027	0.0838
	GPC.PCh	0.018	0.006	0.0020
WM	Cr.PCr	0.081	0.017	<0.0001
	Glu	0.108	0.042	0.0102
	Ins	0.062	0.028	0.0260
	NAA	0.213	0.033	<0.0001
	GPC.PCh	0.003	0.007	0.7005
GM	Cr.PCr	0.140	0.027	<0.0001
	Glu	0.131	0.055	0.0172
	Ins	0.088	0.027	0.0012
	NAA	0.102	0.036	0.0048
	GPC.PCh	0.022	0.006	0.0005

The effect of HIV on metabolite concentrations has been investigated from two perspectives. First, without any HIV Status*Age interaction terms as this further complicates the already complex model and from the previous chapter we saw this interaction effect to be mostly non-significant (Figure 4.4A and Table 4.5). And secondly, with the HIV Status*Age interaction terms included in the model as we have seen previously that the effect of HIV on NAA concentration in the BG region was not constant over time (Figure 4.4B-C and Table 4.6-4.7). We use both perspectives to fully interrogate this model and ensure we completely understand the effects of HIV on these metabolite concentrations.

The simpler model without age*HIV Status interactions shows us the effect of HIV across all ages (Figure 4.4A and Table 4.5). Figure 4.4A compares the metabolite concentrations of HIV- children to HIV+ children. We see significant increases in GPC+PCh across all ages in all three regions and a significant increase in Ins across all ages in the MFGM region for HIV+ children compared to HIV- (Figure 4.4A and Table 4.5). This validates what we previously observed from the univariate model outputs.

Figure 4.4B shows the comparison of metabolite concentrations between HIV+ and HIV- children specifically at age 5, while Figure 4.4C shows the modification of this comparison with an increase in age.

Figure 4.4: Effect of (A) HIV Status (HIV- as the reference) from the model without HIV*Age interactions, (B) HIV Status from the model with HIV*Age interactions and (C) the HIV*Age interaction on the respective metabolites given different regions along with 95% confidence bands.

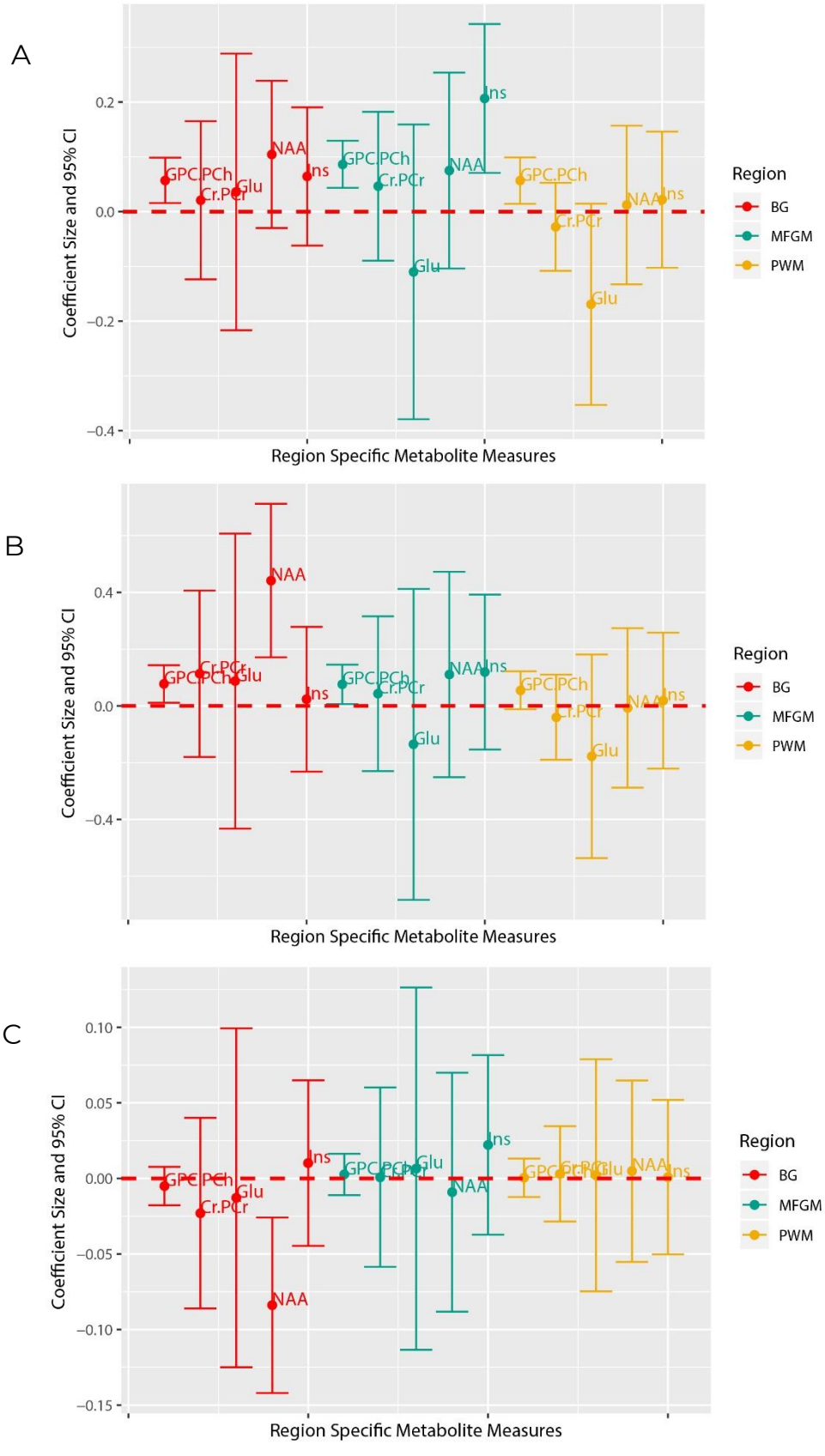

At age 5 we see significantly higher levels of NAA and GPC+PCh in the BG region and GPC+PCh in the MFGM region in HIV+ children compared to HIV- children (Figure 4.4B and Table 4.6). Figure 4.4C and Table 4.7 show that the only metabolite effected differently by HIV as time progresses is NAA in the BG region. We see this comparison of BG-NAA concentrations among HIV+ and HIV- children starts with HIV+ children having greater BG-NAA concentrations, and as these children grow older this difference decreases (Figure 4.4C and Table 4.7). Thus, the interaction of age and HIV status has a negative effect size, meaning the effect of HIV on NAA in the BG region decreases with age. These findings also validate the results previously seen in chapter 3.

Table 4.5: The estimates of HIV Status effect size for the multilevel mixed effect model (without an age*status interaction) with different metabolite-region references.

Reference Region	Reference Metabolite	β estimate	Standard Error	P-value
BG	Cr.PCr	0.021	0.073	0.7778
	Glu	0.036	0.128	0.7807
	Ins	0.064	0.064	0.3172
	NAA	0.104	0.068	0.1279
	GPC.PCh	0.057	0.021	0.0073
WM	Cr.PCr	-0.028	0.041	0.4942
	Glu	-0.169	0.093	0.0708
	Ins	0.022	0.063	0.7288
	NAA	0.012	0.073	0.8714
	GPC.PCh	0.057	0.021	0.0093
GM	Cr.PCr	0.046	0.069	0.5017
	Glu	-0.110	0.136	0.4206
	Ins	0.207	0.069	0.0031
	NAA	0.075	0.091	0.4096
	GPC.PCh	0.086	0.022	0.0001

Table 4.6: The estimates of HIV Status effect size from the multilevel mixed effect model (with an age*status interaction) with different metabolite-region references.

Reference Region	Reference Metabolite	β estimate	Standard Error	P-value
BG	Cr.PCr	0.113	0.148	0.4469
	Glu	0.087	0.263	0.7406
	Ins	0.024	0.129	0.8558
	NAA	0.442	0.137	0.0015
	GPC.PCh	0.077	0.033	0.0221
WM	Cr.PCr	-0.040	0.076	0.6009
	Glu	-0.178	0.182	0.3297
	Ins	0.018	0.121	0.8792
	NAA	-0.007	0.142	0.9600
	GPC.PCh	0.055	0.034	0.1037
GM	Cr.PCr	0.043	0.138	0.7555
	Glu	-0.136	0.278	0.6258
	Ins	0.119	0.138	0.3897
	NAA	0.111	0.183	0.5457
	GPC.PCh	0.076	0.035	0.0323

Table 4.7: The estimates of HIV Status-Age interaction effect size from the multilevel mixed effect model with different metabolite-region references.

Reference Region	Reference Metabolite	β estimate	Standard Error	P-value
BG	Cr.PCr	-0.023	0.032	0.4746
	Glu	-0.013	0.057	0.8231
	Ins	0.010	0.028	0.7163
	NAA	-0.084	0.030	0.0046
	GPC.PCh	-0.005	0.006	0.4350
WM	Cr.PCr	0.003	0.016	0.8512
	Glu	0.002	0.039	0.9576
	Ins	0.001	0.026	0.9730
	NAA	0.005	0.031	0.8753
	GPC.PCh	0.000	0.006	0.9532
GM	Cr.PCr	0.001	0.030	0.9776
	Glu	0.006	0.061	0.9159
	Ins	0.022	0.030	0.4648
	NAA	-0.009	0.040	0.8214
	GPC.PCh	0.003	0.007	0.7104

Comparing the effects of age between the model with and without the age*HIV status interaction term is equivalent to comparing the effect of age on the respective metabolite concentrations across all children (for the model without age*HIV status) and for HIV- children only (the model with the age*HIV status interaction). These estimates are illustrated in Tables 4.4 and 4.8. The effect of age on metabolite concentrations of HIV- children is very similar to the effect on the

group as a whole (Table 4.8 and 4.4). The effect sizes show very little change between the two models, apart from the estimate of the age effect on BG-NAA levels which has increased from 0.046 to 0.103 and which was previously non-significant but with this inclusion on HIV*Age interaction we see the age effect is now significant. The effect of age on BG-Glu, WM-Ins and GM-Glu concentration was significant across all children, but when looking specifically at the HIV- group this effect is no longer significant.

Table 4.8: The estimates of age effect size from the multilevel mixed effect model with an age*status interaction, given different metabolite-region references.

Reference Region	Reference Metabolite	β estimate	Standard Error	P-value
BG	Cr.PCr	0.202	0.036	<0.0001
	Glu	0.113	0.064	0.0775
	Ins	0.089	0.031	0.0043
	NAA	0.103	0.033	0.0020
	GPC.PCh	0.021	0.007	0.0035
WM	Cr.PCr	0.079	0.020	0.0001
	Glu	0.106	0.049	0.0317
	Ins	0.061	0.033	0.0617
	NAA	0.210	0.039	<0.0001
	GPC.PCh	0.002	0.008	0.7666
GM	Cr.PCr	0.140	0.034	<0.0001
	Glu	0.126	0.069	0.0652
	Ins	0.074	0.034	0.0304
	NAA	0.108	0.045	0.0165
	GPC.PCh	0.021	0.008	0.0100

Figure 4.5 reiterates the importance of including MRI scanner and relative % of GM as covariates in this model. We see relative % of GM has a significant effect on almost all metabolite concentrations with some large effect sizes (Figure 4.5A). We generally see an increase in relative GM% leading to an increase in metabolite concentrations, apart from the concentration of GPC+PCh in the PWM region which decreased as GM% increased.

We also see the scanner used had a significant effect on all but one metabolite measured with consistently positive effect sizes (Figure 4.5B). Again, reiterating that greater concentrations were recorded using the Skyra MRI scanner compared to the Allegra scanner.

Figure 4.5: The effects of (A) relative GM% and (B) MRI Scanner (Allegra as the reference) for the respective metabolites given different regions along with 95% confidence bands.

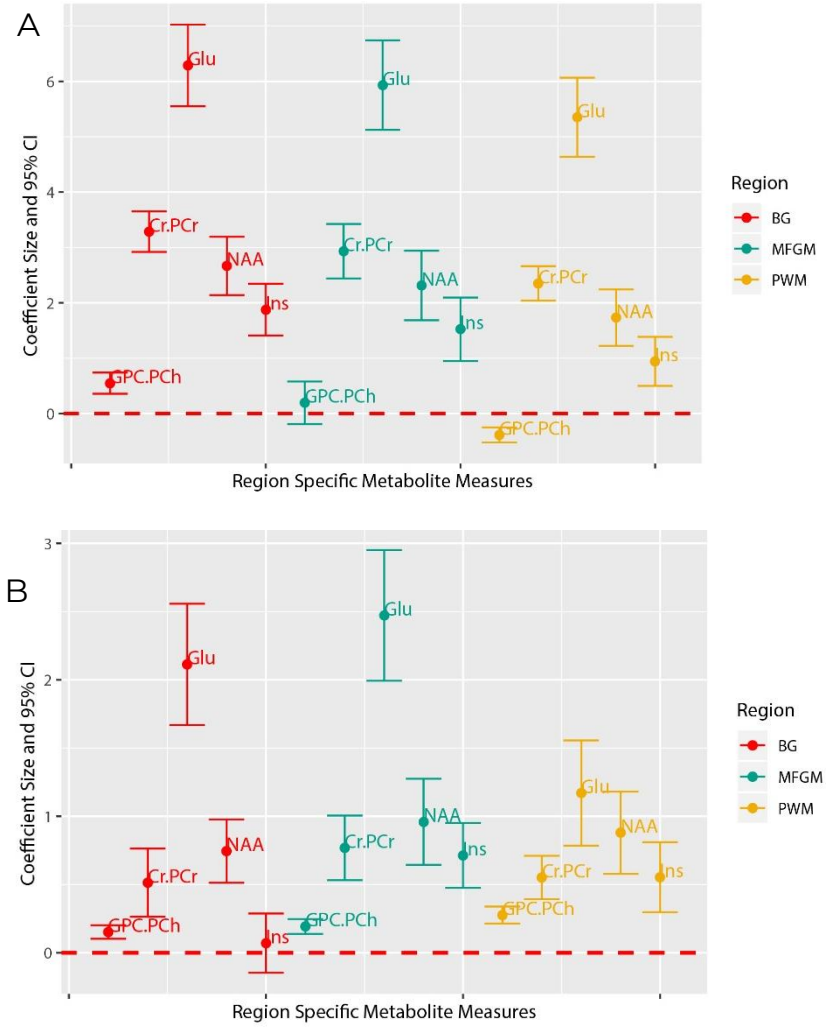

The residual plots of fitted values against residuals show no obvious data structures that would lead to questioning the model validity (Figure 4.6A,). However, we see a deviation from normality in the histogram of residuals (Figure 4.6B). This deviation is not due to skewness, but instead due to both positive and negative outliers.

Figure 4.6: (A) Residuals vs Fitted Values and (B) histogram of residuals from the model not considering age*status interaction.

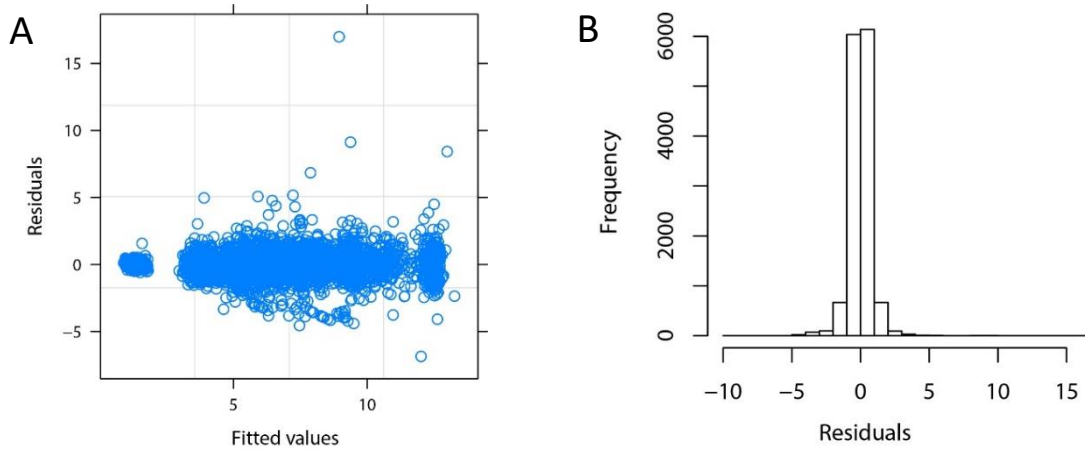

Generally, this multilevel mixed effect model approach has validated all previous findings from the univariate modelling approach. We have seen significance in the interaction terms allowing for formal inferential comparison of effects across metabolites and regions and reinforcing the need to study this in a multivariate setting.

However, the huge number of interaction terms has also complicated the interpretation of this model. Because of the complexity seen in this model we moved onto the CRM approach to try a different multivariate analysis approach in the hopes of once again validating previous findings and improving the interpretability of the final model.

4.3.2 Correlated Response Models:

For the correlated response model approach, three models were fit and compared; a purely latent response model, a model with a linear component of the subject covariates added to the latent response model and a model that allows the linear model coefficients to vary with response variable traits.

The latent response model:

The formulation of the latent response model is:

$$E(Y_{ijt}) = \beta_{0j} + z_i^T \theta_j + u_i \ .$$

In this formulation θ_j values are the column-specific coefficients (the factor loadings) relating to the created latent factors, β_{0j} accounts for differences between the metabolite concentrations while u_i represents a subject specific random effect and accounts for the correlation within the data due to repeated subjects over time(Hui and Blanchard, 2018).

Typically, one to three latent variables are used to allow the comparison of these variables through the use of plots and easy interpretation of these latent variables

(Hui and Blanchard, 2018). We have chosen to include three latent variables in this latent factor model and all subsequent correlated response models. Three variables were included for ease of plotting and interpretation and because the source of variability was largely explained by the first latent factor and then less and less was observed in the second and third factors (Table 4.9).

Table 4.9: The proportion of variance explained by the respective factors from a FA model with 2, 3 and 4 latent factors.

	Factor 1	**Factor 2**	**Factor 3**	**Factor 4**	**Cumulative Variance**
Model with Two Factors	0.324	0.287	-	-	0.611
Model with Three Factors	0.273	0.205	0.196	-	0.674
Model with Four Factors	0.259	0.205	0.141	0.115	0.720

The extracted factor loadings for this model are presented in Table 4.10. The first factor appears to represent a metabolite factor where Glu has large positive values across all three regions while GPC+PCh has the smallest values across all three regions (Table 4.10). This may be due to the differences in scale when looking at metabolite concentrations where Glu has the largest concentrations and GPC+PCh has the smallest, though this is largely accounted for by β_0 (Figure 3.4). In chapter 2 we observed the greatest variability within the measurements of Glu and the smallest variability within the observations of GPC+PCh. This first latent factor may also be identifying this difference in variability. Hence, the first factor may be an 'accuracy'/scale factor which represents the greatest source of variability within residuals. The second and third factors point toward region factors where the MFGM is being contrasted to the BG and WM regions – this is clear for the second factor whereas factor three does not appear to contribute much new interpretable information (Table 4.10).

Table 4.10: Estimated coefficients from a purely latent factor model.

Region	Metabolite	β_0	θ_1	θ_2	θ_3
MFGM	Glu	10.958	1.953	0.000	0.000
	Ins	5.832	0.744	0.107	0.000
	NAA	6.868	1.012	0.203	0.041
	GPC.PCh	1.341	0.166	0.020	-0.007
	Cr.PCr	6.144	1.003	0.071	0.051
PWM	Glu	6.193	0.835	-0.111	-0.645
	Ins	4.414	0.434	-0.056	-0.109
	NAA	6.318	0.918	-0.141	-0.480
	GPC.PCh	1.309	0.148	-0.026	-0.010
	Cr.PCr	4.123	0.492	-0.067	-0.276
BG	Glu	9.438	1.201	-0.601	-0.120
	Ins	3.728	0.191	-0.162	0.016
	NAA	5.862	0.448	-0.197	-0.082
	GPC.PCh	1.345	0.119	-0.062	-0.010
	Cr.PCr	6.674	0.756	-0.386	-0.007

The latent response and GLM model:

To investigate the longitudinal trends, we included a GLM component:

$$E(Y_{ijt}) = \beta_{0j} + X_i^T \beta_j + z_i^T \theta_j + u_i \ .$$

Once again, the latent variable (LV) component ($z_i^T \theta_j$) induces a residual covariance among the columns of the response matrix Y_{ijt} (Hui and Blanchard, 2018). We can look at these latent factor estimates to try understand the relationships among the residuals and hence, the latent connections within the data.

Table 4.11: Estimated latent factor loadings from a model with a latent factor and GLM component.

Region	Metabolite	β_0	θ_1	θ_2	θ_3
MFGM	Glu	2.805	1.077	0.000	0.000
	Ins	3.238	0.468	0.170	0.000
	NAA	2.200	0.649	0.211	0.152
	GPC.PCh	0.847	0.072	0.050	0.006
	Cr.PCr	2.200	0.670	0.093	-0.047
PWM	Glu	2.927	0.162	-0.366	0.416
	Ins	2.499	0.156	-0.107	0.067
	NAA	3.757	0.252	-0.373	0.392
	GPC.PCh	1.121	0.058	-0.033	0.027
	Cr.PCr	3.394	0.153	-0.191	0.154
BG	Glu	4.452	0.367	-0.610	-0.260
	Ins	1.561	-0.012	-0.066	-0.146
	NAA	4.996	0.167	-0.287	-0.028
	GPC.PCh	0.863	0.037	-0.057	-0.023
	Cr.PCr	3.959	0.412	-0.495	-0.317

While previously the first factor appeared to be a metabolite factor (Table 4.10), this metabolite effect has now been overshadowed and instead the first factor appears to be a MFGM region factor (Table 4.11). The differences in metabolite responses is largely explained by the covariates within the GLM model, which is likely why this first factor now presents as a MFGM region factor. The second factor shows large negative loadings for responses from the BG and smaller negative loading for responses from the PWM with small positive loadings for responses from the MFGM region (Table 4.11). This suggests the second factor contrasts MFGM responses against those from the PWM and BG regions. The third factor shows large positive loadings for responses from the PWM and large negative loadings for responses from the BG region, hence the third factor contrasts BG responses to PWM responses.

The CRM provides a GLM for each response variable and is thus a true multivariate model. This GLM component ($X_i^T \beta_j$) allows us to understand the effect of covariates on the different response variables. We have illustrated these estimates in Table 4.12 and Figures 4.7-4.10. Three covariates are included for relative GM % as this was measured in each region. We see the relative GM% measured in the MFGM has a large effect on the metabolites also measured in the MFGM region, with small (and

non-significant) effects in other regions (Table 4.12). This is consistent for the relative GM% measured in all three regions and is completely expected as the percentage of GM % measured in one voxel should be entirely independent of the concentration of metabolites measured in another region. The relative GM% covariates are further illustrated in Appendix A.4 in Figure A.4.2.

Table 4.12: The Estimated GLM coefficient sizes from the CRM with both the GLM and LV components.

Region	Metabolite	Age	Machine (Skyra =1)	HIV Status (HIV=1)	Relative GM (MFGM)	Relative GM (PWM)	Relative GM (BG)
MFGM	Glu	0.098	2.644	-0.038	6.268	1.100	0.202
	Ins	0.110	0.629	0.261	1.435	0.417	0.352
	NAA	0.075	1.101	0.085	3.867	0.426	-0.105
	GPC.PCh	0.036	0.141	0.096	0.041	0.151	0.251
	Cr.PCr	0.118	0.928	0.119	2.720	0.502	0.344
PWM	Glu	0.133	1.123	-0.118	0.887	5.765	0.492
	Ins	0.047	0.593	0.035	1.438	0.424	-0.120
	NAA	0.228	0.867	0.036	0.278	2.900	0.625
	GPC.PCh	0.007	0.264	0.061	-0.018	-0.479	0.139
	Cr.PCr	0.097	0.509	-0.012	-0.258	2.582	-0.241
BG	Glu	0.137	2.043	0.059	0.151	0.465	5.059
	Ins	0.133	-0.006	0.122	-0.131	-0.029	2.845
	NAA	0.042	0.674	0.065	0.436	0.071	-0.228
	GPC.PCh	0.015	0.192	0.067	-0.085	-0.016	0.605
	Cr.PCr	0.178	0.608	0.081	-0.085	0.286	2.771

The response specific intercepts (β_{0j}) from this model show the metabolite concentrations when all covariates are zero (Figure 4.7). This shows different scales and differing variability across metabolites and across regions (Figure 4.7). In particular, the metabolite with the smallest concentration in all three regions was GPC+PCh, and NAA was the most abundant metabolite within both the PWM and BG regions (Figure 4.7). The metabolite with the greatest variability in measurement across all three regions was Glu (Figure 4.7).

Figure 4.7: The β_{0j} estimates with 95% CI* for each of the response variables from the CRM model with both the LV and GLM components.

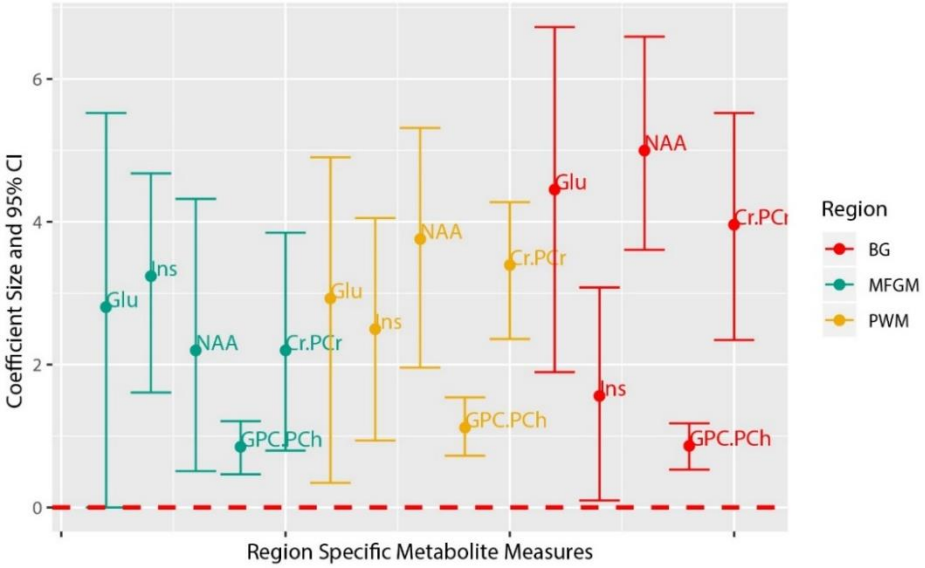

The effect of age on metabolite concentrations is positive for all metabolites (Figure 4.8). In the MFGM region Ins, NAA and Cr+PCr have significant increases with age. In the PWM region Glu, NAA and Cr+PCr are significantly increasing with age (Figure 4.8). Finally, in the BG region all metabolites apart from NAA increased significantly with age. In the MFGM and BG regions Cr+PCr showed the biggest increase across age, and in the PWM NAA showed the largest increase (Figure 4.8).

Figure 4.8: The Age effect size estimates with 95% CI* for each of the response variables from the CRM model with both the LV and GLM components.

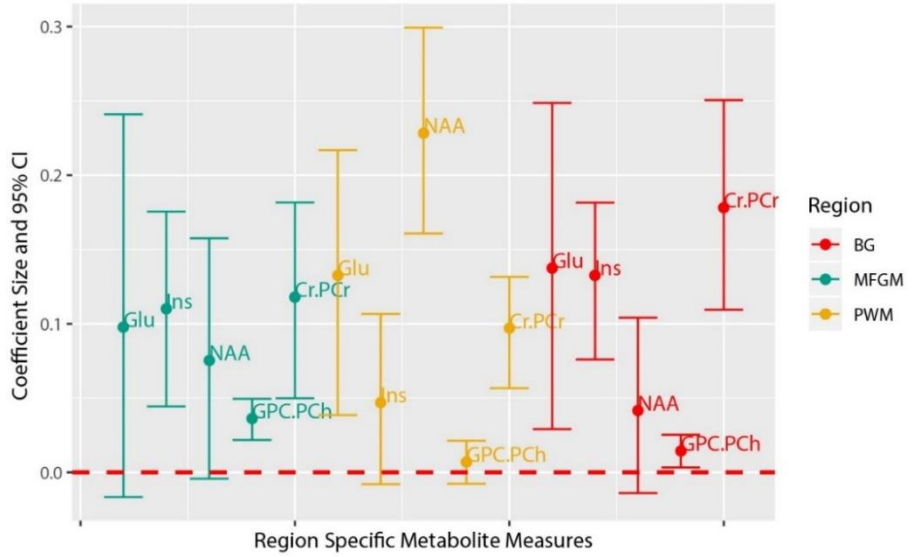

The results discussed thus far were extracted from the CRM model without an Age*HIV Status interaction term. These results were shown as the model without this interaction term had better model fit and allows for easier interpretation. To observe the effect of this term we have presented the effect of HIV status on metabolite concentrations when considering an Age*HIV Status interaction and when this term is omitted (Figure 4.9).

Figure 4.9: The Effect and 95% CI* of (A) HIV Status from the CRM model without an Age*HIV interaction term, (B) HIV Status from the CRM model with an Age*HIV interaction term and (C) the HIV*Age interaction term. Here a positive value indicates greater concentrations observed for HIV+ children compared to HIV- controls.

(A)

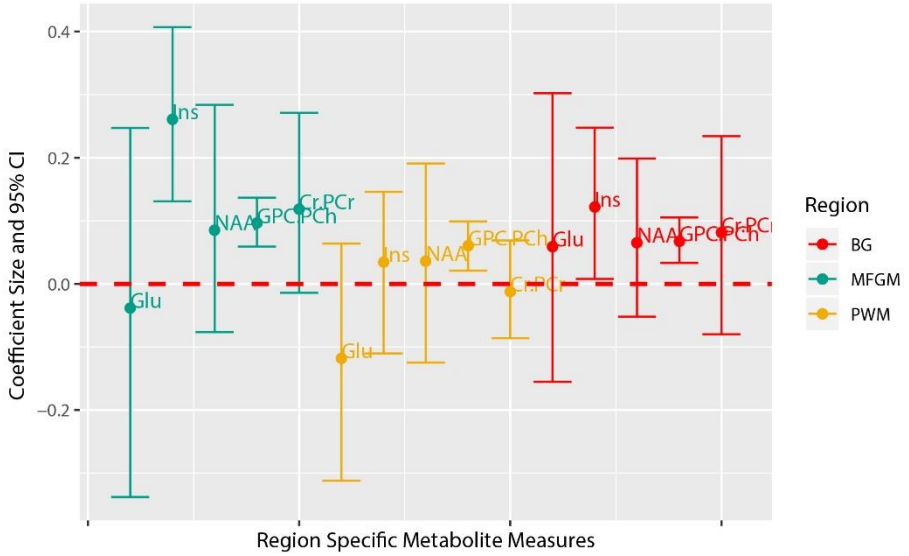

(B)

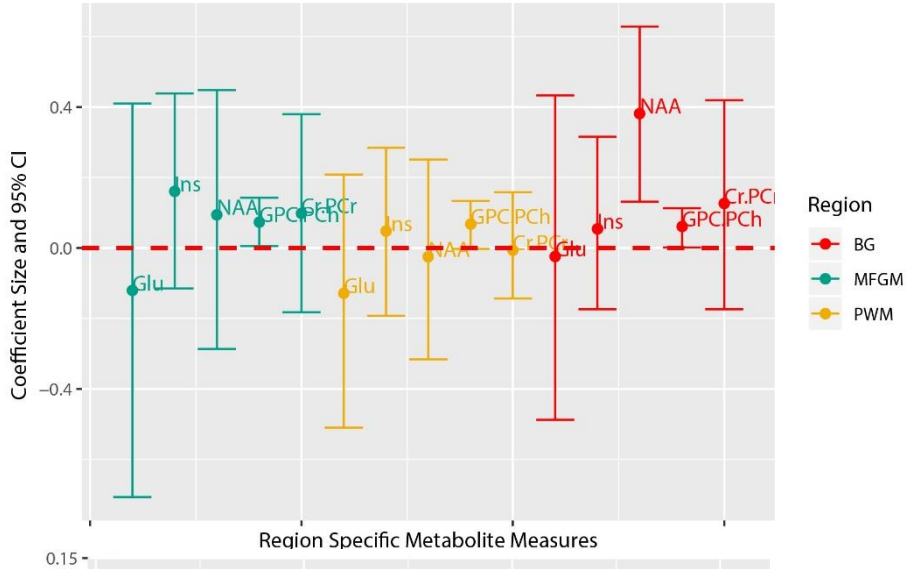

(C)

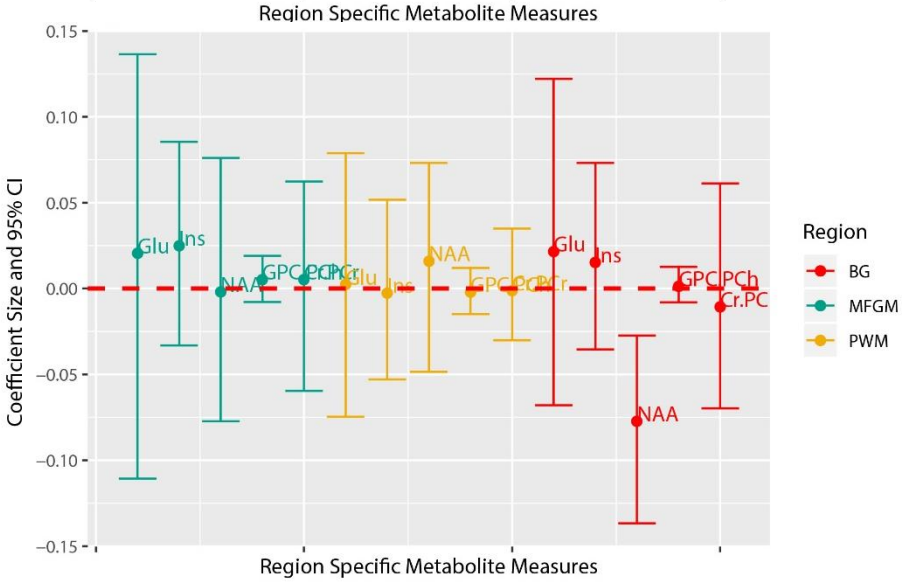

The effect of HIV from the CRM without the Age*HIV status interaction term refers to the differences in metabolite concentrations between HIV+ and HIV- children across all ages, while the model with this interaction term refers to the differences at age 5. Across all ages we see elevated levels of MFGM and BG levels of Ins and GPC+PCh in HIV+ children; the only metabolite with significantly increased concentrations in the PWM is GPC+PCh (Figure 4.9A). Thus, across all ages and regions we see elevated GPC+PCh levels in HIV+ children (Figure 4.9A).

When the HIV*Age interaction term is included, we see NAA in the BG region is significantly elevated within HIV+ children (Figure 4.9B). We also see GPC+PCh is significantly elevated in all three regions, but the significance here is not as strong as seen in the model without the interaction term (Figure 4.9B). This means that at age 5 BG-NAA concentration is clearly higher in HIV+ children. Looking at the Age*HIV Status interaction term, the effect sizes are small and non-significant for all metabolites with the exception of NAA in the BG region (Figure 4.9C). Hence, the elevated concentrations of NAA seen at age 5 progressively decreases over time. These results are completely in line with the results obtained from the univariate models and multilevel mixed effect models.

The machine effect was significant for each metabolite in each region of the brain, except for Ins in the BG, which reiterates why scanner was added as a covariate in this model (Figure 4.10). The effect was consistent, that the use of Skyra lead to an increased metabolite concentration, however the size of these effects were not consistent across the regions or metabolites measured (Figure 4.10).

Figure 4.10: The scanner effect size estimates with 95% CI* for each of the response variables from the CRM model with both the LV and GLM components.

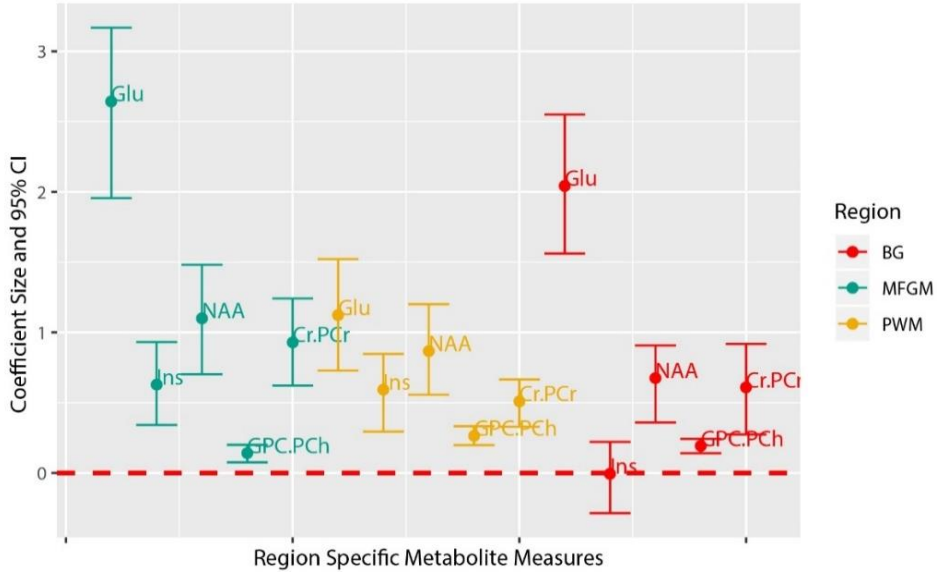

The correlation due to covariates shows the strong positive relationship between all metabolites in all regions (Figure 4.11). Hence, an increase in one metabolite is generally correlated with an increase in another. We are unsurpised to see this as the largest effect on these metabolites is due to age and machine which both have an increasing effect on the metabolite concentrations.

Looking at the residual correlation we see the next level of association is due to region related relationships more than metabolites across regions (Figure 4.11). Almost no associations exist between the concentrations in the BG and MFGM regions, while the PWM-BG and MFGM-PWM shows weak associations. The strong positive correlations seen here are showing that the relationship within a region between metabolites is greater than the relationship of metabolites between different regions.

Figure 4.11: The correlation among the data due to covariates and residual correlation.

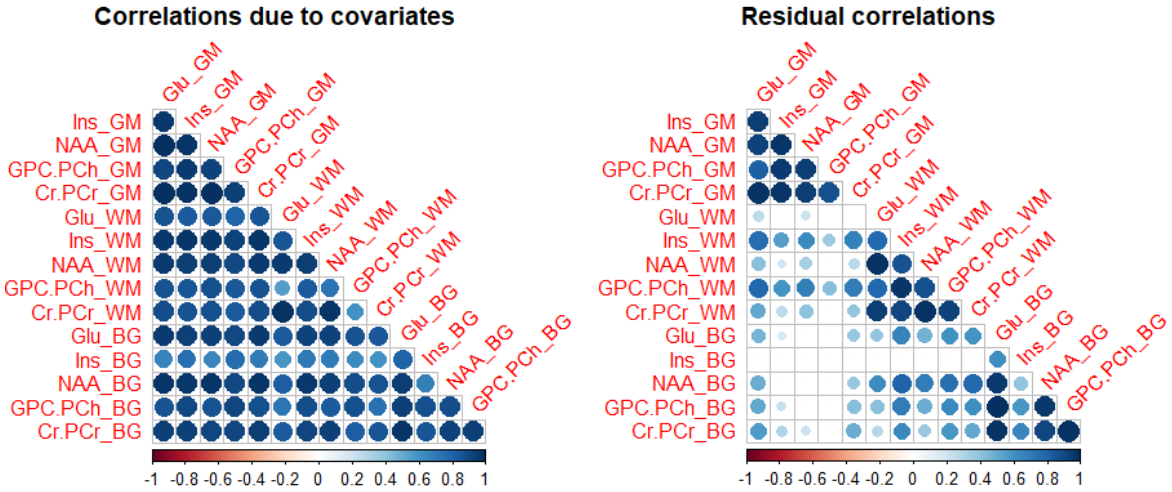

The latent component of the CRM can be illustrated by creating biplots of observations and variables in the dimensions determined by the latent variables. Figure 4.12 illustrates these biplots of the purely latent model and the latent model of the residuals after the GLM component was added.

When comparing the biplots for the purely latent models to those from the correlated response models we see slightly different loadings as a result of including the covariates in the model (Figure 4.12). In both the latent factor (LF) and CR model biplots we see rough grouping of response variables by region, except for the GPC+PCh metabolites which cluster together instead of with the relative regions these observations were measured in (Figure 4.12). This suggests that generally a stronger within-region association is present between metabolite concentrations, apart from the GPC+PCh metabolites which have a strong association between concentrations across the regions (indicated using the orange arrows). This reiterates what we have observed in the correlation plots in Figure 4.11. The biplots do not show any particular grouping of observations by HIV status (Figure 4.12).

Figure 4.12: The biplots for the purely latent model and the correlated response model, comparing the three latent factors.

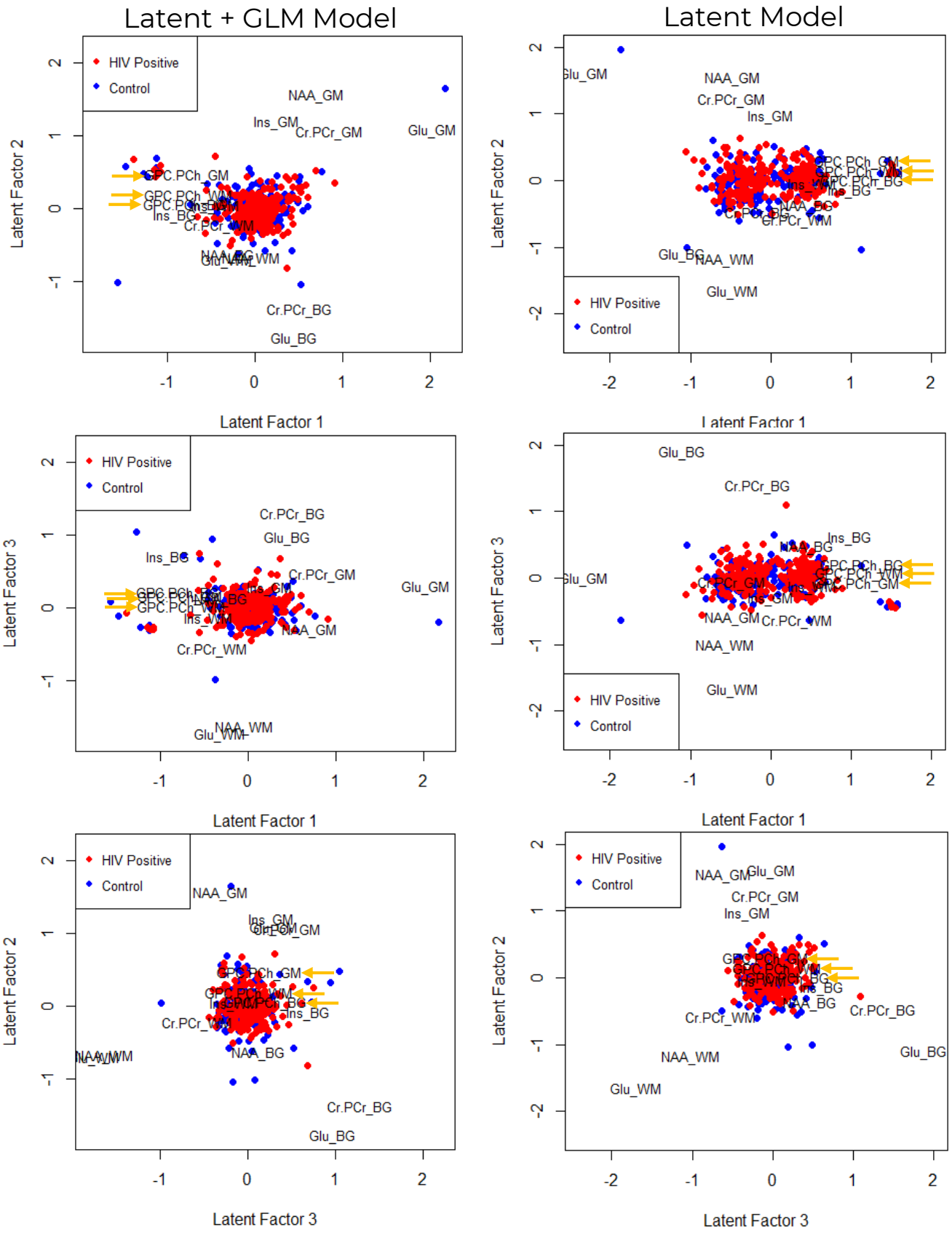

The CR-traits model:

The CRM can be extended to include variable (as opposed to sample) characteristics and thus model the interaction between variable and sample characteristics. This is done through the inclusion of so-called 'traits'. We thus extend the CRM without the Age*HIV status interaction in the following manner:

$$E(Y_{ijt}) = \beta_{0j} + X_{it}^T \beta_j + z_i^T \theta_j + u_i$$
$$\beta_{0j} \sim N(\boldsymbol{t}_j{}^T \boldsymbol{\kappa}_0,\ \sigma^2{}_0)$$
$$\beta_{jk} \sim N(\boldsymbol{t}_j{}^T \boldsymbol{\kappa}_k,\ \sigma^2{}_k)$$

$j = 1\ to\ 15$ (3 metabolites x 5 regions),

$k = 1\ to\ 3$ (three covariates of interest: age, HIV status and machine),

where β_{jk} is the kth regression coefficient in β_j. This relates the response column specific coefficients β_{0j} and β_j to their corresponding traits using the trait coefficients ($\boldsymbol{\kappa}_k$).

The latent factor ($z_i^T \theta_j$) and GLM ($X_i^T \beta_j$) estimates from this model were very similar to the estimates obtained from the model without the traits component and are reported in Appendix A.4 in Tables A.4.6 and A.4.7 and Figure A.4.3. The traits estimates give us an insight into the marginal effects of our sample/subject covariates of interest on the different regions or metabolites as a whole, thus the effects are measured across all metabolites within a region or for the same metabolite across the three regions. Table 4.13 gives average estimates for β_{0j} and the modification due to metabolite or region. The inference is estimated and illustrated using 95% CI (Figure 4.13). Unfortunately, this technique is not very powerful and accordingly the estimates of these modification effects have very large credibility intervals (Figure 4.13).

Table 4.13: Effect sizes of the Traits portion of the correlated response model for selected covariates.

	κ_0	Cr+PCr	Glu	GPC+ PCh	Ins	NAA	BG	GM	WM	σ
Intercept	1.979	0.820	1.200	-1.644	0.067	1.487	0.676	0.668	0.835	0.765
Age (years)	0.100	0.014	0.004	-0.098	-0.016	-0.002	0.012	0.024	0.013	0.064
Machine (Skyra)	0.431	0.012	1.275	-0.450	-0.248	0.236	0.111	0.404	0.107	0.378
Status (HIV+)	-0.028	0.069	-0.036	0.110	0.175	0.085	-0.048	0.027	-0.015	0.031

As we have previously observed, the effects of the different covariates on metabolites is not consistent across regions or metabolites and this aspect of the CR Model further confirms that. We see large CI* bands and small effect sizes (Figure 4.13 and Table 4.13) because the different regions and same metabolites from different regions all interact independently from one another. Contrary to what this model aims to show, which is a conserved region or metabolite effect we

see relationships within a region to be more important. Thus, increases and decreases that are metabolite-region specific cancel out and we are left with small non-significant effect sizes (Figure 4.13 and Table 4.13).

Figure 4.13: The (A) baseline marginal concentration across regions and metabolites and global effects due to (B) the scanner, (C) HIV Status and (D) Age on different metabolite concentrations across all three regions, as given by the inclusion of traits in the model, with 95% CI*.

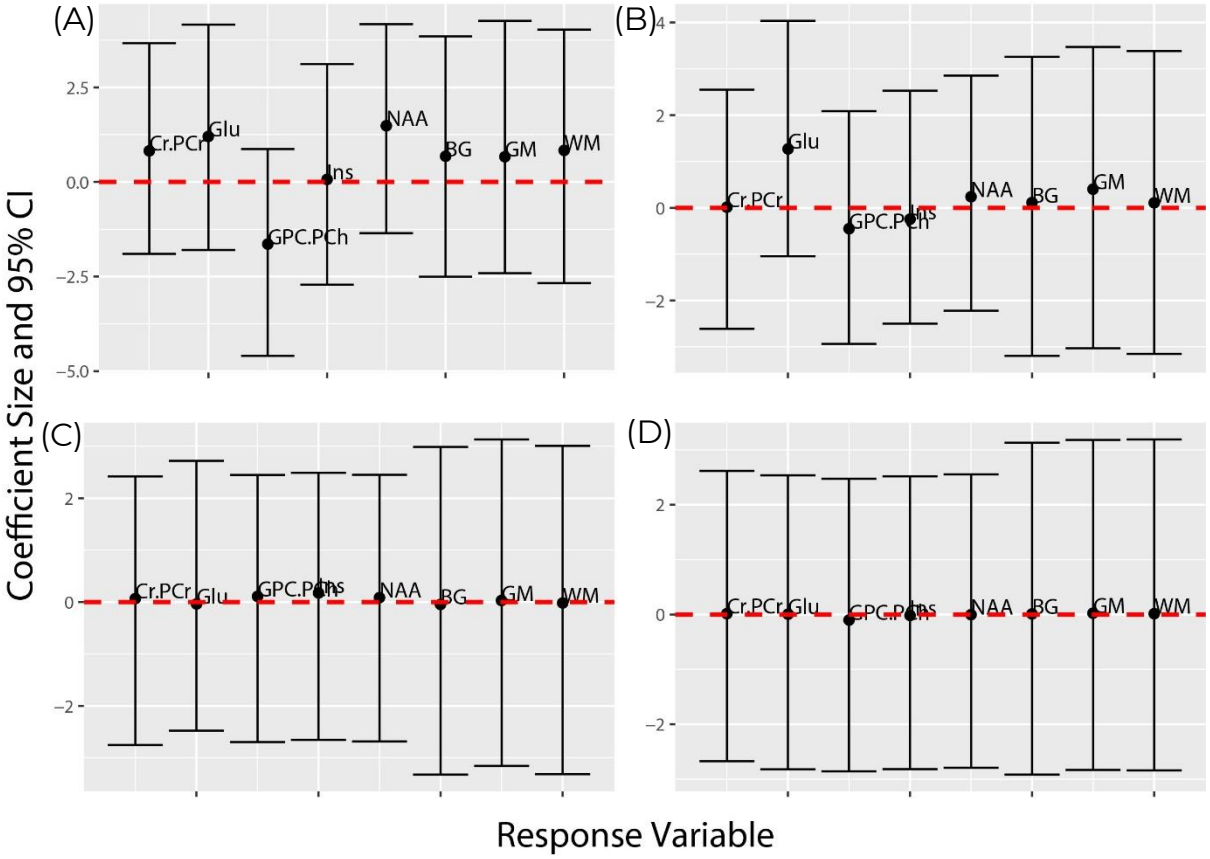

The estimates within Table 4.13 reflect two-way interactions between age, machine, status and either metabolite or region. To investigate three-way metabolite-region-age (or status/ scanner) interactions metabolite-region interaction traits may also have been included. We chose not to do so as this model already proved to be underpowered and from the multilevel LMEM we saw these three-way interactions were seldom significant and informative.

Model Validation:

The change in relative residual correlation was used to measure model improvement. A very small change indicates little improvement in the model. Starting with the latent model, we see that adding the GLM structure improved the model fit substantially (Table 4.14). However, adding the traits matrix component to the model and the age*status interaction made a very little change in the model fit. This is expected as the traits component of the results showed no significance and no results of interest, and the age*status interaction also did not show any significance or large effect sizes for most metabolites. Hence, we conclude that the basic CR Model without the traits component and an age*status interaction best explains the data.

Table 4.14: CR Model fit improvements due to the model changes.

Model 1	**Model 2**	**Change in relative residual correlation due to model 2**
Latent variable Model	Basic Correlated Response Model	0.669
Basic Correlated Response Model	Basic Correlated Response Model with Age*HIV Status	0.054
Basic Correlated Response Model	Correlated Response Model and traits matrix incorporated	0.0004

The residual plots show that there are no data structures that need to be corrected in this model, and the qq-plot shows the within subject residuals are indeed normally distributed apart from some outlying observations (Figure 4.14).

Figure 4.14: The model validity investigation for the final correlated response model.

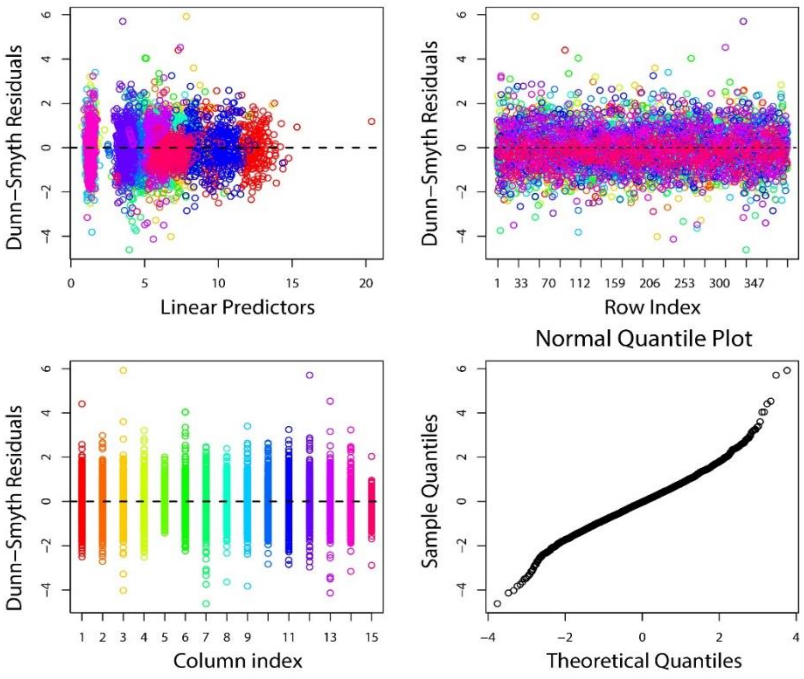

4.4 Discussion:

This chapter presented two approaches to modelling the multivariate response vector of metabolite concentrations in three brain regions. The multilevel LME's achieved this by transforming the multilevel responses to a long univariate response vector and modelling this as a function of metabolite type and region in addition to HIV status, age and the other confounding variables. The advantage of this approach is the inclusion of the interaction terms of metabolite type and region with HIV status and age that allows for formal inference with respect to the different effects of HIV status and different age profiles across metabolites and across regions. Unfortunately, the inclusion of many higher order interactions complicates the interpretation.

The long univariate response vector reflects a multilevel design of repeated measures across age for each metabolite within each region for each subject. We captured the within subject association through the inclusion of a subject-specific random effect. This imposed an equal and exchangeable correlation structure on all measurements taken for the same subject across age, metabolite type and region. We allowed for different variance estimates by metabolite and region through the use of a stratified variance function. To allow for different levels of correlation within specific metabolite type and region we could have added complex within subject correlation measures or added region within subject and metabolite within region within subject specific random effects. For the sake of model parsimony, we chose not to do so.

The correlated response model is a true multivariate approach in that it models the multivariate response vector, thus giving separate model estimates for each metabolite and region specific element of that vector while capturing the correlation between the multiple responses through a latent component. One benefit of the latent modelling approach is parameter reduction through the choice of the two or three most important latent variables.

This approach leads to a simple interpretation of the association between the covariates of interest and the different response variables. The inference related to the interaction terms of the multilevel LME is replaced by the traits component. Additionally, the model incorporates an ordination component that captures unmeasured and modelled residual associations.

The preliminary hierarchical model shows that there is a significant region-metabolite interaction, confirming the need for the multivariate modelling approach. Both the CRM and multilevel LMEM approaches further validated our previous findings from Chapter 3. Age had a consistently positive effect on most metabolites, apart from BG-NAA and PWM-GPC+PCh which was not significantly affected over time, seen from both the multilevel LMEM output and the CRM output with the traits component. Interestingly, without the traits component, MFGM-Glu, MFGM-NAA, PWM-Ins, PWM-GPC+PCh and BG-NAA was not significantly affected by age.

The multilevel LMEM and CRM showed GPC+PCh was significantly increased in HIV+ children in all three regions of the brain and MFGM-Ins was also increased in HIV+ children. The CRM also showed a significant increase of BG-Ins in HIV+ children. At age 5 GPC+PCh was elevated in all three regions of the brain, as was BG-NAA. The Age*HIV Status interaction significantly affected BG-NAA, showing that as time progressed the difference in NAA concentrations between HIV+ and HIV- children decreased.

Generally, the effect of scanner and relative % GM was also significant across all metabolites and regions and metabolites measured using the Skyra scanner had greater concentrations recorded compared to those measured using the Allegra scanner. The results from the CRM and multi-level approaches are almost identical, apart from a few differences particularly relating to the effect of age and HIV on metabolite concentrations. As this is an exploratory study both approaches have given us further insights into the possible underlying effects we may not have captured had we used only one of the approaches. Hence, the use of both has proved to be very beneficial.

From the CRM latent factor output and correlation between covariates and residuals we can see a clear association between GPC+PCh concentrations across regions and associations between different metabolites within the same region. This is a key advantage to using the CRM approach as we would not have identified these patterns if we only used the multilevel LMEM approach.

Other advantages of the CRM approach include the ease of interpretation and that fewer parameters need to be estimated compared to if one was using the multilevel LME approach. Hence, there is greater power when using this approach. While the multilevel LMEM is easy to program and adapt once a univariate model has been created, the interpretation thereof is extremely complicated. Another limitation for this approach is the large positive and negative residuals.

The CRM approach also has the benefit of both GLM and FA output which allows further investigation of the data with no extra effort. One limitation of the CRM is that only individuals that were scanned in all three brain regions and where all metabolites were recorded may be used as the response profiles must be complete with no missingness, hence some data is lost. The CRM approach does not have the benefit of formal inference on two- and three-way interaction terms as the multilevel LME does. In theory, the traits component of the model is an equivalent method of investigating these interactions, however in practice it did not prove to give as informative results as the multilevel LME approach.

The CRM approach also did not offer a clear method of including the different relative GM%'s measured, which were different for responses measured within the three regions of the brain. Three relative GM% covariates (measured for the BG, PWM and MFGM voxels respectively) were included within the CR model which allowed the effect of these to be observed on the response variables related to these covariates. However, for example, it also means the effect of relative GM%

measured within the PWM is examined for an effect on concentrations measured within the BG and MFGM region (see Appendix A.4 for the illustration hereof), which we know should be zero as the responses from one region and relative GM% from another are entirely independent. Hence, the CRM model does not allow for clear incorporation of response specific covariates within the model.

Chapter 5: Conclusion

This dissertation focused on an analysis aimed at characterising the impact of HIV infection on longitudinal brain metabolite profiles of children ages 5 to 11. The structure of the data and features of the data collection process lead to interesting statistical challenges. These included:

i) a change in MRI scanner during data acquisition,
ii) repeated measures due to repeated observations within subjects,
iii) a multivariate response vector as a result of repeated metabolites measured across different regions, which were also repeated over time.

The key statistical aim was to create a model that performed three functions: i) account for the scanner effect within the data, ii) account for correlation due to repeated subjects over time and to iii) account for correlation due to repeated regions and metabolites at the same time point.

The change in MRI scanner introduced a source of variability which was investigated using linear regression and Bland-Altman tests. This also involved looking at inter- and intra-scanner variability to identify the severity of the bias introduced by the scanner, relative to normal variability present in our data. From the inter- and intra-scanner analysis it was clear that the variability introduced by the change in scanner was greater than normal intra-scanner variability. This linear regression analysis showed a consistent scale effect, but a random association between unit changes on the two scanners. It thus necessitates inclusion of a scanner effect in the models. One concern is the confounding caused by age and scanner. We see a clear increase in metabolite concentrations with age, as well as an increase due to the change in scanner. The scanner change occurred during the age nine follow-up visits with an average time of 10.8 months between the observations used to harmonize this scanner effect, thus it is difficult to entirely separate the scanner and age effects.

As this study was longitudinal, correlation induced by the repeated observations from the same subjects had to be addressed during analysis. This led to the use of

linear mixed effect models which were created separately for each metabolite measured within each region. We created linear mixed effect models with a subject-specific random effect which imposes an equal and exchangeable correlation structure and hence captures the correlation between observations. Linear models were used as the concentrations appeared to be following a positive linear relationship with age.

As the data was truly multivariate in nature, we created a multivariate model to allow analysing all the given data at once, instead of separate independent analyses. This was performed using a multilevel linear mixed effect model and a correlated response model. The correlation within the data due to measurements from the same brain regions and of the same metabolites may be captured by the multilevel LME model in two ways: i) through the use of nested region-within-subject random effects and metabolite-within-region-within-subject random effects or ii) using specified variance structures. We chose to specify a stratified variance structure by metabolite-region grouping. The correlated response model is composed of GLM and latent factor components. Separate GLMs are fit to each of the response variables producing response-specific estimates of effect sizes. The CRM accounts for the correlation due to repeated measurements from the same region/metabolite with a latent factor component within the CR model. This latent factor component uses the residuals to create factors that describe the variability and latent relationships present within the data.

The central clinical focus was to identify the effect of HIV status over the ages 5 to 11 on seven metabolites measured in three regions of the brain. We also included relative GM% and scanner as covariates to accurately understand the effect of HIV and to create reliable longitudinal profiles of these metabolite concentrations over development.

Looking at the effect sizes in Table 5.1 we can see that all three approaches of longitudinally modelling our data produced very similar results. The estimated effect sizes obtained using the multilevel- and univariate mixed effect modelling approaches are more similar than those estimated using the correlated response model approach, however all three appear to have a strong agreement between estimates (Table 5.1). The multilevel- and univariate mixed effect modelling approaches both use maximum likelihood estimation while the CRM approach employs Bayesian estimation techniques, this may be a reason for the slightly varied estimates. The CRM approach could only make use of observations that were complete (all metabolites measured in all three regions at a time point) which may be another cause for slightly different estimates.

Table 5.1: Summarised findings from each of the approaches used in this report to investigate the effect of HIV on metabolite concentrations.

Region	Metabolite	Univariate Mixed Effects Models		Multilevel Mixed Effects Model		Correlated Response Model	
		Estimate	95% CI	Estimate	95% CI	Estimate	95% CI*
MFGM	Glu	-0.115	[-0.390; 0.161]	-0.110	[-0.379; 0.159]	-0.038	[-0.338; 0.247]
	Glu+Gln	-0.200	[-0.554; 0.155]	-	-	-	-
	Ins	0.213	[0.059; 0.366]	0.207	[0.071; 0.343]	0.261	[0.131; 0.407]
	NAA	0.073	[-0.115; 0.261]	0.075	[-0.104; 0.254]	0.085	[-0.077; 0.284]
	NAA+NAAG	0.002	[-0.179; 0.184]	-	-	-	-
	Cr+PCr	0.046	[-0.094; 0.186]	0.046	[-0.090; 0.182]	0.119	[-0.014; 0.271]
	GPC+PCh	0.092	[0.052; 0.132]	0.086	[0.043; 0.129]	0.096	[0.059; 0.137]
PWM	Glu	-0.168	[-0.365; 0.029]	-0.169	[-0.353; 0.015]	-0.118	[-0.312; 0.064]
	Glu+Gln	-0.234	[-0.490; 0.022]	-	-	-	-
	Ins	0.023	[-0.133; 0.178]	0.022	[-0.102; 0.146]	0.035	[-0.110; 0.146]
	NAA	0.018	[-0.143; 0.178]	0.012	[-0.133; 0.157]	0.036	[-0.125; 0.191]
	NAA+NAAG	-0.005	[-0.173; 0.164]	-	-	-	-
	Cr+PCr	-0.036	[-0.125; 0.053]	-0.028	[-0.108; 0.052]	-0.012	[-0.086 ; 0.069]
	GPC+PCh	0.059	[0.016; 0.101]	0.057	[0.014; 0.099]	0.061	[0.021; 0.099]
BG	Glu	0.029	[-0.236; 0.293]	0.036	[-0.217; 0.288]	0.059	[-0.155; 0.302]
	Glu+Gln	-0.080	[-0.425; 0.265]	-	-	-	-
	Ins	0.053	[-0.093; 0.199]	0.064	[-0.062; 0.190]	0.122	[0.008; 0.248]
	NAA (HIV)	0.425	[0.162; 0.688]	0.442	[0.171; 0.712]	0.094	[0.131 ; 0.628]
	NAA (HIV*age)	-0.078	[-0.134; -0.021]	-0.084	[-0.142; -0.025]	-0.077	[-0.137; -0.027]
	NAA+NAAG	0.041	[-0.087; 0.168]	-	-	-	-
	Cr+PCr	0.026	[-0.123; 0.175]	0.021	[-0.124; 0.165]	0.081	[-0.080; 0.234]
	GPC+PCh	0.052	[0.014; 0.091]	0.057	[0.016; 0.098]	0.067	[0.033; 0.105]

*As Bayesian estimation processes were used these are credibility intervals instead of confidence intervals.

In all three models we found significant differences between HIV+ and HIV- children indicating:

i) Increased MFGM-Ins in HIV+ children,
ii) Increased MFGM-GPC+PCh in HIV+ children,
iii) Increased PWM-GPC+PCh in HIV+ children,
iv) Increased BG-GPC+PCh in HIV+ children,
v) Decreased BG-NAA in HIV+ children,
vi) Increasing BG-NAA over time within HIV+ children.

The only observation not consistently identified was the difference in BG-Ins, seen using the CRM approach only.

The increases in GPC+PCh, as previously mentioned in chapter three, along with increases in Ins suggest inflammation within the BG, MFGM and PWM regions of HIV+ children. The elevated BG-NAA see at age five appears to be normalised by the age of nine, which is promising as it shows no evidence for neuronal dysfunction within these children. This validates the previous cross sectional findings (Mbugua et al., 2016, Robertson et al., Unpublished, Robertson et al., 2019).

Interestingly, in previous work, GPC+PCh was only identified as elevated at age 5 within the BG region, and at ages 7 and 11 within the MFGM (Mbugua et al., 2016 ; Robertson et al., Unpublished; Graham et al., Unpublished), while we observed clear increases in the concentration of GPC+PCh in all three regions across all ages. Glu was also found to be decreased within HIV+ children in the BG and MFGM regions

at age 9 (Robertson et al., 2018; Robertson et al., Unpublished) which contradicts our observations as no significant differences in Glu concentrations were detected between HIV+ and HIV- children. At age 11 PWM-NAA and PWM-Cr were also found to be significantly lower in HIV+ children (Graham et al., unpublished) which we have not identified throughout our analysis. This may suggest a non-linear modelling approach may be more appropriate when looking at the profiles of Glu, NAA and Cr+PCr across developmental ages.

The effects of age were generally positive and significant according to all approaches. The scanner effect was consistently significant and indicated greater concentrations measured using the Skyra scanner. The relative GM% showed to also have significantly increasing effects on most metabolite concentrations across all three regions. Thus, in future studies involving MRS data, we recommend the inclusion of a site or scanner variable, a measure of relative GM% and age.

The univariate mixed effect modelling approach was simple and proved to produce just as accurate results as the more complex multivariate models. This approach allowed for metabolite specific model building, which meant terms such as age*scanner or age*HIV could be included when relevant and when improving model fit.

All three approaches involved estimating a huge number of parameters and performing numerous hypothesis tests. The multivariate mixed effect modelling approach was particularly problematic in this regard as many of the estimated parameters were three- and four-way interaction terms, which are very difficult to interpret.

The correlated response model and multivariate mixed effects model allowed a look at the region-metabolite interactions at play, and lead to the conclusion that within-region effects among metabolite concentrations plays a bigger role than within-metabolite across regions effects. Only the concentrations of GPC+PCH seemed to be associated across regions, which ties in with the clinical significance of elevated GPC+PCH within HIV+ children.

Table 5.2: Summarised advantages and disadvantages of the three longitudinal modelling approaches used within this dissertation.

Method	Advantages	Disadvantages
Univariate LMEs	• Simple.	• Do not allow inference across metabolites or region, • Do not take multivariate nature of responses into account.
Multilevel LMEs	• Allow specific inference of effects across metabolites and regions.	• Complex.
CRM	• True multivariate model, • Allows for inference across regions and metabolites through traits, • Adds latent component to capture residual associations.	• Traits component lacks power, • Requires complete data.

The univariate- and multilevel mixed effect approaches produced residuals with very large and very small outliers. Thus, the correlated response model appeared to have the best model fit in terms of meeting assumptions about normality of residuals and also had a random scatter of residuals showing no need for imposing variance structures upon the data.

A normal distribution of data was assumed throughout this dissertation which generally appeared to produce adequate results. However, we see in some cases due to outlying residuals the model fit was not perfect. Not entirely resolving these outlying residuals is the first shortcoming within this dissertation. If one was to try account for these extremely large and small residuals one could consider assuming a Cauchy or t distribution when analysing this data.

Another limitation is that we are unable to make any distinction between the effects of HIV and the effects of AR treatment as all children that are HIV+ must be taking treatment. We may have clinical conclusions about what we have observed, but we do not know if separate interventions must be employed to resolve these effects due to HIV or if treatment must be altered to prevent these effects in the first place.

We fear that the scanner effect may still be present within the data due to the fact that the observations taken 'at the same age point - 9' are in fact not from the same age and actually have an average of 10.8 months between observations. Hence, the increases in concentration seen with age and seen due to the Skyra scanner confound one another and cannot be completely separated. This is the key limitation of this dissertation and unfortunately we were unable to hypothesise a means to resolve this.

An alternative approach, that one may try in future, to remove the scanner effect is through the use of ComBat (Johnson et al., 2007), a tool initially designed to remove 'batch effects' within microarray experiments, and recently applied to two multicentre studies looking at structural MRI and DTI data (Fortin et al., 2018, 2017). The general approach of ComBat is that it assumes the MRS data can be modelled as a linear combination of variables of interest, scanner parameters, the scanner effects and an error term that includes additive and multiplicative scanner-specific scaling factors (Fortin et al., 2018, 2017; Johnson et al., 2007).

If we would give recommendations to multicentre studies or studies that make use of more than one scanner the key advice would be to use a phantom sample when acquiring data. Phantoms are vials of fluid containing specifically known concentrations of metabolites that are placed within the MRI and analysed using the same protocols as when acquiring data from a subject. This allows exact quantification of the scanner bias which is clearly the difference between the concentration measured by the scanner and what was truly present within the vial. This approach was used by Harezlak et al., (2011) to account for site-specific differences within their study (Harezlak et al., 2011).

We would also recommend the study design to specify a time of day for data acquisition from each child as it is known that circadian rhythms effect metabolite concentrations all over the body throughout the day and this may also play a role in the variability seen within our data.

References

Aickin, M., Gensler, H., 1996. Adjusting for multiple testing when reporting research results: the Bonferroni vs Holm methods. Am. J. Public Health 86, 726–728.

Altman, D.G., Bland, J.M., 1983. Measurement in Medicine: The Analysis of Method Comparison Studies. J. R. Stat. Soc. Ser. Stat. 32, 307–317. https://doi.org/10.2307/2987937

Ashby, J., Foster, C., Garvey, L., Wan, T., Allsop, J., Paramesparan, Y., Taylor-Robinson, S.D., Fidler, S., Winston, A., 2015. Cerebral function in perinatally HIV-infected young adults and their HIV-uninfected sibling controls. HIV Clin. Trials 16, 81–87. https://doi.org/10.1179/1528433614Z.0000000003

Bandyopadhyay, S., Ganguli, B., Chatterjee, A., 2011. A review of multivariate longitudinal data analysis. Stat. Methods Med. Res. 20, 299–330. https://doi.org/10.1177/0962280209340191

Barreto, F.R., Otaduy, M.C.G., Salmon, C.E.G., 2014. Evaluation of nuclear magnetic resonance spectroscopy variability. Rev. Bras. Eng. Bioméd. 30, 242–247. https://doi.org/10.1590/rbeb.2014.023

Belman, A.L., Lantos, G., Horoupian, D., Novick, B.E., Ultmann, M.H., Dickson, D.W., Rubinstein, A., 1986. AIDS: calcification of the basal ganglia in infants and children. Neurology 36, 1192–1199. https://doi.org/10.1212/wnl.36.9.1192

Biberacher, V., Schmidt, P., Keshavan, A., Boucard, C.C., Righart, R., Sämann, P., Preibisch, C., Fröbel, D., Aly, L., Hemmer, B., Zimmer, C., Henry, R.G., Mühlau, M., 2016. Intra- and interscanner variability of magnetic resonance imaging based volumetry in multiple sclerosis. NeuroImage 142, 188–197. https://doi.org/10.1016/j.neuroimage.2016.07.035

Chang, L., Ernst, T., Witt, M.D., Ames, N., Walot, I., Jovicich, J., DeSilva, M., Trivedi, N., Speck, O., Miller, E.N., 2003. Persistent brain abnormalities in antiretroviral-naive HIV patients 3 months after HAART. Antivir. Ther. 8, 17–26.

Chong, W.K., Sweeney, B., Wilkinson, I.D., Paley, M., Hall-Craggs, M.A., Kendall, B.E., Shepard, J.K., Beecham, M., Miller, R.F., Weller, I.V., 1993. Proton spectroscopy of the brain in HIV infection: correlation with clinical, immunologic, and MR imaging findings. Radiology 188, 119–124. https://doi.org/10.1148/radiology.188.1.8099750

Cichocka, M., Bereś, A., 2018. From fetus to older age: A review of brain metabolic changes across the lifespan. Ageing Res. Rev. 46, 60–73. https://doi.org/10.1016/j.arr.2018.05.005

Cotton, M.F., Violari, A., Otwombe, K., Panchia, R., Dobbels, E., Rabie, H., Josipovic, D., Liberty, A., Lazarus, E., Innes, S., van Rensburg, A.J., Pelser, W., Truter, H., Madhi, S.A., Handelsman, E., Jean-Philippe, P., McIntyre, J.A., Gibb, D.M.,

Babiker, A.G., CHER Study Team, 2013. Early time-limited antiretroviral therapy versus deferred therapy in South African infants infected with HIV: results from the children with HIV early antiretroviral (CHER) randomised trial. Lancet Lond. Engl. 382, 1555–1563. https://doi.org/10.1016/S0140-6736(13)61409-9

Ernst, T., Kreis, R., Ross, B.D., 1993. Absolute Quantitation of Water and Metabolites in the Human Brain. I. Compartments and Water. J. Magn. Reson. B 102, 1–8. https://doi.org/10.1006/jmrb.1993.1055

Flowers, C.H., Mafee, M.F., Crowell, R., Raofi, B., Arnold, P., Dobben, G., Wycliffe, N., 1990. Encephalopathy in AIDS patients: evaluation with MR imaging. AJNR Am. J. Neuroradiol. 11, 1235–1245.

Fortin, J.-P., Cullen, N., Sheline, Y.I., Taylor, W.D., Aselcioglu, I., Cook, P.A., Adams, P., Cooper, C., Fava, M., McGrath, P.J., McInnis, M., Phillips, M.L., Trivedi, M.H., Weissman, M.M., Shinohara, R.T., 2018. Harmonization of cortical thickness measurements across scanners and sites. NeuroImage 167, 104–120. https://doi.org/10.1016/j.neuroimage.2017.11.024

Fortin, J.-P., Parker, D., Tunç, B., Watanabe, T., Elliott, M.A., Ruparel, K., Roalf, D.R., Satterthwaite, T.D., Gur, R.C., Gur, R.E., Schultz, R.T., Verma, R., Shinohara, R.T., 2017. Harmonization of multi-site diffusion tensor imaging data. bioRxiv 116541. https://doi.org/10.1101/116541

Govender, R., Eley, B., Walker, K., Petersen, R., Wilmshurst, J.M., 2011. Neurologic and Neurobehavioral Sequelae in Children With Human Immunodeficiency Virus (HIV-1) Infection. J. Child Neurol. 26, 1355–1364. https://doi.org/10.1177/0883073811405203

Graaf, R.A. de, 2008. In Vivo NMR Spectroscopy: Principles and Techniques. Wiley.

Graham, A.S., Holmes, M.J., Little, F., Dobbels, E., Cotton, M.F., Laughton, B., van der Kouwe, A.J.W., Meintjes, E.M., Robertson, F.C., Unpublished. Altered neurometabolic activity and interregional coupling at 11 years in perinatally HIV-infected children in a South African context.

Harezlak, J., Buchthal, S., Taylor, M., Schifitto, G., Zhong, J., Daar, E., Alger, J., Singer, E., Campbell, T., Yiannoutsos, C., Cohen, R., Navia, B., 2011. Persistence of HIV− Associated Cognitive Impairment, Inflammation and Neuronal Injury in era of Highly Active Antiretroviral Treatment. AIDS Lond. Engl. 25, 625–633. https://doi.org/10.1097/QAD.0b013e3283427da7

Haris, M., Cai, K., Singh, A., Hariharan, H., Reddy, R., 2011. In vivo Mapping of Brain Myo-Inositol. NeuroImage 54, 2079–2085. https://doi.org/10.1016/j.neuroimage.2010.10.017

Hedeker, D., Gibbons, R.D., 2006. Longitudinal Data Analysis. John Wiley & Sons.

Hoare, J., Ransford, G.L., Phillips, N., Amos, T., Donald, K., Stein, D.J., 2014. Systematic review of neuroimaging studies in vertically transmitted HIV positive children and adolescents. Metab. Brain Dis. 29, 221–229. https://doi.org/10.1007/s11011-013-9456-5

Holm, S., 1979. A Simple Sequentially Rejective Multiple Test Procedure. Scand. J. Stat. 6, 65–70.

Holmes, M.J., Robertson, F.C., Little, F., Randall, S.R., Cotton, M.F., Kouwe, A.J.W. van der, Laughton, B., Meintjes, E.M., 2017. Longitudinal increases of brain metabolite levels in 5-10 year old children. PLoS ONE 12. https://doi.org/10.1371/journal.pone.0180973

Hui, F.K.C., 2016. boral – Bayesian Ordination and Regression Analysis of Multivariate Abundance Data in r. Methods Ecol. Evol. 7, 744–750. https://doi.org/10.1111/2041-210X.12514

Hui, F.K.C., Blanchard, with contributions from W., 2018. boral: Bayesian Ordination and Regression AnaLysis.

Jessen, F., Gür, O., Block, W., Ende, G., Frölich, L., Hammen, T., Wiltfang, J., Kucinski, T., Jahn, H., Heun, R., Maier, W., Kölsch, H., Kornhuber, J., Träber, F., 2009. A multicenter (1)H-MRS study of the medial temporal lobe in AD and MCI. Neurology 72, 1735–1740. https://doi.org/10.1212/WNL.0b013e3181a60a20

Johnson, W., Li, C., Rabinovic, A., 2007. Adjusting batch effects in microarray expression data using empirical Bayes methods. Biostatistics 8, 118–127.

Keller, M.A., Venkatraman, T.N., Thomas, A., Deveikis, A., LoPresti, C., Hayes, J., Berman, N., Walot, I., Padilla, S., Johnston-Jones, J., Ernst, T., Chang, L., 2004. Altered neurometabolite development in HIV-infected children: correlation with neuropsychological tests. Neurology 62, 1810–1817. https://doi.org/10.1212/01.wnl.0000125492.57419.25

Keller, M.A., Venkatraman, T.N., Thomas, M.A., Deveikis, A., LoPresti, C., Hayes, J., Berman, N., Walot, I., Ernst, T., Chang, L., 2006. Cerebral metabolites in HIV-infected children followed for 10 months with 1H-MRS. Neurology 66, 874–879. https://doi.org/10.1212/01.wnl.0000203339.69771.d8

Kerr, S.J., Puthanakit, T., Vibol, U., Aurpibul, L., Vonthanak, S., Kosalaraksa, P., Kanjanavanit, S., Hansudewechakul, R., Wongsawat, J., Luesomboon, W., Ratanadilok, K., Prasitsuebsai, W., Pruksakaew, K., Lugt, J. van der, Paul, R., Ananworanich, J., Valcour, V., Team, on B. of the S. 012 S., 2014. Neurodevelopmental outcomes in HIV-exposed-uninfected children versus those not exposed to HIV. AIDS Care 26, 1327–1335. https://doi.org/10.1080/09540121.2014.920949

Kreis, R., Ernst, T., Ross, B.D., 1993. Absolute Quantitation of Water and Metabolites in the Human Brain. II. Metabolite Concentrations. J. Magn. Reson. B 102, 9–19. https://doi.org/10.1006/jmrb.1993.1056

Lee, P.L., Yiannoutsos, C.T., Ernst, T., Chang, L., Marra, C.M., Jarvik, J.G., Richards, T.L., Kwok, E.W., Kolson, D.L., Simpson, D., Tang, C.Y., Schifitto, G., Ketonen, L.M., Meyerhoff, D.J., Lenkinski, R.E., Gonzalez, R.G., Navia, B.A., 2003. A multi-center 1H MRS study of the AIDS dementia complex: Validation and preliminary analysis. J. Magn. Reson. Imaging 17, 625–633. https://doi.org/10.1002/jmri.10295

Lu, D., Pavlakis, S.G., Frank, Y., Bakshi, S., Pahwa, S., Gould, R.J., Sison, C., Hsu, C., Lesser, M., Hoberman, M., Barnett, T., Hyman, R.A., 1996. Proton MR spectroscopy of the basal ganglia in healthy children and children with AIDS. Radiology 199, 423–428. https://doi.org/10.1148/radiology.199.2.8668788

Madhi, S.A., Adrian, P., Cotton, M.F., McIntyre, J.A., Jean-Philippe, P., Meadows, S., Nachman, S., Käyhty, H., Klugman, K.P., Violari, A., Comprehensive International Program of Research on AIDS 4 Study Team, 2010. Effect of HIV infection status and anti-retroviral treatment on quantitative and qualitative antibody responses to pneumococcal conjugate vaccine in infants. J. Infect. Dis. 202, 355–361. https://doi.org/10.1086/653704

Mbugua, K.K., Holmes, M.J., Cotton, M.F., Ratai, E.-M., Little, F., Hess, Aaron.T., Dobbels, E., Van der Kouwe, A.J.W., Laughton, B., Meintjes, E.M., 2016. HIV-associated CD4/8 depletion in infancy is associated with neurometabolic reductions in the basal ganglia at age 5 years despite early antiretroviral therapy. Aids 30, 1. https://doi.org/10.1097/QAD.0000000000001082

Minati, L., Aquino, D., Bruzzone, M.G., Erbetta, A., 2010. Quantitation of normal metabolite concentrations in six brain regions by in-vivo 1H-MR spectroscopy. J. Med. Phys. Assoc. Med. Phys. India 35, 154–163. https://doi.org/10.4103/0971-6203.62128

Moffett, J.R., Ross, B., Arun, P., Madhavarao, C.N., Namboodiri, M.A.A., 2007. N-Acetylaspartate in the CNS: From Neurodiagnostics to Neurobiology. Prog. Neurobiol. 81, 89–131. https://doi.org/10.1016/j.pneurobio.2006.12.003

Paley, M., Cozzone, P. j., Alonso, J., Vion-Dury, J., Confort-Gouny, S., Wilkinson, I. d., Chong, W. k., Hall-Craggs, M. a., Harrison, M. j. g., Gili, J., Rovira, A., Capellades, J., Rio, J., Ocana, I., Nicoli, F., Dhiver, C., Gastaut, J. l., Gastaut, J. a., Wicklow, K., Sauter, R., 1996. A Multicenter Proton Magnetic Resonance Spectroscopy Study of Neurological Complications of AIDS. AIDS Res. Hum. Retroviruses 12, 213–222. https://doi.org/10.1089/aid.1996.12.213

Pinheiro, J., Bates, D., 2006. Mixed-Effects Models in S and S-PLUS. Springer Science & Business Media.

Pinheiro J, Bates D, DebRoy S, Sarkar D, R Core Team, 2019. nlme: Linear and Nonlinear Mixed Effects Models. R package version 3.1-143, https://CRAN.R-project.org/package=nlme.

Prado, P.T.C., Escorsi-Rosset, S., Cervi, M.C., Santos, A.C., 2011. Image evaluation of HIV encephalopathy: a multimodal approach using quantitative MR techniques. Neuroradiology 53, 899. https://doi.org/10.1007/s00234-011-0869-8

Provencher, S.W., 2001. Automatic quantitation of localized in vivo 1H spectra with LCModel. NMR Biomed. 14, 260–264. https://doi.org/10.1002/nbm.698

Provencher, S.W., 1993. Estimation of metabolite concentrations from localized in vivo proton NMR spectra. Magn. Reson. Med. 30, 672–679. https://doi.org/10.1002/mrm.1910300604

Rie, A.V., Mupuala, A., Dow, A., 2008. Impact of the HIV/AIDS Epidemic on the Neurodevelopment of Preschool-Aged Children in Kinshasa, Democratic Republic of the Congo. Pediatrics 122, e123–e128. https://doi.org/10.1542/peds.2007-2558

Robertson, F.C., Holmes, M.J., Cotton, M.F., Dobbels, E., Little, F., Laughton, B., van der Kouwe, A.J.W., Meintjes, E.M., 2018. Perinatal HIV Infection or Exposure Is Associated With Low N-Acetylaspartate and Glutamate in Basal Ganglia

at Age 9 but Not 7 Years. Front. Hum. Neurosci. 12. https://doi.org/10.3389/fnhum.2018.00145

Robertson, F.C., Holmes, M.J., Cotton, M.F., Dobbels, E., Little, F., Laughton, B., van der Kouwe, A.J.W., Meintjes, E.M., Unpublished. Perinatal HIV infection and exposure are associated with distinct neurometabolite alterations in gray matter and basal ganglia at 7 and 9 years.

RStudio Team, 2018. RStudio: Integrated Development for R. RStudio, Inc., Boston, MA URL http://www.rstudio.com/.

Sacktor, N., Skolasky, R.L., Ernst, T., Mao, X., Selnes, O., Pomper, M.G., Chang, L., Zhong, K., Shungu, D.C., Marder, K., Shibata, D., Schifitto, G., Bobo, L., Barker, P.B., 2005. A multicenter study of two magnetic resonance spectroscopy techniques in individuals with HIV dementia. J. Magn. Reson. Imaging 21, 325–333. https://doi.org/10.1002/jmri.20272

Verbeke, G., Fieuws, S., Molenberghs, G., Davidian, M., 2014. The analysis of multivariate longitudinal data: A review. Stat. Methods Med. Res. 23, 42–59. https://doi.org/10.1177/0962280212445834

Violari, A., Cotton, M.F., Gibb, D.M., Babiker, A.G., Steyn, J., Madhi, S.A., Jean-Philippe, P., McIntyre, J.A., 2008. Early Antiretroviral Therapy and Mortality among HIV-Infected Infants. N. Engl. J. Med. 359, 2233–2244. https://doi.org/10.1056/NEJMoa0800971

Wang, Y., Li, S.-J., 1998. Differentiation of metabolic concentrations between gray matter and white matter of human brain by in vivo 1H magnetic resonance spectroscopy. Magn. Reson. Med. 39, 28–33. https://doi.org/10.1002/mrm.1910390107

Wright, S.P., 1992. Adjusted P-Values for Simultaneous Inference. Biometrics 48, 1005–1013. https://doi.org/10.2307/2532694

Zahr, N.M., Mayer, D., Rohlfing, T., Sullivan, E.V., Pfefferbaum, A., 2014. Imaging Neuroinflammation? A Perspective from MR Spectroscopy. Brain Pathol. Zurich Switz. 24, 654–664. https://doi.org/10.1111/bpa.12197

Zeisel, S.H., da Costa, K.-A., 2009. Choline: An Essential Nutrient for Public Health. Nutr. Rev. 67, 615–623. https://doi.org/10.1111/j.1753-4887.2009.00246.x

Zhu, H., Barker, P.B., 2011. MR Spectroscopy and Spectroscopic Imaging of the Brain. Methods Mol. Biol. Clifton NJ 711, 203–226. https://doi.org/10.1007/978-1-61737-992-5_9

Appendix

A.1:

Previous research into the effects of HIV on the developing brain completed using MRS.

Table A.1.1: The previous studies performed using the data that was also used within this research project and the regions and age groups they focussed on.

Regions	5	7	9	11
BG	Mbugua et al. (2016); Holmes et al., (2017)	Robertson et al. (2018); Holmes et al., (2017)	Robertson et al. (2018); Holmes et al., (2017)	Graham et al., (unpublished)
PWM				Graham et al., (unpublished)
MFGM		Robertson et al., (unpublished)	Robertson et al., (unpublished)	Graham et al., (unpublished)

Table A.1.2: Previous findings from studies that also looked at the effects of HIV on metabolite concentrations within our regions of interest, that compared concentrations between HIV+ and HIV- children.

Region	Metabolite	Increase	Decrease
BG	**Glu**		Robertson et al. 2018
	Glu+Gln		
	GPC+PCh	Mbugua et al. 2016 Ashby et al. 2015[1]	Keller et al. 2004 Lu et al. 1996[1]
	Ins	Ashby et al. 2015[1]	Keller et al. 2004[2]
	NAA	Mbugua et al. 2016	Pavlakis et al. 1995 [1, 3] Lu et al. 1996[1] Robertson et al. 2018 Keller et al. 2004[4]
	NAA+NAAG		
	Cr+PCr		Keller et al. 2004[4]
PWM	**Glu**		
	Glu+Gln		
	GPC+PCh		
	Ins		
	NAA		
	NAA+NAAG		Graham et al. (Unpublished)
	Cr+PCr		Graham et al. (Unpublished)
MFGM	**Glu**	Nagarajan et al. 2012[1] Iqbal et al. 2016[1]	Robertson et al. (Unpublished)
	Glu+Gln		
	GPC+PCh	Van Dalen et al. 2016[1] Keller et al. 2004[1] Iqbal et al. 2016 Robertson et al. (Unpublished) Prado et al. 2011[1]	Graham et al. (Unpublished)
	Ins	Banakar et al. 2008[1]	
	NAA	Banakar et al. 2008[1]	
	NAA+NAAG		
	Cr+PCr		

[1]lower Metabolite/Cr ratio, absolute metabolite change was not investigated.
[2]in children with low viral load.
[3]children with AIDS.
[4]in children with higher viral load.

Table A.1.3: Previous findings from studies that also looked at the effects of HIV on metabolite concentrations within our regions of interest, that compared concentrations between HEU and HUU children.

Region	Metabolite	Increase	Decrease
BG	**Glu**		Robertson et al. 2018
	Glu+Gln		
	GPC+PCh		Robertson et al. 2018
	Ins		
	NAA		Robertson et al. 2018
	NAA+NAAG		
	Cr+PCr		Robertson et al. 2018
PWM	**Glu**		
	Glu+Gln		
	GPC+PCh		
	Ins		
	NAA		
	NAA+NAAG		
	Cr+PCr		
MFGM	**Glu**		
	Glu+Gln		
	GPC+PCh	Robertson et al. (Unpublished)	
	Ins		
	NAA		
	NAA+NAAG		
	Cr+PCr		

A.2:

BG and PWM results from inter- and intra-scanner investigations.

Figure A.2.1: Box and Whisker plots of Repeated Scans at Five years old in the BG illustrating the intra-scanner variability present

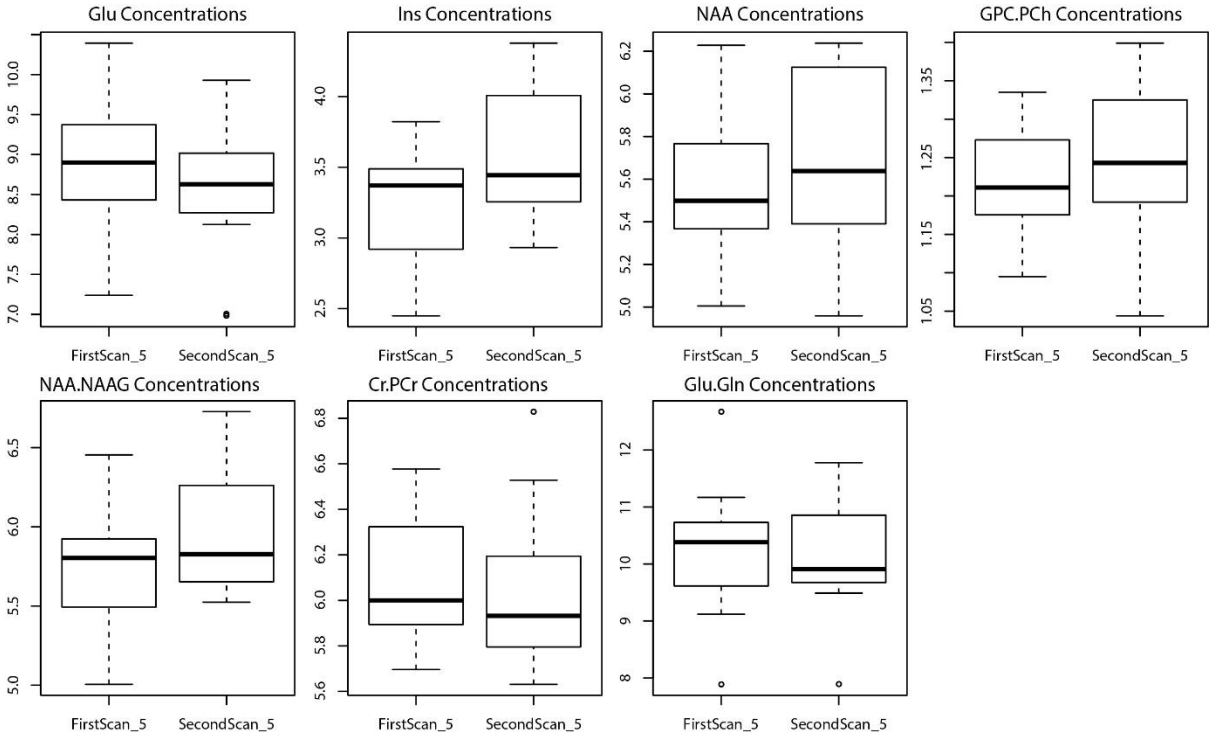

Fig A.2.2: Box and Whisker plots of Repeated Scans at 'nine' years old in the BG illustrating the inter-scanner variability present

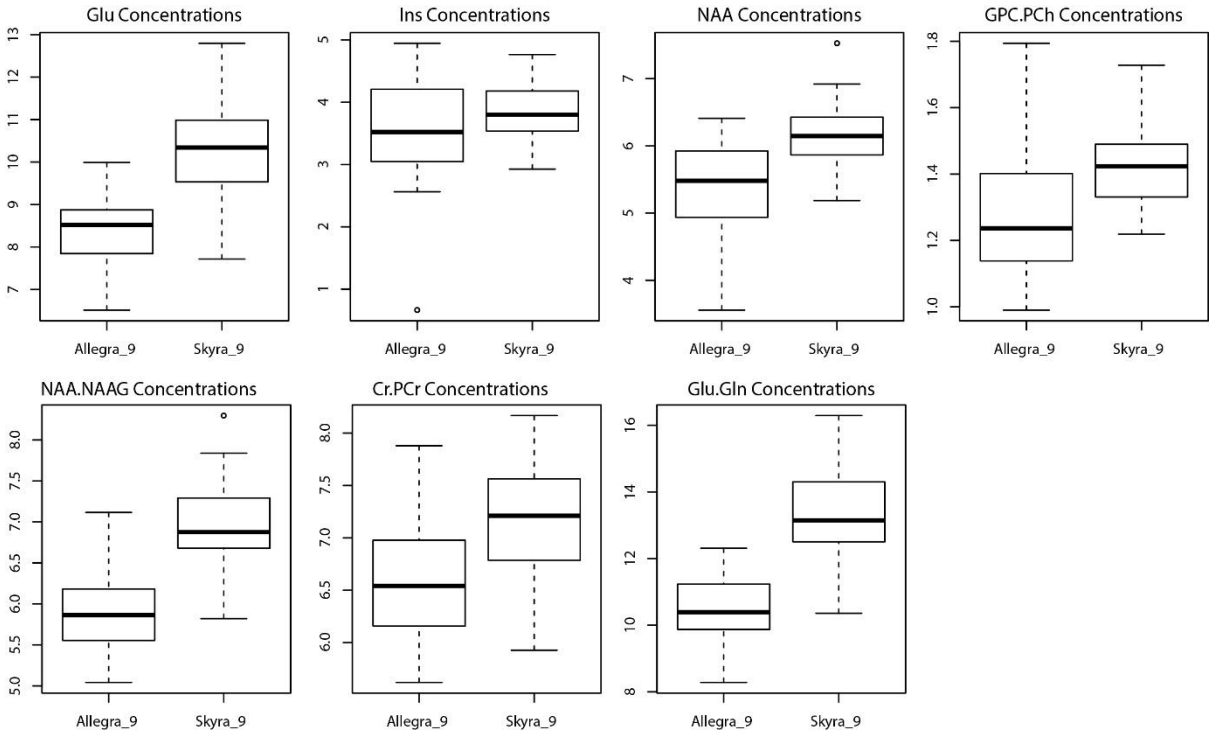

Fig A.2.3: Box and Whisker plots of the difference between metabolite concentrations within the BG region from repeated scans taken at ages five and nine with the significance of t-tests comparing these differences.

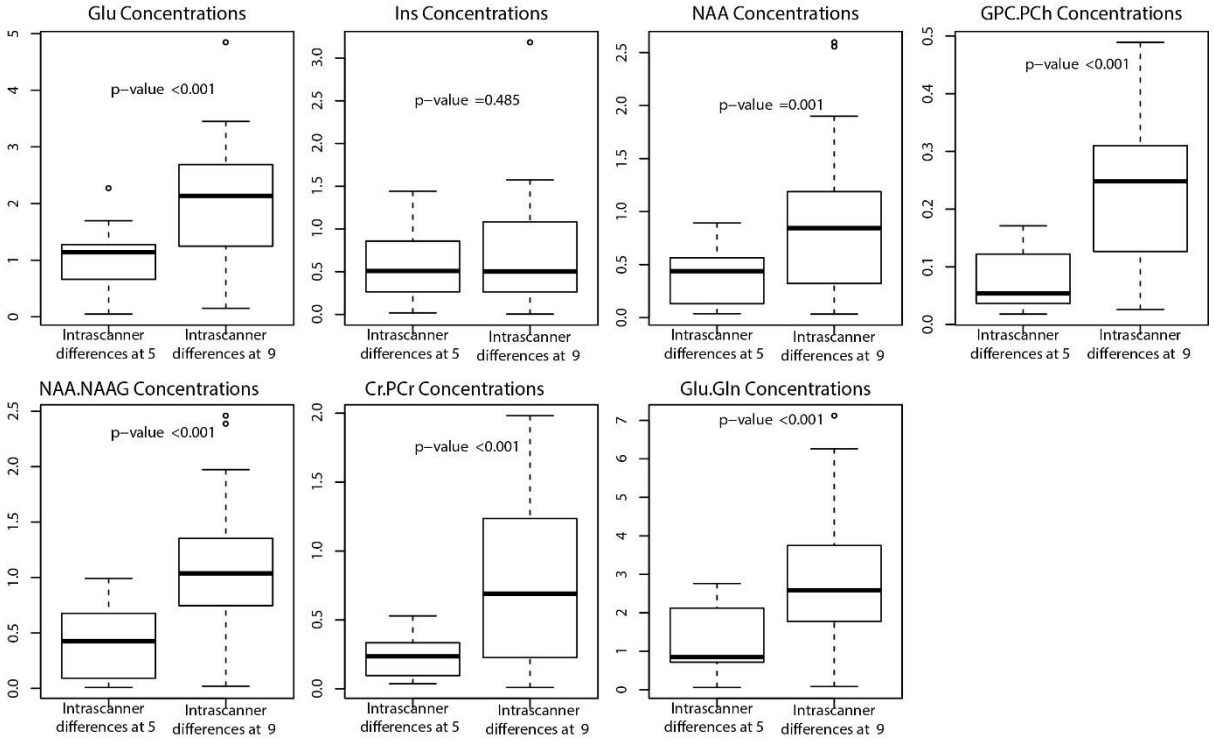

Figure A.2.4: The relationship between the various concentrations measured within the BG using the Allegra and Skyra scanners.

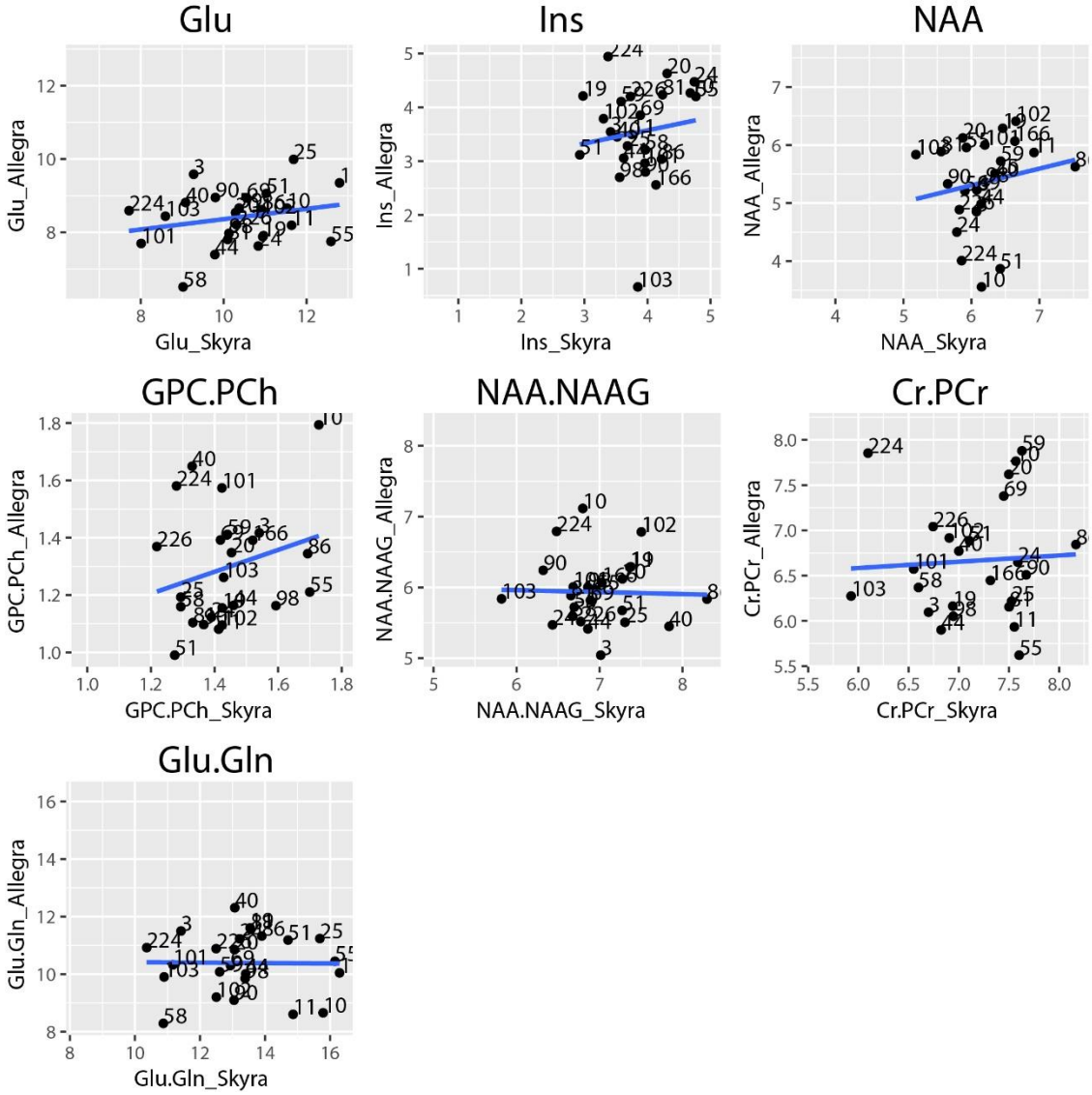

Figure A.2.5: Bland-Altman output for inter- and intra-scanner repeated observations in the BG region. These Bland-Altman plots show an average difference between observations (the bias) and a 95% CI around this difference, along with the actual differences seen.

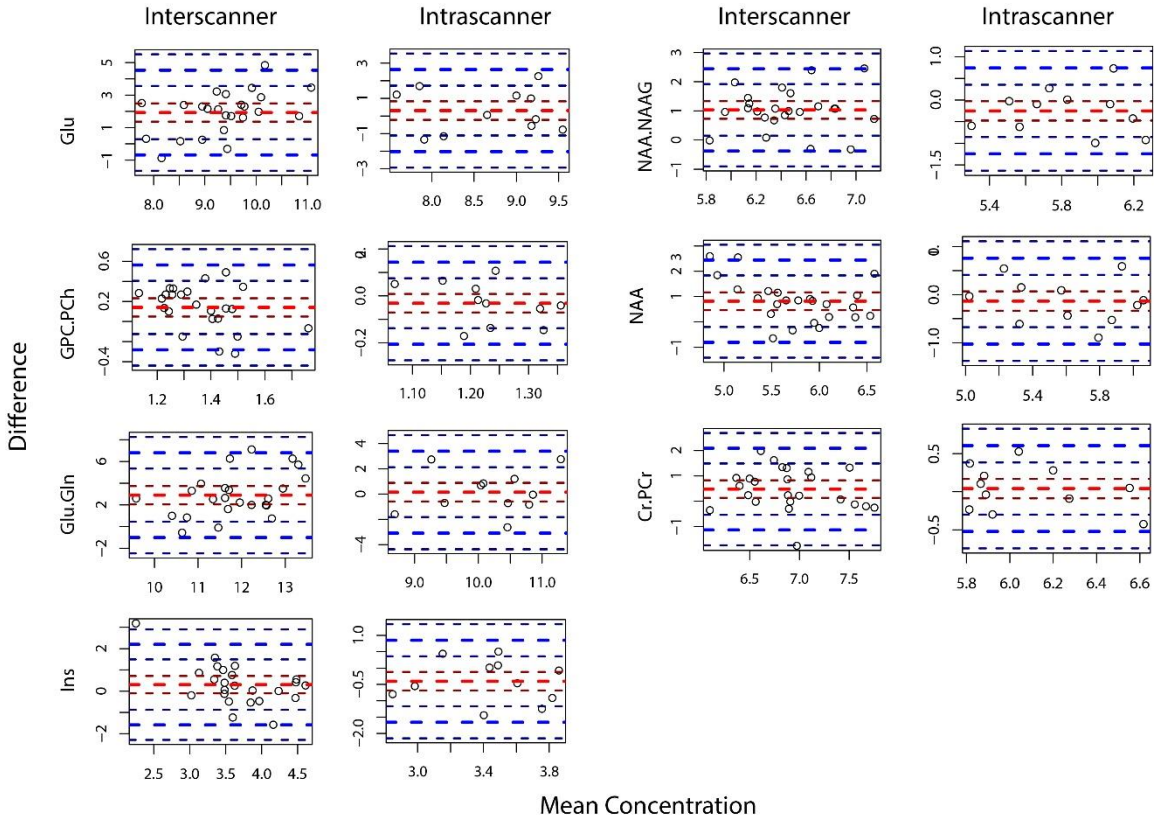

Table A.2.1: Intercepts and Beta Coefficients for separate linear models of Allegra Concentration ~ Skyra Concentration of each metabolite in the BG region.

Metabolites		Estimate	Standard error	P-value
Glu	(Intercept)	6.954	1.268	<0.0001
	Coef	0.141	0.122	0.2609
Ins	(Intercept)	2.592	1.481	0.0940
	Coef	0.245	0.382	0.5282
NAA	(Intercept)	3.577	2.061	0.0966
	Coef	0.288	0.333	0.3961
GPC	(Intercept)	0.747	0.444	0.1069
	Coef	0.382	0.308	0.2287
NAA.NAAG	(Intercept)	6.128	1.395	<0.0001
	Coef	-0.028	0.200	0.8906
Cr.PCr	(Intercept)	6.167	1.841	0.0029
	Coef	0.069	0.257	0.7898
Glu.Gln	(Intercept)	10.491	1.816	<0.0001
	Coef	-0.008	0.136	0.9561

Table A.2.2: Intercepts and Beta Coefficients for separate linear models of Allegra Concentration ~ Skyra Concentration of each metabolite with various covariates in the BG region.

Metabolite		Estimate	Standard Error	P-value
Cr.PCr	Intercept	7.538	2.650	0.0107
	Skyra Conc	0.298	0.163	0.0831
	Allegra GM%	0.030	0.035	0.4032
	Skyra GM%	-0.070	0.031	0.0381
	Time Between Scans	0.180	0.979	0.8564
	HIV Status (HIV)	0.171	0.515	0.7430
GPC	Intercept	4.181	2.962	0.1751
	Skyra Conc	0.072	0.325	0.8271
	Allegra GM%	-0.013	0.035	0.7207
	Skyra GM%	-0.013	0.025	0.5912
	Time Between Scans	1.005	1.000	0.3284
	HIV Status (HIV)	-0.856	0.515	0.1137
NAA	Intercept	2.764	3.266	0.4085
	Skyra Conc	0.130	0.367	0.7279
	Allegra GM%	0.007	0.037	0.8465
	Skyra GM%	0.017	0.026	0.5072
	Time Between Scans	0.141	1.106	0.8998
	HIV Status (HIV)	0.643	0.575	0.2783
NAA.NAAG	Intercept	1.964	0.790	0.0231
	Skyra Conc	0.255	0.295	0.3999
	Allegra GM%	-0.005	0.009	0.5514
	Skyra GM%	-0.016	0.006	0.0170
	Time Between Scans	0.284	0.255	0.2807
	HIV Status (HIV)	0.104	0.134	0.4475
Ins	Intercept	10.310	2.012	0.0001
	Skyra Conc	-0.199	0.192	0.3153
	Allegra GM%	-0.030	0.022	0.1824
	Skyra GM%	-0.025	0.015	0.1107
	Time Between Scans	0.275	0.616	0.6601
	HIV Status (HIV)	0.432	0.324	0.1990
Glu	Intercept	8.515	2.868	0.0082
	Skyra Conc	0.329	0.286	0.2648
	Allegra GM%	-0.024	0.030	0.4466
	Skyra GM%	-0.038	0.022	0.1069
	Time Between Scans	-0.413	0.854	0.6346
	HIV Status (HIV)	-0.433	0.461	0.3597
Glu.Gln	Intercept	4.325	3.685	0.2557
	Skyra Conc	0.085	0.156	0.5922
	Allegra GM%	0.079	0.048	0.1169
	Skyra GM%	-0.023	0.040	0.5750
	Time Between Scans	1.658	1.360	0.2386
	HIV Status (HIV)	0.006	0.711	0.9937

Figure A.2.6: Box and Whisker plots of Repeated Scans at Five years old in the PWM illustrating the intra-scanner variability present

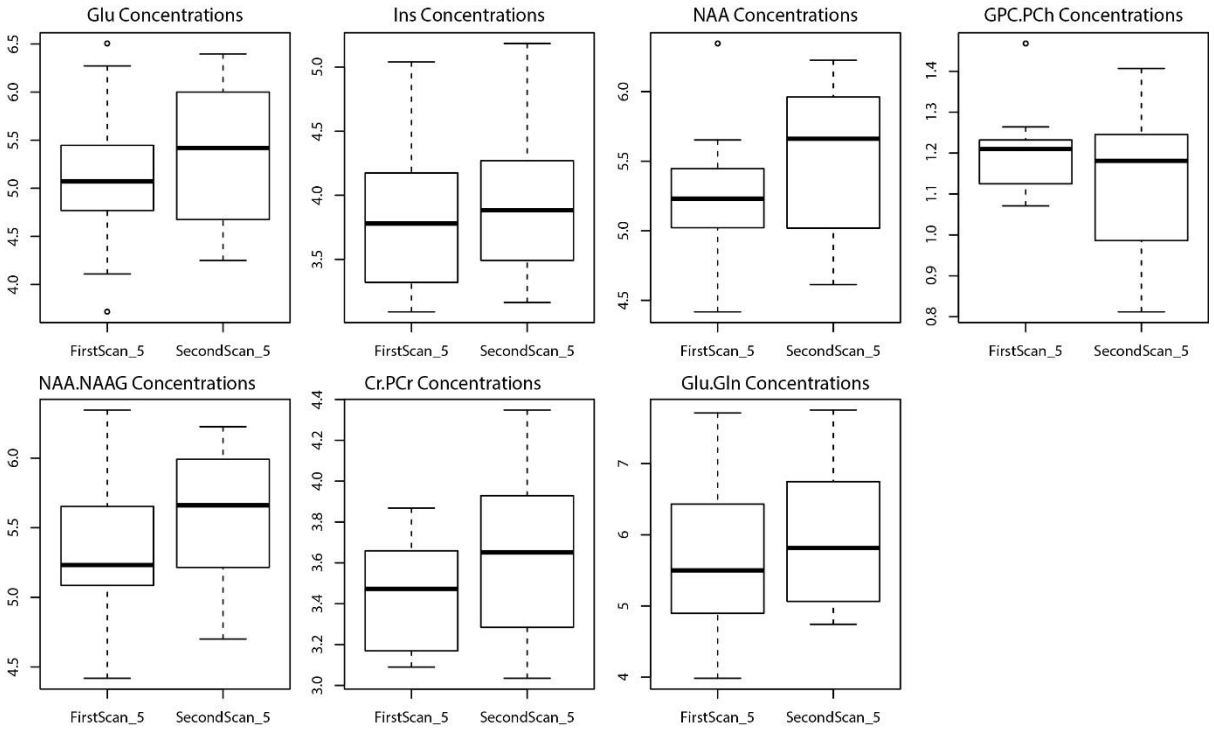

Fig A.2.7: Box and Whisker plots of Repeated Scans at 'nine' years old in the PWM illustrating the inter-scanner variability present

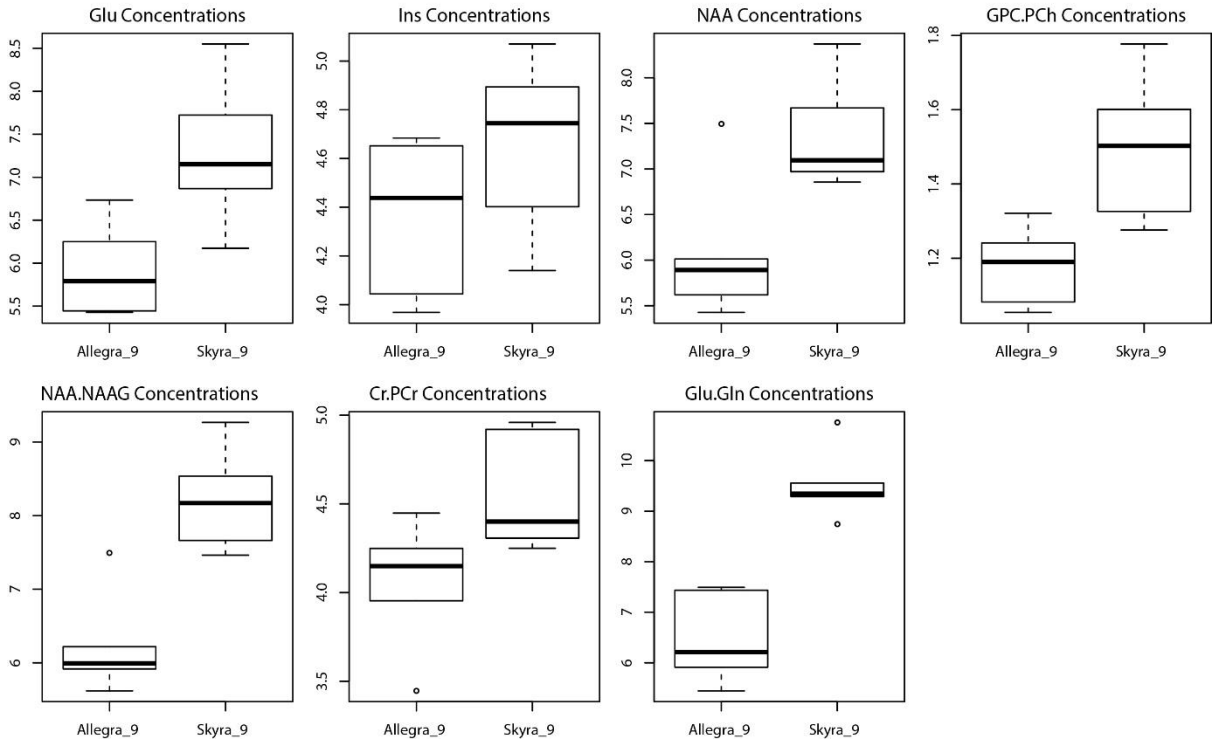

Fig A.2.8: Box and Whisker plots of the difference between metabolite concentrations within the PWM region from repeated scans taken at ages five and nine with the significance of t-tests comparing these differences.

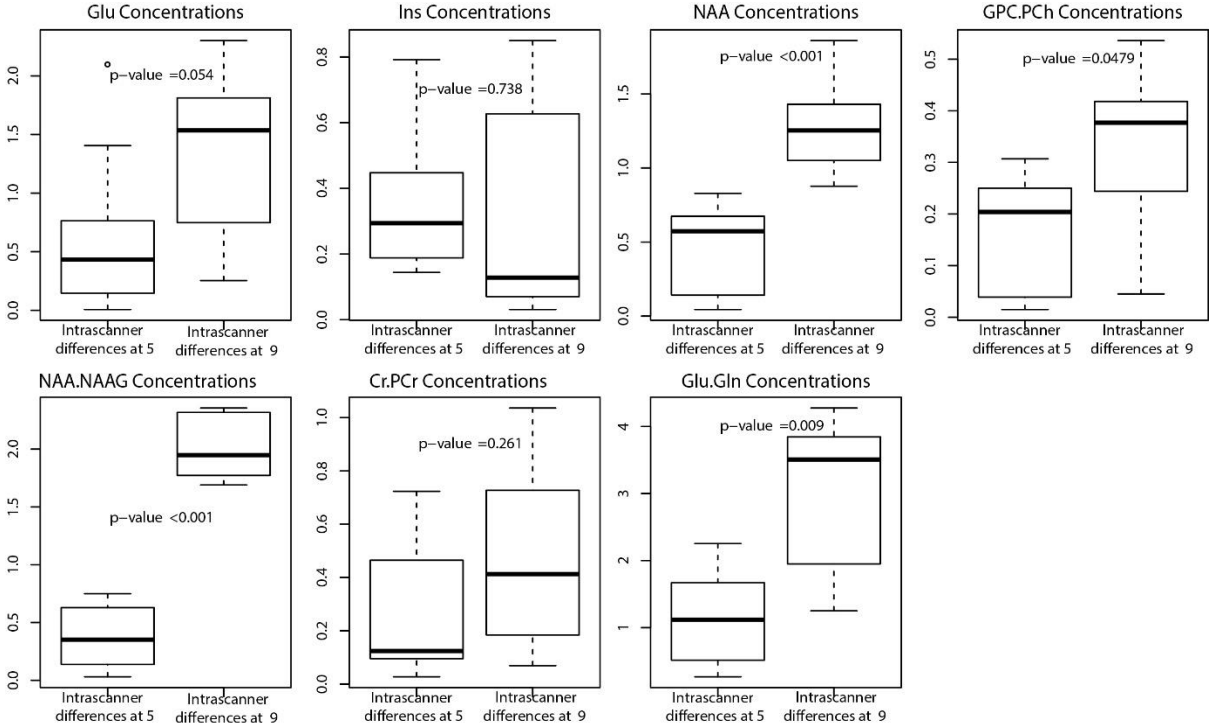

Figure A.2.9: The relationship between the various concentrations measured within the PWM using the Allegra and Skyra scanners.

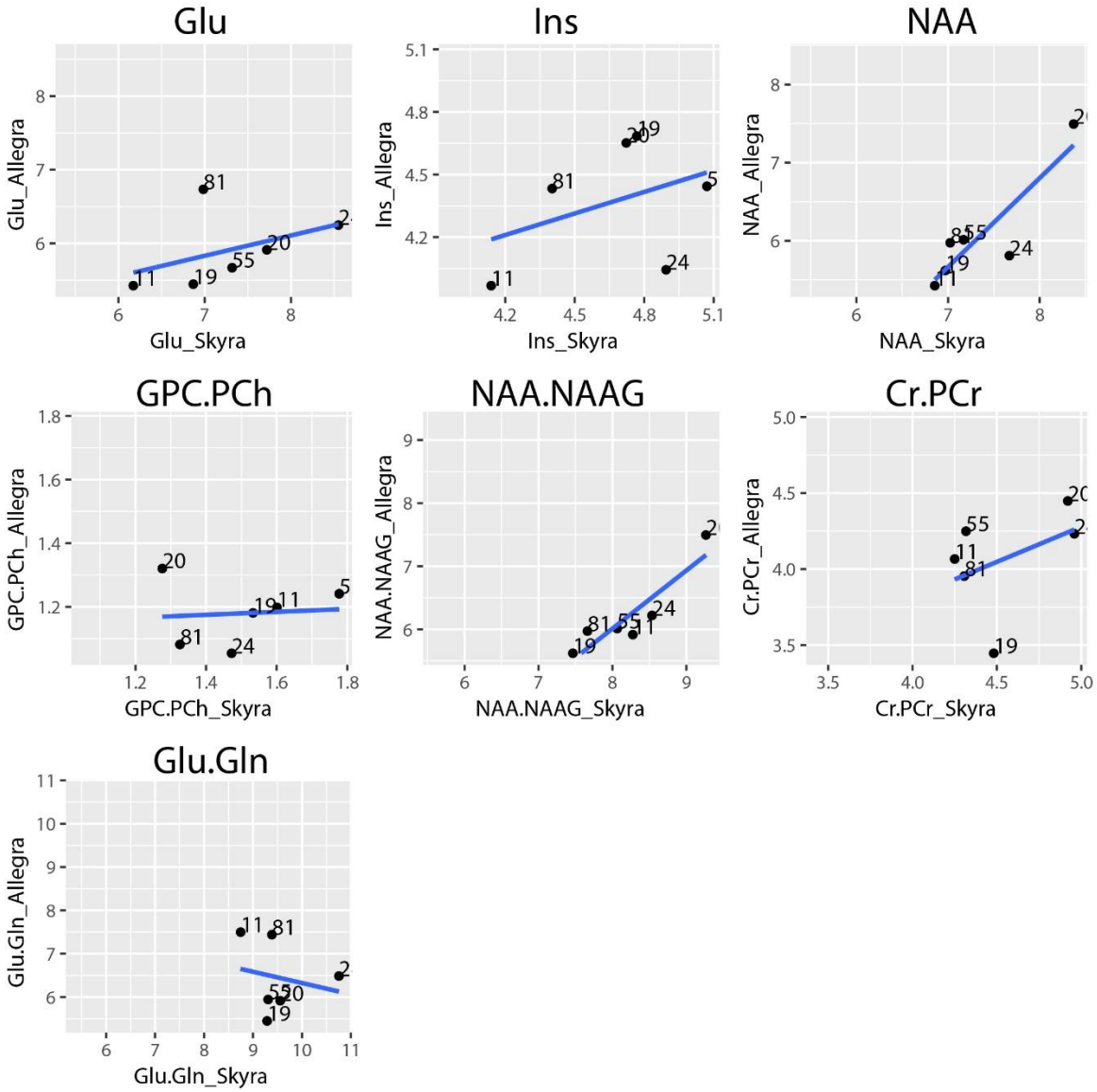

Figure A.2.10: Bland-Altman output for inter- and intra-scanner repeated observations in the PWM region. These Bland-Altman plots show an average difference between observations (the bias) and a 95% CI around this difference, along with the actual differences seen.

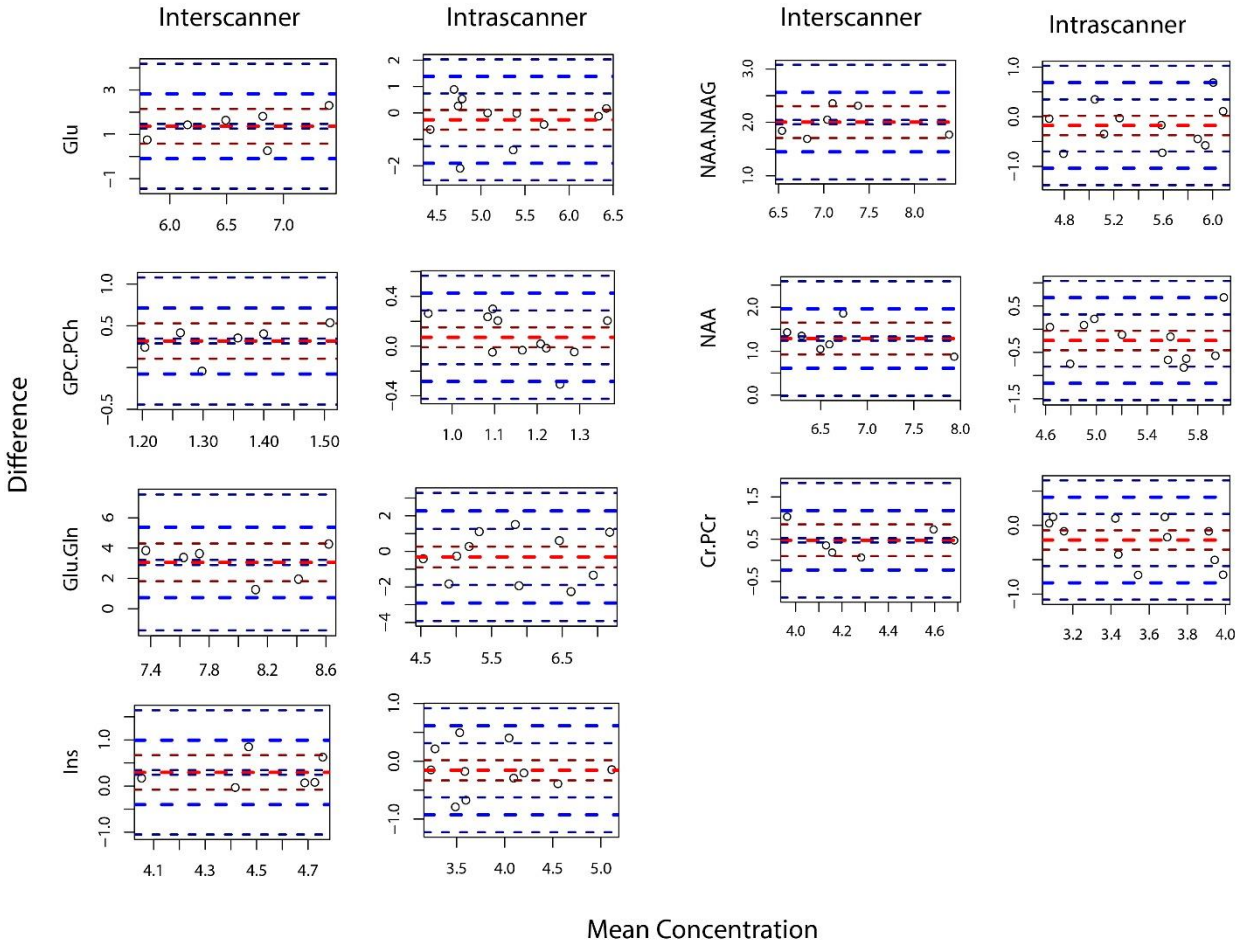

Table A.2.3: Intercepts and Beta Coefficients for separate linear models of Allegra Concentration ~ Skyra Concentration of each metabolite in the PWM region.

Metabolites		Estimate	Standard error	P-value
Glu	(Intercept)	3.897	2.066	0.1324
	Coef	0.276	0.283	0.3838
Ins	(Intercept)	2.766	1.919	0.2229
	Coef	0.344	0.410	0.4490
NAA	(Intercept)	-2.294	2.134	0.3430
	Coef	1.137	0.290	0.0172
GPC	(Intercept)	1.110	0.406	0.0521
	Coef	0.046	0.269	0.8717
NAA.NAAG	(Intercept)	-1.365	1.770	0.4838
	Coef	0.922	0.215	0.0128
Cr.PCr	(Intercept)	1.968	2.238	0.4288
	Coef	0.462	0.492	0.4008
Glu.Gln	(Intercept)	8.927	5.919	0.2060
	Coef	-0.260	0.621	0.6967

Table A.2.4: Intercepts and Beta Coefficients for separate linear models of Allegra Concentration ~ Skyra Concentration of each metabolite with various covariates in the PWM region (In this model HIV status was not included as a covariate as the entire group scanned twice was HIV-).

Metabolite		Estimate	Standard Error	P-value
Cr.PCr	Intercept	13.417	3.912	0.1806
	Skyra Conc	0.089	0.354	0.8439
	Allegra GM%	-0.032	0.030	0.4727
	Skyra GM%	-0.001	0.040	0.9883
	Time Between Scans	-6.950	2.419	0.2132
GPC	Intercept	1.837	0.618	0.2066
	Skyra Conc	1.251	0.190	0.0958
	Allegra GM%	-0.062	0.006	0.0601
	Skyra GM%	-0.011	0.010	0.4578
	Time Between Scans	-1.832	0.358	0.1228
NAA	Intercept	0.690	2.944	0.8535
	Skyra Conc	0.836	0.291	0.2130
	Allegra GM%	-0.048	0.022	0.2703
	Skyra GM%	0.058	0.035	0.3443
	Time Between Scans	-1.035	1.886	0.6805
NAA.NAAG	Intercept	0.027	0.381	0.9546
	Skyra Conc	-0.015	0.168	0.9438
	Allegra GM%	-0.004	0.005	0.6083
	Skyra GM%	0.012	0.004	0.2023
	Time Between Scans	0.902	0.432	0.2844
Ins	Intercept	1.413	0.250	0.1114
	Skyra Conc	0.857	0.022	0.0160
	Allegra GM%	-0.041	0.002	0.0331
	Skyra GM%	0.043	0.003	0.0419
	Time Between Scans	-2.202	0.196	0.0565
Glu	Intercept	1.446	7.174	0.8734
	Skyra Conc	0.278	1.078	0.8392
	Allegra GM%	0.010	0.051	0.8790
	Skyra GM%	0.020	0.068	0.8175
	Time Between Scans	0.720	4.510	0.8992
Glu.Gln	Intercept	19.603	18.423	0.4803
	Skyra Conc	-0.484	1.354	0.7814
	Allegra GM%	0.006	0.106	0.9612
	Skyra GM%	-0.112	0.108	0.4877
	Time Between Scans	-5.863	8.745	0.6240

A.3:

Extended and repetitive output from the univariate mixed effect models.

Figure A.3.1: The β estimates with 95% CI for the effect of (A) gender and (B) race on metabolite concentrations from different regions, identified using univariate LMEM.

(A)

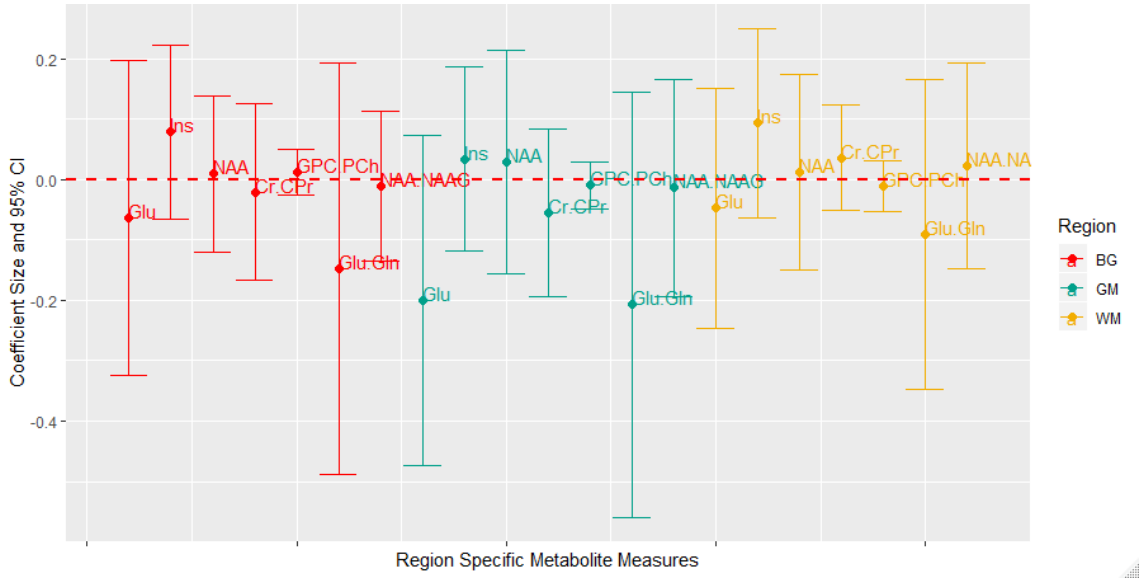

(B)

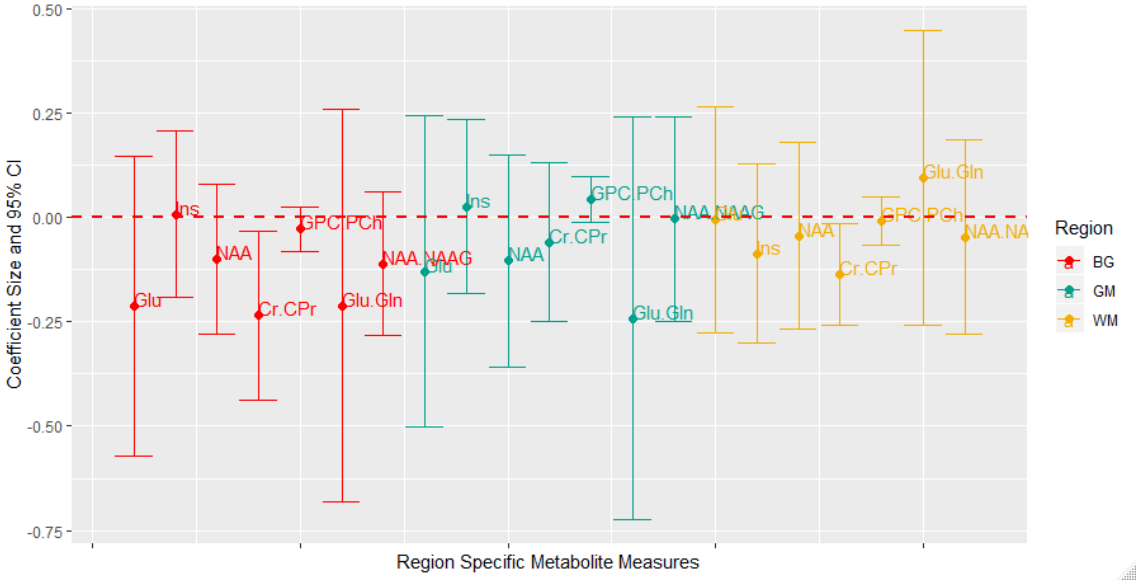

Table A.3.1: Mixed effect model with HIV Exposure for each metabolite measured in the Peritrgonal White Matter region

Metabolite		Estimate	Standard Error	P-value
Glu	Intercept	9.414	0.377	<0.0001
	Age	0.239	0.065	0.0003
	Machine (Skyra vs Allegra)	1.736	0.320	<0.0001
	Exposure (HEU vs HIV+)	-0.187	0.127	0.1433
	Exposure (HEU vs HUU)	-0.037	0.153	0.8096
	Exposure (HIV+ vs HUU)	0.151	0.124	0.2277
	Relative WM %	-5.334	0.416	<0.0001
	Age*Machine	-0.193	0.082	0.0197
Ins	Intercept	4.250	0.251	<0.0001
	Age	0.050	0.025	0.0425
	Machine (Skyra vs Allegra)	0.611	0.114	<0.0001
	Exposure (HEU vs HIV+)	0.049	0.100	0.6258
	Exposure (HEU vs HUU)	0.050	0.117	0.6712
	Exposure (HIV+ vs HUU)	0.001	0.097	0.9899
	Relative WM %	-0.495	0.277	0.0745
NAA	Intercept	7.304	0.292	<0.0001
	Age	0.212	0.031	<0.0001
	Machine (Skyra vs Allegra)	0.898	0.144	<0.0001
	Exposure (HEU vs HIV+)	-0.022	0.104	0.8292
	Exposure (HEU vs HUU)	-0.077	0.123	0.5329
	Exposure (HIV+ vs HUU)	-0.055	0.101	0.5891
	Relative WM %	-2.790	0.324	<0.0001
GPC.PCh	Intercept	0.766	0.068	<0.0001
	Age	0.004	0.007	0.5767
	Machine (Skyra vs Allegra)	0.274	0.031	<0.0001
	Exposure (HEU vs HIV+)	0.069	0.027	0.0122
	Exposure (HEU vs HUU)	0.020	0.032	0.5344
	Exposure (HIV+ vs HUU)	-0.049	0.027	0.0666
	Relative WM %	0.408	0.075	<0.0001
NAA.NAAG	Intercept	7.304	0.314	<0.0001
	Age	0.158	0.053	0.0033
	Machine (Skyra vs Allegra)	0.790	0.262	0.0028
	Exposure (HEU vs HIV+)	-0.029	0.109	0.7901
	Exposure (HEU vs HUU)	-0.047	0.130	0.7188
	Exposure (HIV+ vs HUU)	-0.018	0.106	0.8667
	Relative WM %	-2.582	0.346	<0.0001
	Age*Machine	0.170	0.067	0.0118
Cr.PCr	Intercept	5.521	0.159	<0.0001
	Age	0.129	0.027	<0.0001
	Machine (Skyra vs Allegra)	0.753	0.131	<0.0001
	Exposure (HEU vs HIV+)	-0.097	0.057	0.0883
	Exposure (HEU vs HUU)	-0.119	0.067	0.0802
	Exposure (HIV+ vs HUU)	-0.022	0.055	0.6960
	Relative WM %	-2.442	0.176	<0.0001
	Age*Machine	-0.069	0.034	0.0414
Glu.Gln	Intercept	10.443	0.499	<0.0001
	Age	0.365	0.087	<0.0001
	Machine (Skyra vs Allegra)	3.125	0.429	<0.0001
	Exposure (HEU vs HIV+)	-0.235	0.166	0.1584
	Exposure (HEU vs HUU)	0.000	0.199	0.9987
	Exposure (HIV+ vs HUU)	0.234	0.162	0.1491
	Relative WM %	-6.005	0.550	<0.0001
	Age*Machine	-0.265	0.110	0.0165

Table A.3.2: Mixed effect model with HIV Exposure for each metabolite measured in the Mid-Frontal Gray Matter

Metabolite		Estimate	Standard Error	P-value
Glu	Intercept	2.760	1.729	0.1116
	Age	0.125	0.057	0.0283
	Machine (Skyra vs Allegra)	2.488	0.248	<0.0001
	Exposure (HEU vs HIV+)	-0.147	0.179	0.4123
	Exposure (HEU vs HUU)	-0.062	0.212	0.7686
	Exposure (HIV+ vs HUU)	0.085	0.173	0.6231
	Relative GM %	6.766	1.831	0.0003
Ins	Intercept	3.722	0.865	<0.0001
	Age	0.040	0.037	0.2728
	Machine (Skyra vs Allegra)	0.244	0.248	0.3251
	Exposure (HEU vs HIV+)	0.198	0.099	0.0476
	Exposure (HEU vs HUU)	-0.029	0.117	0.8059
	Exposure (HIV+ vs HUU)	-0.227	0.096	0.0192
	Relative GM %	1.413	0.915	0.1233
	Age*Machine	0.116	0.053	0.0303
NAA	Intercept	1.174	1.132	0.3005
	Age	0.085	0.037	0.0222
	Machine (Skyra vs Allegra)	1.001	0.161	<0.0001
	Exposure (HEU vs HIV+)	-0.006	0.122	0.9590
	Exposure (HEU vs HUU)	-0.152	0.144	0.2932
	Exposure (HIV+ vs HUU)	-0.145	0.117	0.2172
	Relative GM %	5.084	1.199	<0.0001
GPC.PCh	Intercept	1.093	0.189	<0.0001
	Age	-0.001	0.008	0.8788
	Machine (Skyra vs Allegra)	-0.028	0.052	0.5874
	Exposure (HEU vs HIV+)	0.081	0.026	0.0019
	Exposure (HEU vs HUU)	-0.020	0.030	0.4982
	Exposure (HIV+ vs HUU)	-0.102	0.025	0.0001
	Relative GM %	0.056	0.200	0.7803
	Age*Machine	0.055	0.011	<0.0001
NAA.NAAG	Intercept	3.052	1.154	0.0086
	Age	0.109	0.038	0.0046
	Machine (Skyra vs Allegra)	1.401	0.166	<0.0001
	Exposure (HEU vs HIV+)	0.005	0.118	0.9648
	Exposure (HEU vs HUU)	0.005	0.139	0.9721
	Exposure (HIV+ vs HUU)	0.000	0.113	0.9977
	Relative GM %	3.364	1.223	0.0063
Cr.PCr	Intercept	2.784	0.869	0.0015
	Age	0.143	0.029	<0.0001
	Machine (Skyra vs Allegra)	0.772	0.124	<0.0001
	Exposure (HEU vs HIV+)	-0.036	0.091	0.6906
	Exposure (HEU vs HUU)	-0.158	0.108	0.1459
	Exposure (HIV+ vs HUU)	-0.121	0.088	0.1698
	Relative GM %	2.580	0.920	0.0054
Glu.Gln	Intercept	3.839	2.109	0.0697
	Age	0.212	0.069	0.0022
	Machine (Skyra vs Allegra)	3.510	0.299	<0.0001
	Exposure (HEU vs HIV+)	-0.237	0.230	0.3030
	Exposure (HEU vs HUU)	-0.073	0.271	0.7894
	Exposure (HIV+ vs HUU)	0.165	0.222	0.4578
	Relative GM %	6.676	2.233	0.0030

Table A.3.3: Mixed effect model with HIV Exposure for each metabolite measured in the Basal Ganglia

Metabolite		Estimate	Standard Error	P-value
Glu	Intercept	4.320	0.599	<0.0001
	Age	0.105	0.052	0.0416
	Machine (Skyra vs Allegra)	2.101	0.228	<0.0001
	Exposure (HEU vs HIV+)	0.006	0.171	0.9703
	Exposure (HEU vs HUU)	-0.041	0.200	0.8372
	Exposure (HIV+ vs HUU)	-0.048	0.164	0.7722
	Relative GM %	5.936	0.892	<0.0001
Ins	Intercept	1.248	0.292	<0.0001
	Age	0.103	0.024	<0.0001
	Machine (Skyra vs Allegra)	0.097	0.105	0.3586
	Exposure (HEU vs HIV+)	0.107	0.094	0.2556
	Exposure (HEU vs HUU)	0.103	0.110	0.3488
	Exposure (HIV+ vs HUU)	-0.004	0.090	0.9629
	Relative GM %	3.258	0.432	<0.0001
NAA	Intercept	5.184	0.322	<0.0001
	Age	0.058	0.040	0.1433
	Machine (Skyra vs Allegra)	0.678	0.114	<0.0001
	Exposure (HEU vs HIV+)	0.372	0.173	0.0326
	Exposure (HEU vs HUU)	-0.108	0.213	0.6145
	Exposure (HIV+ vs HUU)	-0.480	0.168	0.0050
	Relative GM %	-0.088	0.445	0.8438
	Age*Exposure (HEU vs HIV+)	-0.052	0.037	0.1612
	Age*Exposure (HEU vs HUU)	0.050	0.046	0.2700
	Age*Exposure (HIV+ vs HUU)	0.102	0.036	0.0051
GPC.PCh	Intercept	0.780	0.075	<0.0001
	Age	0.019	0.006	0.0020
	Machine (Skyra vs Allegra)	0.153	0.027	<0.0001
	Exposure (HEU vs HIV+)	0.045	0.025	0.0671
	Exposure (HEU vs HUU)	-0.013	0.029	0.6462
	Exposure (HIV+ vs HUU)	-0.059	0.024	0.0145
	Relative GM %	0.642	0.111	<0.0001
NAA.NAAG	Intercept	5.492	0.097	<0.0001
	Age	0.063	0.026	0.0157
	Machine (Skyra vs Allegra)	1.176	0.115	<0.0001
	Exposure (HEU vs HIV+)	0.058	0.082	0.4800
	Exposure (HEU vs HUU)	0.034	0.097	0.7289
	Exposure (HIV+ vs HUU)	-0.025	0.079	0.7534
Cr.PCr	Intercept	3.795	0.350	<0.0001
	Age	0.257	0.039	<0.0001
	Machine (Skyra vs Allegra)	1.149	0.264	<0.0001
	Exposure (HEU vs HIV+)	-0.046	0.096	0.6366
	Exposure (HEU vs HUU)	-0.135	0.113	0.2322
	Exposure (HIV+ vs HUU)	-0.089	0.092	0.3345
	Relative GM %	3.024	0.507	<0.0001
	Age*Machine	-0.158	0.057	0.0060
Glu.Gln	Intercept	4.603	0.780	<0.0001
	Age	0.263	0.067	0.0001
	Machine (Skyra vs Allegra)	3.078	0.296	<0.0001
	Exposure (HEU vs HIV+)	-0.024	0.223	0.9143
	Exposure (HEU vs HUU)	0.106	0.261	0.6850
	Exposure (HIV+ vs HUU)	0.130	0.214	0.5441
	Relative GM %	7.590	1.161	<0.0001

A.4:

Extended output from multilevel LME and CR Models.

A.4.1 Multilevel LME:

Table A.4.1: Machine effect estimates from the Multilevel LMEM without the age*HIV Status and age*scanner interaction terms.

Reference Region	Reference Metabolite	β Estimate	Standard Error	P-value
BG	Cr.PCr	0.514	0.128	0.0001
	Glu	2.113	0.227	<0.0001
	Ins	0.070	0.111	0.5247
	NAA	0.745	0.119	<0.0001
	GPC.PCh	0.152	0.025	<0.0001
WM	Cr.PCr	0.552	0.081	<0.0001
	Glu	1.170	0.197	<0.0001
	Ins	0.554	0.131	<0.0001
	NAA	0.880	0.154	<0.0001
	GPC.PCh	0.276	0.032	<0.0001
GM	Cr.PCr	0.769	0.121	<0.0001
	Glu	2.472	0.244	<0.0001
	Ins	0.713	0.121	<0.0001
	NAA	0.960	0.161	<0.0001
	GPC.PCh	0.192	0.028	<0.0001

Table A.4.2: Relative GM% effect estimates from the Multilevel LMEM without the age*HIV Status and age*scanner interaction terms.

Reference Region	Reference Metabolite	β Estimate	Standard Error	P-value
BG	Cr.PCr	3.286	0.187	<0.0001
	Glu	6.287	0.376	<0.0001
	Ins	1.877	0.238	<0.0001
	NAA	2.668	0.268	<0.0001
	GPC.PCh	0.548	0.098	<0.0001
WM	Cr.PCr	2.351	0.159	<0.0001
	Glu	5.352	0.365	<0.0001
	Ins	0.942	0.226	<0.0001
	NAA	1.732	0.260	<0.0001
	GPC.PCh	-0.387	0.069	<0.0001
GM	Cr.PCr	2.932	0.251	<0.0001
	Glu	5.933	0.412	<0.0001
	Ins	1.523	0.292	<0.0001
	NAA	2.314	0.321	<0.0001
	GPC.PCh	0.194	0.196	0.3227

Table A.4.3: Age effect estimates from the Multilevel LMEM with an Age*Scanner interaction term.

Reference Region	Reference Metabolite	β Estimate	Standard Error	P-value
BG	Cr.PCr	0.283	0.045	<0.0001
	Glu	0.164	0.081	0.042
	Ins	0.079	0.040	0.045
	NAA	0.128	0.042	0.002
	GPC.PCh	0.022	0.009	0.017
WM	Cr.PCr	0.114	0.030	<0.0001
	Glu	0.226	0.074	0.002
	Ins	0.055	0.049	0.265
	NAA	0.139	0.058	0.016
	GPC.PCh	0.006	0.012	0.623
GM	Cr.PCr	0.168	0.042	<0.0001
	Glu	0.017	0.042	0.684
	Ins	0.017	0.042	0.684
	NAA	0.111	0.056	0.049
	GPC.PCh	0.984	0.184	<0.0001

Table A.4.4: MRI Scanner effect estimates from the Multilevel LMEM with an Age*Scanner interaction term.

Reference Region	Reference Metabolite	β Estimate	Standard Error	P-value
BG	Cr.PCr	1.179	4.546	<0.0001
	Glu	2.532	5.439	<0.0001
	Ins	-0.005	-0.023	0.9813
	NAA	0.939	3.890	0.0001
	GPC.PCh	0.161	3.107	0.0019
WM	Cr.PCr	0.728	5.349	<0.0001
	Glu	1.756	5.304	<0.0001
	Ins	0.521	2.357	0.0184
	NAA	0.536	2.070	0.0385
	GPC.PCh	0.294	5.434	0.0000
GM	Cr.PCr	1.021	4.068	<0.0001
	Glu	0.229	0.913	0.3613
	Ins	0.229	0.913	0.3613
	NAA	0.983	2.935	0.0033
	GPC.PCh	-0.003	-0.310	0.7562

Table A.4.5: Age*Scanner modification estimates from the Multilevel LMEM with an Age*Scanner interaction term.

Reference Region	Reference Metabolite	β Estimate	Standard Error	P-value
BG	Cr.PCr	-0.167	0.056	0.0031
	Glu	-0.105	0.101	0.3008
	Ins	0.020	0.049	0.6919
	NAA	-0.053	0.052	0.3136
	GPC.PCh	-0.002	0.011	0.8469
WM	Cr.PCr	-0.056	0.035	0.1106
	Glu	-0.186	0.085	0.0284
	Ins	0.010	0.057	0.8559
	NAA	0.110	0.066	0.0977
	GPC.PCh	-0.006	0.014	0.6888
GM	Cr.PCr	-0.062	0.054	0.2538
	Glu	0.121	0.054	0.0255
	Ins	0.121	0.054	0.0255
	NAA	-0.006	0.072	0.9331
	GPC.PCh	0.050	0.012	<0.0001

Figure A.4.1: The Effect of (A) Age, (B) Scanner and (C) the age*scanner interaction term on metabolite concentration in the respective regions. These estimates were obtained from a Multilevel LMEM with an Age*Scanner interaction.

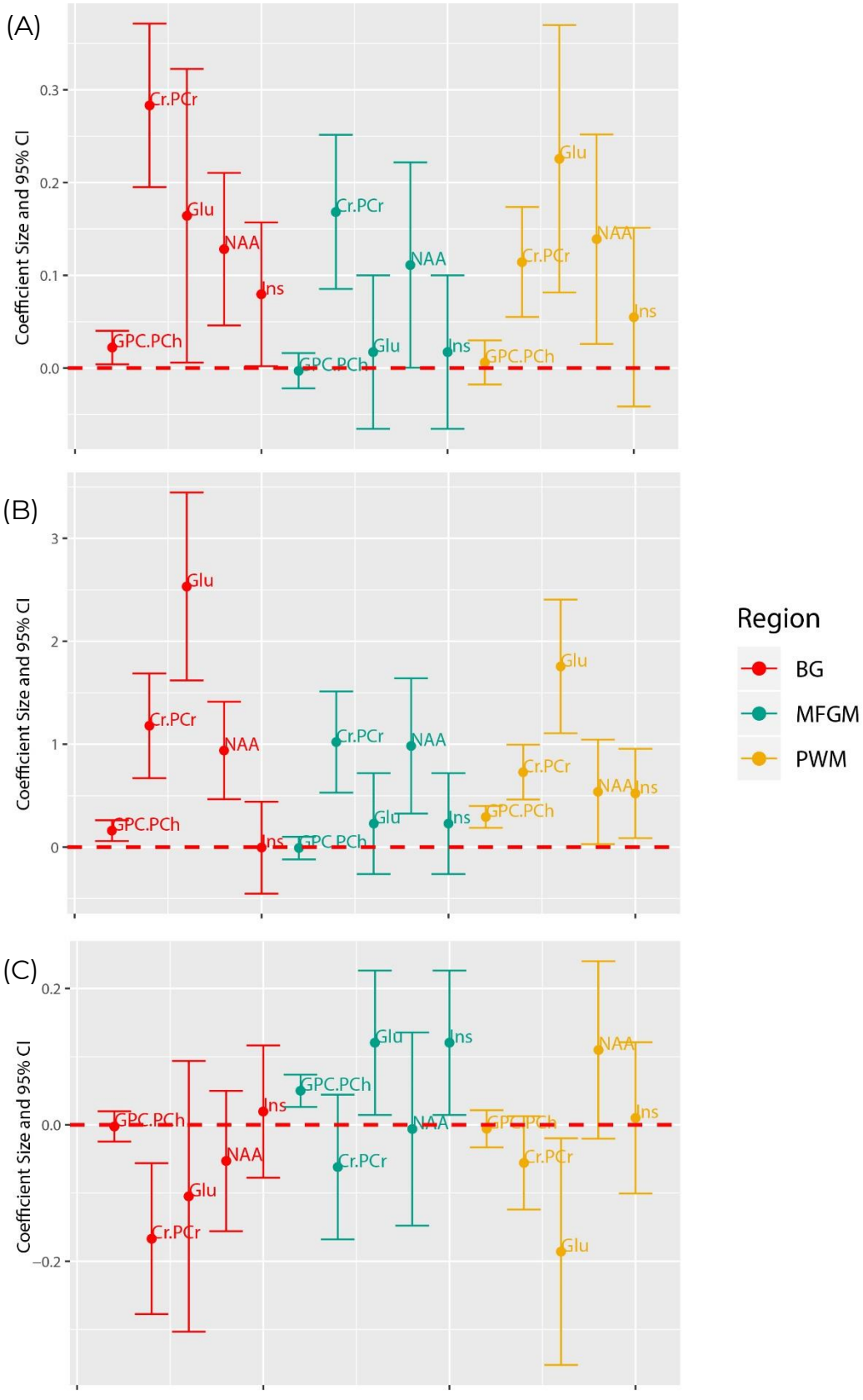

A.4.2 CRM:

Figure A.4.2: The Effect of Relative GM% recorded for the (A) BG, (B) MFGM and (C) PWM voxels on metabolite concentrations determined using the CRM without the traits component.

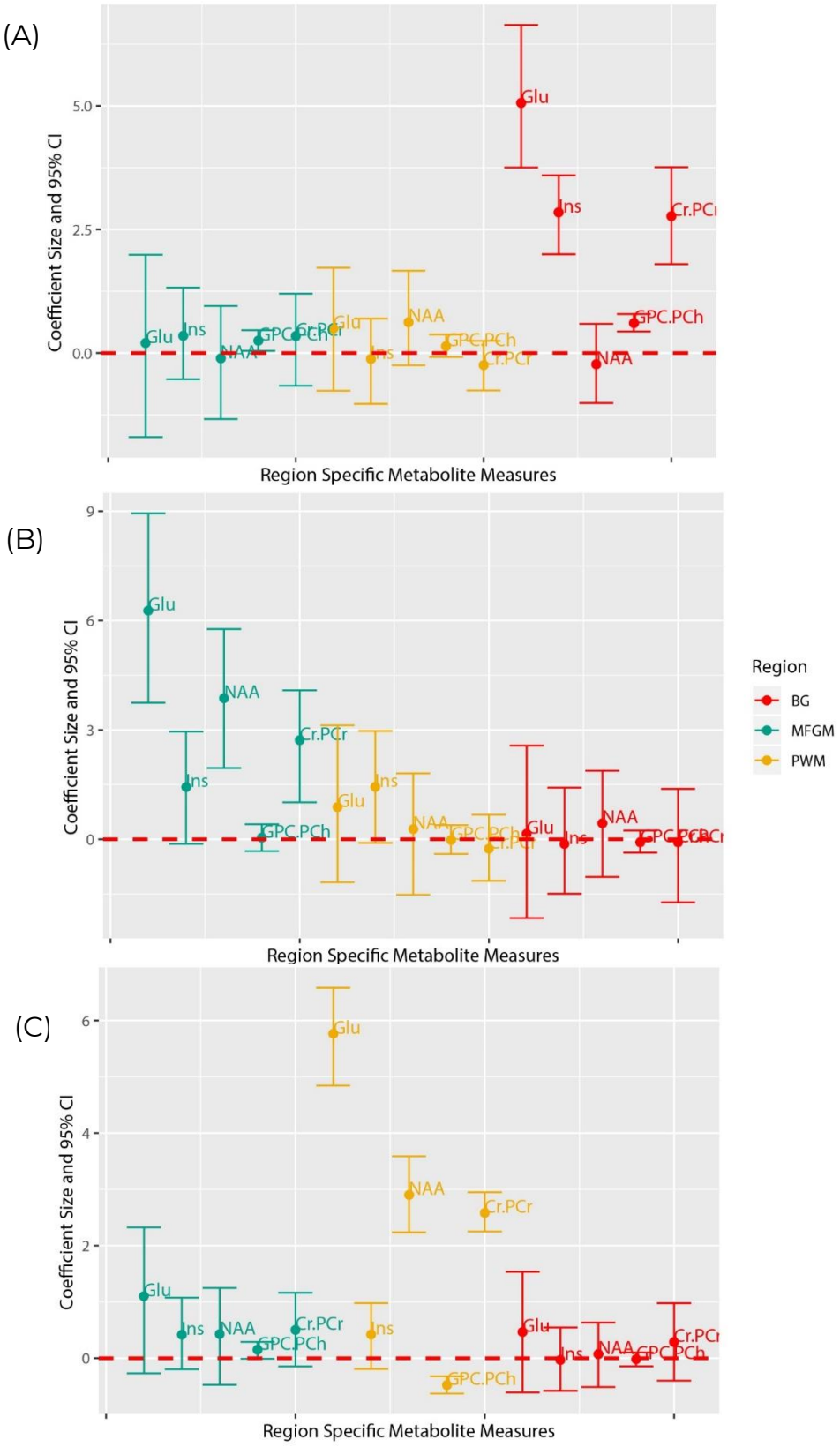

CRM with the Traits Component:

Table A.4.6: Estimated latent factor loadings from a model with a latent factor, traits and GLM component.

Region	Metabolite	β_0	θ_1	θ_2	θ_3
MFGM	Glu	4.213	1.071	0.000	0.000
	Ins	3.194	0.469	0.126	0.000
	NAA	3.727	0.651	0.220	0.032
	GPC.PCh	0.936	0.073	0.038	0.015
	Cr.PCr	3.103	0.676	0.048	0.060
PWM	Glu	3.427	0.140	-0.057	-0.457
	Ins	2.941	0.150	-0.039	-0.107
	NAA	4.107	0.232	-0.070	-0.453
	GPC.PCh	1.194	0.057	-0.009	-0.037
	Cr.PCr	3.512	0.145	-0.059	-0.193
BG	Glu	4.210	0.345	-0.535	-0.118
	Ins	2.192	-0.015	-0.109	0.059
	NAA	4.748	0.156	-0.207	-0.119
	GPC.PCh	0.904	0.035	-0.049	-0.013
	Cr.PCr	4.040	0.398	-0.485	-0.022

Table A.4.7: The Estimated GLM coefficient sizes from the CRM with the Traits, GLM and LV components.

Region	**Metabolite**	**Age**	**Machine (Skyra =1)**	**HIV Status (HIV=1)**	**Relative GM (MFGM)**	**Relative GM (PWM)**	**Relative GM (BG)**
MFGM	Glu	0.140	2.445	-0.044	4.610	1.343	0.347
	Ins	0.114	0.595	0.190	1.483	0.482	0.409
	NAA	0.099	0.996	0.078	2.381	0.472	-0.337
	GPC.PCh	0.038	0.131	0.096	-0.047	0.159	0.237
	Cr.PCr	0.133	0.854	0.072	1.820	0.605	0.264
PWM	Glu	0.099	1.282	-0.117	0.514	5.702	0.347
	Ins	0.066	0.515	0.086	0.893	0.470	-0.098
	NAA	0.203	0.955	0.012	0.114	2.945	0.397
	GPC.PCh	0.006	0.267	0.052	-0.082	-0.460	0.127
	Cr.PCr	0.092	0.524	-0.013	-0.341	2.616	-0.299
BG	Glu	0.125	2.031	-0.068	0.718	0.741	4.694
	Ins	0.122	0.044	0.123	-0.661	-0.044	2.670
	NAA	0.046	0.655	0.042	0.599	0.164	-0.092
	GPC.PCh	0.014	0.191	0.062	-0.120	-0.001	0.595
	Cr.PCr	0.173	0.605	0.026	-0.087	0.444	2.686

Figure A.4.3: The (A) baseline metabolite concentrations when all covariates are zero and the (B) Age, (C) scanner and (D) HIV Status effect size estimates with 95% CI for each of the response variables from the CRM model with Traits, LV and GLM components.

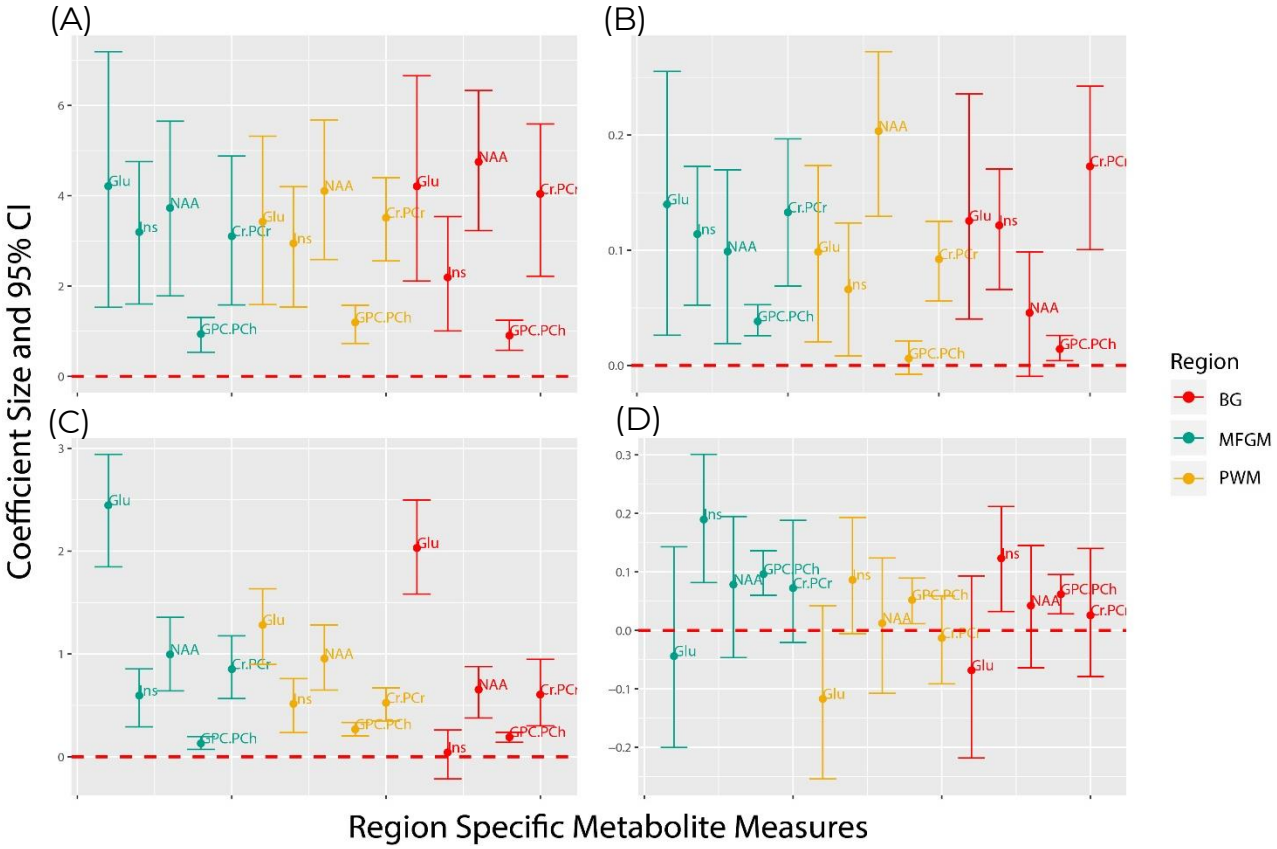

B:

Code used for the analyses described within this dissertation.

Code for Chapter 2:

1. The simple LR Model

```
        lm(Allegra$Glu ~ Skyra$Glu)
```

Cycle through and repeat for all metabolites and regions

2. The LR Model with covariates

```
        lm(Allegra$Glu ~ Skyra$Glu + Allegra$GM + Skyra$GM +
        demographics$TimeBetweenScans + demographics $status)
```

Cycle through and repeat for all metabolites and regions

3. Bland Altman Plot

```
        a <- Age5_FirstObservation_GM$Glu
        b <- Age5_SecondObservation_GM$Glu
        plot_ba <- bland.altman.plot(a,b, xlab="Mean Concentration",
        ylab="Difference", silent=FALSE,conf.int=.95)
```

Cycle through and repeat for all metabolites and regions

Code for Chapter 3:

1. Creating relative GM%, relative WM% and scaled age variables:

```
WM$RelativeWM <- WM$WM/(100-WM$CSF)
WM$Age0 <- WM$Age-4.94182
```

2. Univariate Mixed Effects Models:

```
WM_Glu <- groupedData(formula = Glu~Age0|ID, data = WM)

WM_Glu.lme <- lme(Glu~Age0+machine+status+ RelativeWM
+Age0*machine, data = WM_Glu, random = ~1|ID)
summary(WM_Glu.lme)
```

3. Univariate Mixed Effects Models with HIV Exposure:

```
BG_Cr.PCr <- groupedData(formula = Cr.PCr~Age0|ID, data = BG)

BG_Cr.PCr.lme <-
lme(Cr.PCr~Age0+machine+Exposure+RelativeBG_GM+Age0*machine,
data = BG_Cr.PCr, random = ~1|ID)
summary(BG_Cr.PCr.lme)
```

4. Model Validation:

```
par(mfrow=c(2,2))
hist(WM_Glu.lme$residuals[,1], xlab="Residuals", main="Between Subject
Residuals")
hist(WM_Glu.lme$residuals[,2], xlab="Residuals", main="Within Subject
Residuals")

plot(WM_Glu.lme$fitted[,1], WM_Glu.lme$residuals[,1], xlab="Fitted
Values", ylab="Residuals", main = "Between Subject")
plot(WM_Glu.lme$fitted[,2], WM_Glu.lme$residuals[,2], xlab="Fitted
Values", ylab="Residuals", main = "Within Subject")
```

Code for Chapter 4:

For the Multilevel LMEM:

1. Set the reference region and metabolite

```
Data_Edit$region <- relevel(Data_Edit$region, ref = 'BG')
Data_Edit$Meta <- relevel(Data_Edit$Meta, ref = 'Glu')
```

2. Describe the data structure

```
Mets_Ed <-  groupedData (formula = Conc~Age0|ID/region/Meta,
            data = Data_Edit)
```

3. Fit the Full Multilevel LMEM

```
lme_Full <-     lme(Conc~Age0 + machine + status + region +
                Meta + RelativeGM + RelativeGM*Meta +
                RelativeGM *region + machine *Meta +
                machine*region + machine*Meta*region +
                status*Age0*Meta*region + status*Meta*region +
                Age0*Meta*region + status*Age0 , data =
                Mets_Ed, random = list(ID=pdDiag(~1)),  weights =
                varIdent(form= ~ 1 | region*Meta))
```

4. Fit the Multilevel LMEM without the age*status interactions

```
lme_WOI <-      lme(Conc~ Age0 + machine + status + region +
                Meta + RelativeGM + RelativeGM*Meta +
                RelativeGM *region + machine*Meta + machine
                *region +
                machine*Meta*region+status*Meta*region +
                Age0 *Meta*region , data = Mets_Ed, random =
                list(ID=pdDiag(~1)),  weights = varIdent(form= ~ 1 |
                region*Meta))
```

Cycle between different reference regions and metabolites to easily obtain estimates of SE and $\boldsymbol{\beta}$ values

For the CRM:

Note: Data must have ID variables in increasing order without gaps and categorical or binary covariates must be coded using 0/1's.

1. The latent factor model

```
fit.lvm <-  boral ( y=Y, family = "normal", lv.control = list(num.lv = 3,
            type = "independent"), row.eff="random", save.model =
            TRUE, row.ids = ID)
```

2. The GLM+LF model

```
fit.X <-    boral ( y=Y, X=X, family="normal", lv.control = list(num.lv
            =3, type="independent"), row.eff = "random",
            save.model = TRUE, row.ids = ID)
```

3. The GLM+LF Model with the Traits component

Making the traits matrix:

```
respvars <-         c("Glu_GM", "Ins_GM", "NAA_GM", "GPC.PCh_GM",
                    "Cr.PCr_GM" ,"Glu_BG", "Ins_BG", "NAA_BG",
                    "GPC.PCh_BG", "Cr.PCr_BG", "Glu_WM",
                    "Ins_WM", "NAA_WM", "GPC.PCh_WM",
                    "Cr.PCr_WM")
Region <-           c("GM", "GM", "GM", "GM", "GM", "BG", "BG", "BG",
                    "BG", "BG", "WM", "WM", "WM", "WM", "WM" )
Metabolite <-       c("Glu", "Ins","NAA","GPC.PCh", "Cr.PCr","Glu",
                    "Ins", "NAA", "GPC.PCh", "Cr.PCr", "Glu", "Ins",
                    "NAA", "GPC.PCh", "Cr.PCr")
Traits_Test <-      as.data.frame(cbind(Region,Metabolite))
Traits <-           cbind(model.matrix(~-1+Metabolite, data =
                    Traits_Test), model.matrix (~-1+Region, data =
                    Traits_Test))
rownames(Traits) <- respvars
colnames(Traits) <- c("Cr.PCr", "Glu", "GPC.PCh", "Ins", "NAA", "BG",
                      "GM", "WM")
which.traits        <- vector("list",ncol(X)+1)
for(i in 1:length(which.traits)) which.traits[[i]] <- 1:ncol(Traits)
```

Fitting the Model:

```
fit.traits <-   boral (y=Y, X=X, family = "normal", traits = Traits,
                which.traits = which.traits, lv.control = list(num.lv = 3,
                type = "independent"), row.eff="random",
                save.model=TRUE, row.ids = ID)
```